



ADDIS ABABA

INSTITUTE OF TECHNOLOGY

CIVIL ENGINEERING DEPARTMENT

**Correlation between Critical State Soil Parameters and
Index Properties of Remolded Red Clay Soils of
Addis Ababa**

By

Yodit Muluneh

Advisor

Prof. Alemayehu Teferra

A Thesis Submitted to the School of Graduate Studies of Addis Ababa
University in Partial Fulfillment of the Requirements for the Degree of
Masters of Science in Civil Engineering (Geotechnical Engineering)

July, 2012

Addis Ababa, Ethiopia



**Correlation between Critical State Soil Parameters and Index
Properties of Remolded Red Clay Soils of Addis Ababa**

By

Yodit Muluneh

July, 2012

Approved by the Board of Examiners

Prof. Alemayehu Teferra

Advisor

External Examiner

Internal Examiner

Chairman

Signature

Signature

Signature

Signature

Date

Date

Date

Date

Abstract

Critical state concept is a modern concept to make estimates of soil responses when one cannot conduct sufficient soil tests to completely characterize a soil at a site or when one needs to predict the soil's response from changes in loading during and after construction. In this study correlations are developed to predict critical state soil parameters (CSSP) from index tests so that one can be able to model Addis Ababa red clay soils with critical state model using simple laboratory tests.

Disturbed soil samples from six different sites of Addis Ababa, where red clay is found, are collected. Laboratory tests like specific gravity, grain size analysis, Atterberge limit and standard compaction for a total of twelve test samples (at 1.5m and 3.0m depths per each six sites) are conducted. By remolding these samples to MDD and OMC Twelve - one dimensional consolidation and six- isotropic consolidation triaxial tests have done. From these tests critical state soil parameters (λ and Γ) are determined. From the results of limited tests, an indicative good correlation is observed between (Γ and LL), (Γ and, PL), (Γ and PI), (λ and LL) and (λ and PL). But, Poor correlation is developed between λ and PI.

The developed correlations will be important inputs in modeling Addis Ababa red clay soils with critical state model using simple index tests. In addition, the results of this study can serve as a basis for further study of such correlations on red clay soils in the country.

Key words: critical state soil parameters (CSSP), index property, standard compaction

Acknowledgement

The professional guidance, valuable advice and support offered by my advisor Prof. Alemayehu Teferra is greatly appreciated. I also value the contributions from AAiT Geotechnical Engineering laboratory staff members, CDSco (Construction Design Share Company) Geotechnical laboratory staff members especially Ato Grma Mekonen for their support while conducting my laboratory tests.

Last but not least, my beloved husband Anteneh Getachew, I am very thankful for your support and encouragements.

Contents

Abstract	I
Acknowledgment.	II
List of tables	V
List of figures	VI
List of acronyms, abbreviations and symbols	VII
1. Introduction.....	1
1.1 Background.....	1
1.2 Objective of the research.....	2
1.3 Methodology.....	2
1.4 Organization of the thesis.....	3
1.5 Scope of the investigation.....	3
2. Literature review.....	4
2.1 Clay soils.....	4
2.1.1 General.....	4
2.1.2 Clay mineralogy.....	4
2.1.3 Origin and mineral composition of Ethiopian red clay.....	5
2.2 Index property.....	10
2.2.1 Specific gravity	10
2.2.2 Grain size analysis	10
2.2.3 Atterberge limits	11
2.3 The critical state concept.....	12
2.3.1 Introduction.....	12
2.3.2 State boundary surface for saturated soils.....	12
2.3.3 Basic concepts in critical state theory	13
2.3.4 Critical state parameters for saturated soils.....	14
2.3.5 Existing correlations between critical state soil parameters and index tests.....	17
3. Laboratory tests and results.....	21

3.1 General	21
3.2 Specific gravity.....	23
3.3 Grain size analysis	23
3.4 Atterberge limits.....	25
3.5 Standard Compaction.....	27
3.6 One dimensional consolidation	30
3.7 Triaxial compression test (isotropic consolidation)	33
4. Regression analysis	36
4.1 General.....	36
4.2 Scatter Plot.....	37
4.3 Correlation between λ and LL, PL and PI.....	40
4.4 Correlation between Γ and LL, PL and PI	41
4.5 Comparison of λ from Oedometer and Triaxial Tests	42
5. Discussion of test results	43
6. Conclusions and recommendations.....	46
6.1 Conclusions.....	46
6.2 Recommendations.....	46
References.....	47
Appendix – A: (Laboratory Tests Results).....	49
I. Grain size analysis test Results.....	50
II. Atterberge limits test Results.....	53
III. Standard Compaction test Results	59
IV. One dimensional consolidation test Results	65
V. Triaxial compression test (isotropic consolidation) Results	104
Appendix – B: (photos of site and laboratory tests).....	110

List of Tables

Table 2.1: Ranges in properties of Ethiopian soils Morin and Perry (1971) as cited by [2]..	6
Table 2.2: Ranges in properties of undisturbed red clay soils of Addis Ababa by Samuel, T. [17]	8
Table 2.3: Ranges in properties of undisturbed red clay soils of Addis Ababa by Merihun, L. [11].	8
Table 2.4: Ranges in properties of undisturbed red clay soils of Addis Ababa by Jibril, J. [9].	9
Table 3.1: Summary of Specific gravity test results.....	23
Table 3.2: Clay fraction	24
Table 3.3: Summary of Atterberge Limits test results and soil classification	25
Table 3.4: Alternative Proctor Test Methods [16]	28
Table 3.5: Summary of standard compaction test results	30
Table 3.6: Summary of compression index, c_c test results	32
Table 3.7 Summary of pre consolidation pressure (P_c) test results.....	33
Table 3.8: Summary of triaxial test result for different locations.....	35
Table 4.1: Summary of the regression analysis results.....	41
Table 4.2: Comparison of value of λ from Oedometer and Triaxial test	42
Table 5.1: Values of compression index (C_C) for undisturbed red clay soils of Addis Ababa [17].....	44
Table 5.2: Values of capital gamma (Γ) for undisturbed red clay soils of Addis Ababa [17].....	45

List of Figures

Figure 2.1:	Consistency of cohesive soils [13].	11
Figure 2.2:	Complete state boundary surface Atkinson (1981), as cited by [8].....	13
Figure 2.3:	Projection of ideal critical state boundaries on the $v - p'$ and $q - p'$ planes [8]	16
Figure 2.4:	Relation between Liquidity Index and Shear Strength of Remolded Clays (After Skempton & Northey) as cited by [14]	18
Figure 2.5:	Family of Experimental Critical State Lines [1]	19
Figure 2.6:	Idealized Families of Critical State Lines [1].....	20
Figure 3.1:	Test pit locations.....	22
Figure 3.2:	Particle Size distribution curves at 3.0 m depth for samples TP1-2, TP2-2, TP3-2, TP4-2, TP5-2 and TP6-2.....	24
Figure 3.3:	Classification of the soil using USCS, plasticity chart	26
Figure 3.4:	Standard compaction curves at 1.5 m depth for samples TP1-1, TP2-1, TP3-1, TP4-1, TP5-1 and TP6-1.....	29
Figure 3.5:	Standard compaction curves at 3.0 m depth for samples TP1-2, TP2-2, TP3-2, TP4-2, TP5-2 and TP6-2.....	29
Figure 3.6:	e versus $\log p$ curves at 1.5 m depth for samples TP1-1, TP2-1, TP3-1, TP4-1, TP5-1 and TP6-1.....	31
Figure 3.7:	e versus $\log p$ curves at 3.0 m depth for samples TP1-2, TP2-2, TP3-2, TP4-2, TP5-2 and TP6-2.....	32
Figure 3.8:	Triaxial compression machine.	34
Figure 4.1:	Scatter plot of λ versus LL.	37
Figure 4.2:	Scatter plot of λ versus PL.	38
Figure 4.3:	Scatter plot of λ versus PI.	38
Figure 4.4:	Scatter plot of Γ versus LL.	39
Figure 4.5:	Scatter plot of Γ versus PL.	39
Figure 4.6:	Scatter plot of Γ versus PI.	40

List of Acronyms, Abbreviations and Symbols

CSSP	Critical state soil parameters
CSL	Critical state line
NCL	Normal consolidation line
MDD	Maximum dry density
OMC	Optimum moisture content
λ	Compression index, slope of normally consolidation line
Γ	Value of specific volume corresponding to $P'=1.0 \text{ Kn/m}^2$ on critical state line
LL	Liquid limit
PL	Plastic limit
PI	Plasticity index
LI	Liquidity index
R^2	Coefficient of determination
AAiT	Addis Ababa institute of technology
CDSco	Construction design Share Company
q	Deviatoric stress
p	Total mean stress
M	Slope of critical state line
ν	Specific volume
κ	Swelling index, slope of over consolidated line
p'	Effective mean stress
ASTM	American society for testing of materials
BS	British standards
G_s	Specific gravity
USCS	Unified soil classification system
AASHTO	American association of state highway and transportation officials
LI	Liquidity index
$\sigma_1, \sigma_2, \sigma_3$	Principal stresses
e	Void ratio
u	Pore pressure

Pc	Pre consolidation stress
w	Water content
TP	Test pit
CH	Inorganic clays of high plasticity
MH	Inorganic silts, micaceous or diatomaceous fine sandy or silty soils, elastic silts.
Cc	Compression index
N	Number of samples
Hs	Height of solids
e_f	Final void ratio
e_o	Initial void ratio
kPa	KiloPascals
wt.	Weight
γ_w	Unit weight of water
γ_{wet}	Wet unit weight
γ_{dry}	Dry unit weight
ρ	Density
V_o	Initial volume of specimen
ν_o	Initial specific volume
cc	Cubic centimeters

Chapter 1

Introduction

1.1 Background

Most engineers in practice make calculations and base their judgment on the model used over two hundred years ago by C. A. Coulomb in his classic analysis of the active and passive pressures of soil against a retaining wall. But in this time, there is a need to create new model which can represent stress-strain behavior of soils better. The critical state concept is a tool to make estimates of soil responses when one cannot conduct sufficient soil tests to completely characterize a soil at a site or when one has to predict the soil's response from changes in loading during and after construction [1].

In critical state model, soils and other granular materials, if continuously deformed until they flow as a frictional fluid, will come into a well-defined critical state determined by two equations:

$$q = Mp \dots\dots\dots (1.1)$$

$$\Gamma = v + \lambda \ln p \dots\dots\dots (1.2)$$

The constants M , Γ and λ represent basic soil-material properties in normally consolidated clays [1].

These critical state soil parameters are determined by conducting triaxial compression (isotropic consolidation) and oedometer tests. So far, different researchers have determined these parameters for soils in different parts of the world.

In this research an attempt has been made to correlate the critical state soil parameters with index properties of remolded red clay soils of Addis Ababa.

1.2 Objective of the research

To correlate the critical state soil parameters with index properties of remolded red clay soils of Addis Ababa.

1.3 Methodology

In order to achieve the objective of the research, specific gravity, grain size analysis, Atterberg limit tests, standard compaction and one dimensional consolidation /oedometer/ tests have been conducted on twelve soil samples and triaxial compression tests (isotropic consolidation) on six remolded red clay soil samples. Test pits are excavated at selected six locations of Addis Ababa city where red clay is found. Two samples from each test pits at two different depths (1.5m and 3.0m) are collected. The samples were transported to the AAiT geotechnical laboratory.

Disturbed samples are used to conduct specific gravity, Atterberg limits, grain size analysis and standard compaction tests. Also by remolding the samples to MDD and OMC, one dimensional consolidation and triaxial compression tests (isotropic consolidation) tests are conducted. ASTM procedures were followed while conducting all tests except, BS procedures for triaxial compression (isotropic consolidation) tests. λ from one dimensional consolidation test and λ and Γ from triaxial compression (isotropic consolidation) test are determined.

Using Microsoft® excel regression analysis software Γ and λ are correlated with liquid limit, Plastic limit and Plasticity index. Linear and Polynomial regressions are employed in the analysis.

1.4 Organization of the Thesis

This thesis work is divided into six Chapters, each covering a specific topic of the research work. In the introductory Chapter background of the problem, objective of the research, methodology, organization of the thesis and scope of the investigation are presented. Literature review is undertaken in Chapter two. Chapter three deals with laboratory tests and results. Regression analysis is presented in the fourth Chapter. Chapter five deals with discussion of test results. The last Chapter, Chapter six, is devoted to conclusions and recommendations. Detailed test results are presented in the appendices.

1.5 Scope of the investigation

This research addresses the described objective and provides correlations between the critical state soil parameters and index properties of remolded red clay soils of Addis Ababa. Collections of the disturbed samples are limited to six representative locations. One test pit was opened at each sampling location and then disturbed samples are collected from two depths (1.5m and 3.0m).

For the intended purpose, oedometer and triaxial tests are conducted on remolded soil samples. In this study remolding of the test samples is according to standard compaction test. Due to the mechanical problems associated with the triaxial machine, it was not possible to conduct tests as many as possible.

Chapter 2

Literature review

2.1 Clay soils

2.1.1 General

Clay refers for soil particles finer than 0.002mm or 0.005mm depending on which classification system used. It has the property of plasticity when mixed with some amount of water. Plasticity refers for the behavior of material that deforms in shape and keeps its deformation even after the removal of the pressure that caused the deformation.

Clay soil may contain clay minerals as well as non clay minerals. The non clay minerals that are found in clay are quartz, feldspar or mica. Clay minerals are mostly in the form of sheets; their thickness is relatively smaller than the width and length of the sheets, their surface area is larger than their volume. Consequently, the behavior of clay is governed by the surface forces as cited by [11].

Soil behavior is attributed to the properties of clay minerals that are found in the specific soil. Therefore, it is vital to know the behavior of clay minerals for understanding the engineering behavior of fine grained soils.

2.1.2 Clay mineralogy

The minerals of clays are formed by chemical weathering of rock forming minerals such as feldspar and micas. The clay minerals include Illite, Kaolinite, Montmorillonite, Halloysite and Vermiculite; however, the first three are the major ones [3]. Most clay minerals of interest to the geotechnical engineers are made up of two basic units, the octahedral and the tetrahedron sheets. The octahedral unit consists of two layers of oxygen or hydroxyls with aluminum atoms embedded in between, the aluminum may be replaced by magnesium or iron. The tetrahedron

sheet consists of a central silica cation surrounded by four oxygen anions, one at each corner of the tetrahedron [4].

On the basis of their crystalline arrangement, clay minerals are divided into three general groups namely Kaolinite, Illite and Montmorillonite. It is found that Kaolinite shows little swelling on wetting whereas Montmorillonite clay minerals are highly expansive and create major engineering problems.

2.1.3 Origin and mineralogical composition of Ethiopian red clay soils

The origin and mineralogical composition of Ethiopian Red clay soils have been studied by different researchers. The Ethiopian red clay soils are principally residual and derived from the weathering of volcanic rocks. The parent rock for black and red clays in Ethiopia is mainly olivine basalt, basalt and trachyte.

Ethiopian red clay soils have developed where rain fall is plentiful and drainage is good, and contain Kaolinite and halloysite as the principal clay minerals, but Montmorillonite is also frequently present in significant amounts. The red color of the Ethiopian soils indicates the presence of iron. The following tables (Table 2.1-Table2.4) show the ranges in the properties of Ethiopian soils by different researchers.

Table 2.1: Ranges in properties of Ethiopian soils Morin and Perry (1971) as cited by [2]

	Black clays	Red clays	Other clays	Lacustrine soils
Parent Rock	Olivine, basalt, basalt, trachyte	Olivine basalt basalt, trachyte	Olivine basalt basalt, trachyte, ignimbrite, etc	-
Rain fall, mm/year	228.6-1346.2	1219.2-2336.8	10.16-1219.2	<203.2-1041.4
Temperature °F	54-68	57-68	62-82	66-80
Drainage	Poor to good	Fair to good	poor-good	poor
Principal clay Minerals	Montmorillonite, kaolinite and halloysite	Kaolinite, halloysite, montmorillonite	Montmorillonite, Kaolinite	Montmorillonite
PH Value	7.2-8.4	5.1-6.8	6.3-9.1	8-9.1
Principal cations	Calcium, magnesium, potassium	Calcium, magnesium, potassium	Calcium	Calcium
Cation exchange capacity, m.e/100g	42-95	30-77	22-90	61(one test)
Clay (2 μ). %	13-75	34-76	5-51	3-41
Liquid limit, %	37-88	44-66	NP-57	NP-70
Plasticity index, %	11-48	14-30	NP-35	NP-35
Shrinkage limit, %	7-28	10-30	11-19	15-20

	Black clays	Red clays	Other clays	Lacustrine soils
Specific gravity...	2.62-2.94	2.61-2.9	2.61-2.9	2.61-2.92
Organic content,%	2-7+	1-4+	2-7+	4+
Compaction test: Maximum Density ,kg/cu.m	1106.27-101	1619.32-1186.32	1170.4-1667.42	1218.5-1442.96
Optimum moisture,%	40-17	38-29	28-21	30-27
California bearing ratio (CBR)test values	2-8	6-9	-	-
Unconfined compressive strength,kpa	96.76-267.28	146.57-250.99	61.79-159.02	64.66-192.56
Expansion pressure ,kpa	11.5-95.8	21.1-95.8	5.75-143.7	19.16-114.96

Table 2.2: Ranges in properties of undisturbed red clay soils of Addis Ababa by Samuel, T. [17].

S.No.	Site	Clay fraction (%)	Atterberg limits			Gs	CC
			LL (%)	PL (%)	PI (%)		
1	Kolfe	58-70	61-75	28-33	15-21	2.66-2.73	0.136
2	Semien Gebeya	53-68	59-72	24-31	33-47	2.7-2.77	0.146
3	Rufael	50-70	56-66	27-34	29-41	2.66-2.74	0.153

Table 2.3: Ranges in properties of undisturbed red clay soils of Addis Ababa by Merihun, L. [11].

S.No.	Site	Gs	Atterberg limits			OMC (%)	MDD (g/cc)	Cc
			LL (%)	PL (%)	PI (%)			
1	Kolfe pit 1	2.72	61	27	34	28	1.53	0.147
2	Kolfe pit 2	2.73	71	33	38	32	1.36	0.195
3	Adisu Gebeya pit 1	2.71	63	28	35	34	1.37	0.152
4	Adisu Gebeya pit 2	2.71	72	33	39	34	1.39	0.172

Table 2.4: Ranges in properties of undisturbed red clay soils of Addis Ababa by Jibril, J. [9].

S.No.	Name of locality	Test pit	Depth (m)	Gs	LL (%)	PL (%)	PI (%)	Cc
1	Addisu Gebeya (Gulele sub-city)	1	1.5	2.77	64.93	25.23	39.70	0.183
			2.5	2.72	70.84	32.66	38.18	0.219
2	Alem Tsehay Dildy (Gulele sub-city)	1	2.0	2.75	66.85	33.09	33.76	0.236
			3.0	2.73	60.50	23.57	36.93	0.173
3	Atari (Gulele sub-city)	1	2.0	2.74	68.58	27.83	40.75	0.186
			3.0	2.71	71.62	29.66	41.96	0.174
4	Kalae (Kolfe sub-city)	1	1.5	2.73	62.60	24.83	37.77	0.176
			2.5	2.72	54.38	22.36	32.02	0.146
5	Kolfe (Kolfe sub-city)	1	2.0	2.80	67.99	32.69	35.30	0.226
			3.0	2.77	68.97	30.89	38.08	0.189
6	Shogele (Gulele sub-city)	1	1.0	2.69	62.63	31.75	30.88	0.193
			3.0	2.69	73.24	33.17	40.07	0.262
7	Traffic seffer (Kolfe sub-city)	1	2.0	2.73	62.93	25.03	37.90	0.179
			3.0	2.74	72.95	33.01	39.94	0.229
8	Rufael (Gulele sub-city)	1	2.0	2.72	63.21	25.08	38.13	0.182
			3.0	2.73	69.19	31.92	37.27	0.196
9	Semen Mazegaja (Gulele sub-city)	1	1.5	2.66	52.94	21.94	31.00	0.143
			2.5	2.68	56.87	23.03	33.84	0.159
10	Asko (Kolfe sub-city)	1	2.0	2.69	69.38	32.43	36.95	0.199
			3.0	2.74	73.07	33.14	39.93	0.252

2.2 Index Property

2.2.1 Specific gravity

Specific gravity of a soil is defined as the ratio of the mass in air of a given volume of soil solid to the mass in air of an equal volume of distilled water at stated temperature [10].

$$G_s = \frac{M_s}{M_w} \dots\dots\dots (2.1)$$

Where: G_s = Specific gravity of soil particle

M_s = Mass in air of a given volume of soil

M_w = Mass in air of an equal volume of water

2.2.2 Grain size distribution

Simple sieve analysis is used for particles larger than 0.075mm while sedimentation /Hydrometer/ analysis for particles smaller than 0.075mm. For soil sample that contains a measurable portion of their grains both coarser and finer than 0.075mm size combined analysis is required [10].

A sieve analysis test consists of shaking the soil through a stack of wire screens with openings of known size (75mm ,50mm ,37.5mm ,25mm ,19mm ,9.5mm ,4.75mm ,2mm ,850 μ m ,425 μ m ,250 μ m,106 μ m and75 μ m).The particle size is defined as the side dimension of a square hole in which the particle is retained. The percentage finer can be calculated from the mass of sample retained on the sieve, the mass of sieve, and the total mass of sample. A curve or table showing the particle size versus the percentage finer on each sieve can present the distribution of the grain size.

Hydrometer test consists of soaking the fine soil particle left in the pan of the sieve analysis, adding dispersion agent and soaking and then followed by filling with distilled water. The highly heavier particle settles immediately and the light particles settle next. And finally, according to the Stoke's law the diameter of the fine particles, less than 0.075mm is calculated [10].

2.2.3 Atterberge limits

If clay slurry is dried, the moisture content will gradually decrease, and the slurry will pass from a liquid state to a plastic state. With further drying, it will change to a semisolid state and finally to a solid state, as shown in Fig. 2.2 below. In 1911, Atterberg, a Swedish scientist, developed a method for describing the limit consistency of fine-grained soils on the basis of moisture content. These limits are the liquid limit, the plastic limit, and the shrinkage limit [12].

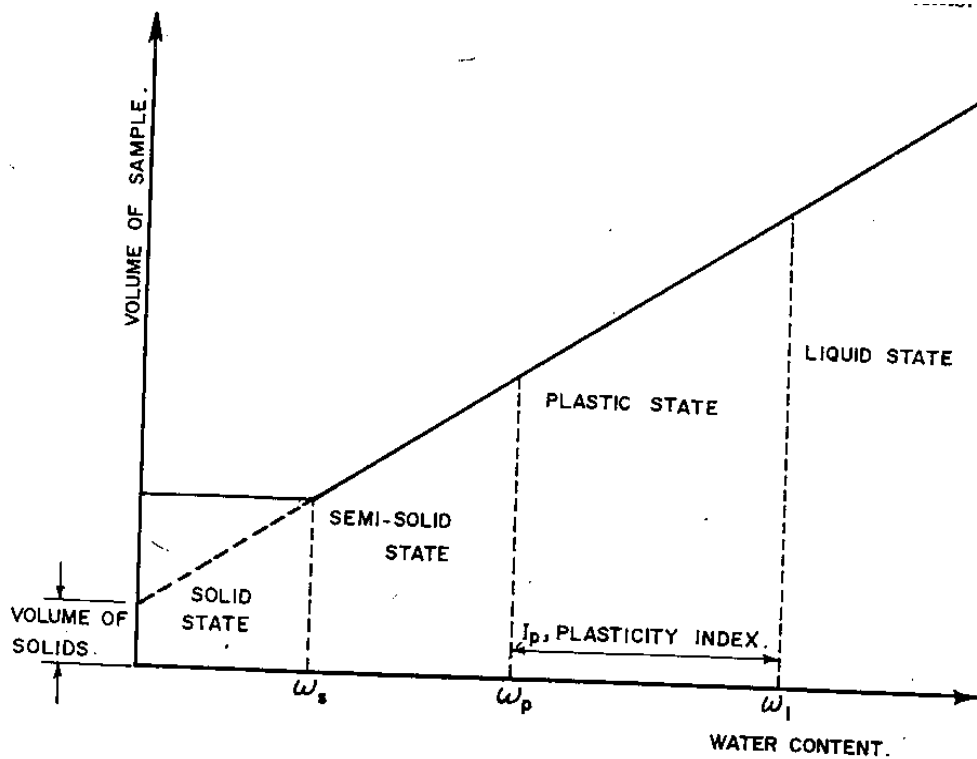


Figure 2.1: consistency of cohesive soils [13].

The liquid and plastic limits are widely used for engineering classification of fine-grained soils. The liquid limit, plastic limit, plasticity index, and liquidity index of soils are used to develop correlation with shear strength, compressibility, permeability, shrink-swell etc.

2.3 The Critical state concept

2.3.1 Introduction

A conceptual model of soil behavior assumes that soil under stress ultimately reaches a state of plastic behavior characterized by continuous deformation without further increases in stress. This concept is the underlying principle of the critical state theory. The critical state framework also idealizes a state boundary surface which defines the limit of possible states at which a soil can exist. The critical state theory was introduced by Roscoe et al. (1958) as cited by [8] as a powerful framework for explaining shear and volume change behavior of saturated soils under external loading. The theory provided for the first time, soil models that combine stresses and the accompanying deformation in a three-dimensional space [8].

2.3.2 State boundary surface for saturated soils

The shape of the complete state boundary surface can be represented graphically in q' , p' and v space, as shown in Fig.2.3 below. The critical state boundary surface for a soil is bounded by lines that define the normal consolidation line (NCL), a unique critical state line (CSL), tension cut off and the v – axis. Generally, soils within the state boundary surface undergo elastic and recoverable strains. State paths cannot cross the state surface; hence soils cannot exist above the surface. However state paths can traverse any of the surfaces; soils in this condition undergo volume change that is plastic, irrecoverable and permanent. The end point of a state path traversing the surface is the critical state line where it continues to deform or flow without any further change in p' , q , or v . The state boundary is made up of three distinct surface namely, Roscoe, Hvorslev and no-tension surface [8].

State paths traversing the Roscoe surface associated with a decrease in volume (compaction), while an increase in volume (loosening or dilation) characterizes the state paths on the Hvorslev surface.

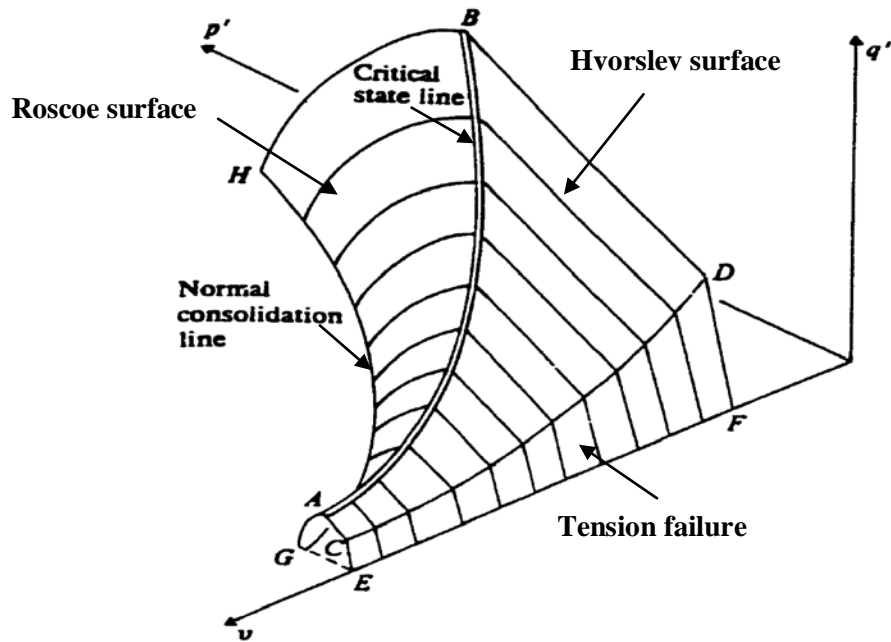


Figure 2.2: Complete state boundary surface Atkinson (1981), as cited by [8].

2.3.3 Basic concepts in critical state theory

Critical state is a failure state at which the specimen under stress continues to deform with no further change in volume or stress. With the assumption that the soil is isotropic, the original and standard critical state variables based on a macroscopic viewpoint, are, p' , q and ν and are defined as: [14]

$$p' = \frac{\sigma_1 + \sigma_2 + \sigma_3}{3} - u \dots \dots \dots (2.2)$$

$$= p - u$$

$$q = \sigma_1 - \sigma_3 \dots \dots \dots (2.3)$$

$$\nu = 1 + e \dots \dots \dots (2.4)$$

- Where,
- p' = effective mean or hydrostatic stress
 - p = total mean stress
 - q = deviatoric stress
 - ν = specific volume
 - e = void ratio

$\sigma_1, \sigma_2, \sigma_3$ = principal stresses

For triaxial conditions, where σ_2 is equal to σ_3 and the above equation can be written as:

$$p' = \frac{\sigma_1 + 2\sigma_3}{3} - u \dots \dots \dots (2.5)$$

Critical state is independent of stress path. Analyzed data for triaxial compression test results of normally consolidated saturated weald clay approached a unique critical state line for both drained and undrained stress paths [14].

Though critical state is independent of stress path, the nature of volume changes that take place are influenced by the soil stress history. Normally consolidated soils generally tend to reach critical state with a decrease in volume in a ductile manner. Brittle or over consolidated soils on the other hand tend to dilate on approaching critical state [8].

2.3.4 Critical state parameters for saturated soils

Different parameters are used to characterize normally consolidated and over consolidated soils using critical state model. A convenient way to represent the critical state condition is by projecting the state boundaries on to the $v - p'$ and $q - p'$ planes as it is shown in Fig.2.4 below [8].

The equations from this representation are:

(i) Isotropic normal consolidation line on $v - p'$ plane

$$v = N - \lambda \ln p \dots \dots \dots (2.6)$$

$$q = 0$$

(ii) Rebound (over consolidation) line on $V - p'$ plane

$$v = v_{\kappa} - \kappa \ln p' \dots \dots \dots (2.7)$$

$$q = 0$$

(iii) Critical state line

$$v = \Gamma - \lambda_{cs} \ln p' \quad \text{on } v - p' \text{ plane}$$

$$q = Mp' \quad \text{on } q - p' \text{ plane}$$

Where, λ = slope of normal consolidation line on the $v - p'$ plane

λ_{cs} = slope of critical state line on the $v - p'$ plane

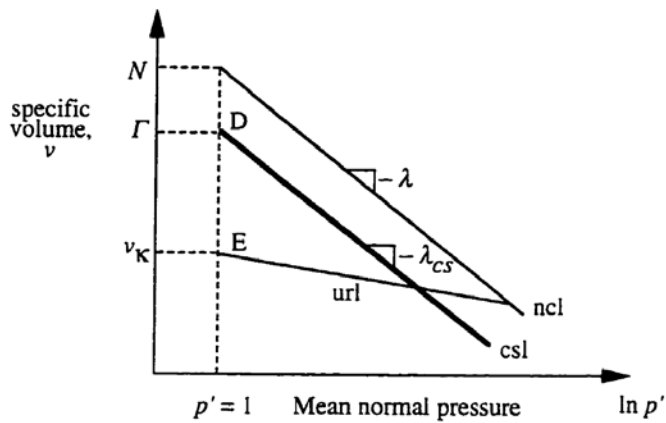
κ = slope of the rebound line on the $v - p'$ plane

M = slope of critical state line on the $q - p'$ plane

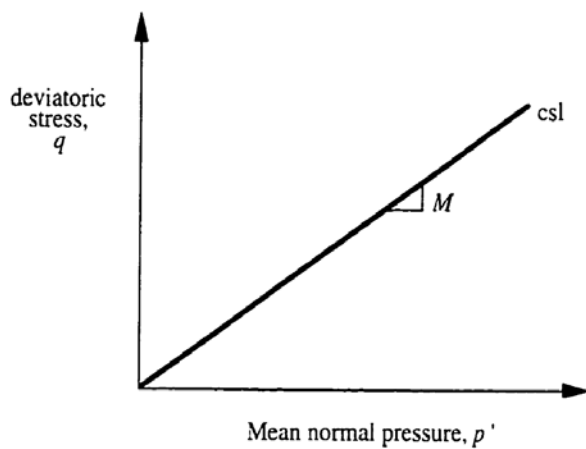
N = intercept of the normal consolidation line with the v -axis

ν_{κ} = intercept of the rebound line with the v -axis

Γ = intercept of the critical state line with the v -axis



a)



b)

Figure 2.3: Projection of ideal critical state boundaries on the $v - p'$ and $q - p'$ planes [8].

For saturated clay, Atkinson and Bransby (1978) observed that λ is equal to λ_{cr} . The parameters λ , λ_{cr} , κ and M are soil constants that can be determined from laboratory experiments. The intercept parameters N , ν_{κ} and Γ are generally obtained from the $v - \ln p'$ graph at reference mean stress of 1 kPa.

The parameter λ (from three-dimensional isotropic consolidation), can be likened to the compression index C_c (from one-dimensional consolidation). Its magnitude determines the relative position of the critical state wall and hence the relative proportions of the Roscoe and Hvorslev surfaces. As λ decrease, the Roscoe surface expands while the Hvorslev surface contracts, and hence the probability of subcritical (ductile) failure is higher. Chances of supercritical (brittle) failure are higher under the reverse conditions.

2.3.5 Existing Correlations between Critical State Soil Parameters and Index Tests

By taking two remolded specimens A and B with different water contents (w_a and w_b) and conducting simple indentation test, their undrained shear strength is determined. w_a and w_b are water contents at liquid limit and plastic limit respectively.

Skempton and Northey (1953) have studied the relationship between undrained shear strength and liquidity index (LI) of four soils (refer Fig.2.5). They found that the shear strength of four soils are very similar both at the plastic and liquid limits. Remarkably, the shear strength at the plastic limit is almost exactly 100 times the shear strength at the liquid limit. One can then write for any clay

$$100q_{ll}=q_{pl} \dots \dots \dots (2.8)$$

Where the subscripts ll and pl refer to the liquid and plastic limits respectively. Using $q=Mp$ and the above equation one can write:

$$100p_{ll}=p_{pl} \dots \dots \dots (2.9)$$

Assuming that the specific gravity G_s of the soil solids is approximately 2.7, we have

$$v_a-v_b = G_s(w_a-w_b) = 2.7(w_a-w_b) \dots \dots \dots (2.10)$$

From the critical state model we have:

$$v_a + \lambda \ln p_a = \Gamma = v_b + \lambda \ln p_b \dots \dots \dots (2.11)$$

Hence,

$$2.7(w_a-w_b) = v_a-v_b = \lambda \ln (p_b/p_a) = \lambda \ln 100 = 4.6\lambda$$

$$\lambda = 0.585(w_a-w_b) \dots \dots \dots (2.12)$$

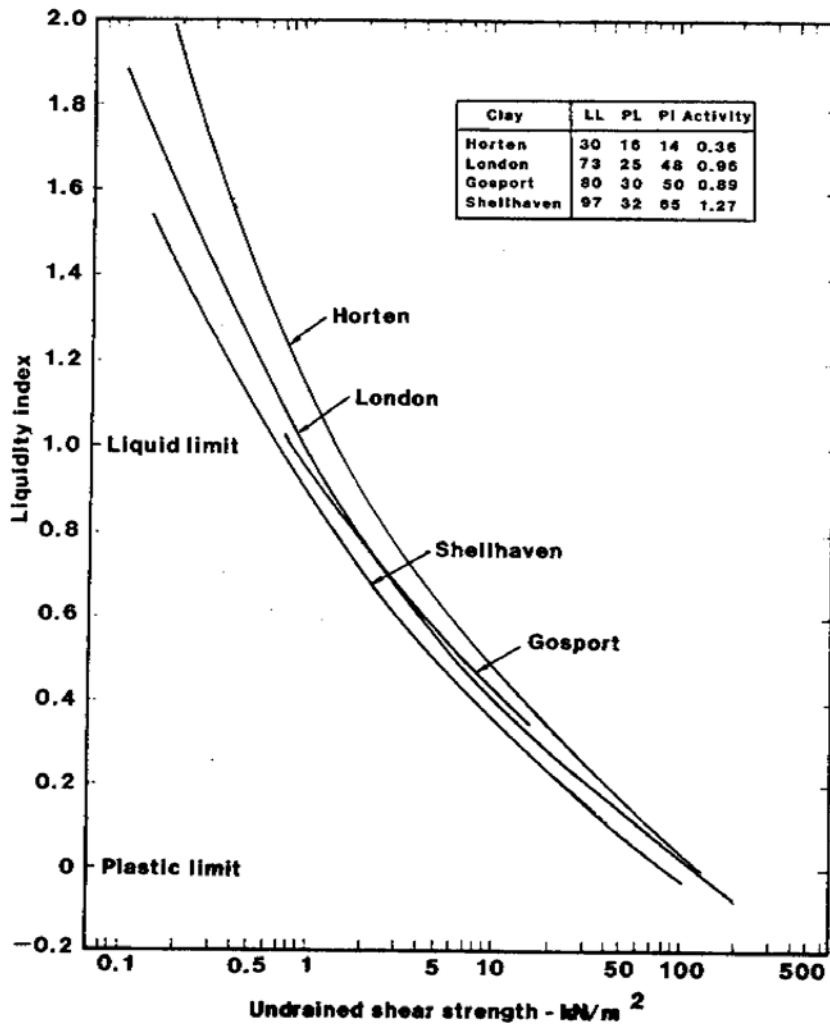


Figure 2.4: Relation between Liquidity Index and Shear Strength of Remolded Clays (After Skempton & Northey) as cited by [14].

The measured difference of water contents ($w_a - w_b$) then corresponds to the plasticity index, and we can write:

$$\lambda = 0.585(w_a - w_b) = 0.585(LL - PL) = 0.585PI \dots \dots \dots (2.13)$$

In Fig. 2.6 below the critical state lines for several soils from the experimental data are displayed. All the lines pass through or very near, the single point Ω given by:

$$\nu_{\Omega} = 1.25 \text{ and } p_{\Omega} = 1500 \text{ lb/in}^2$$

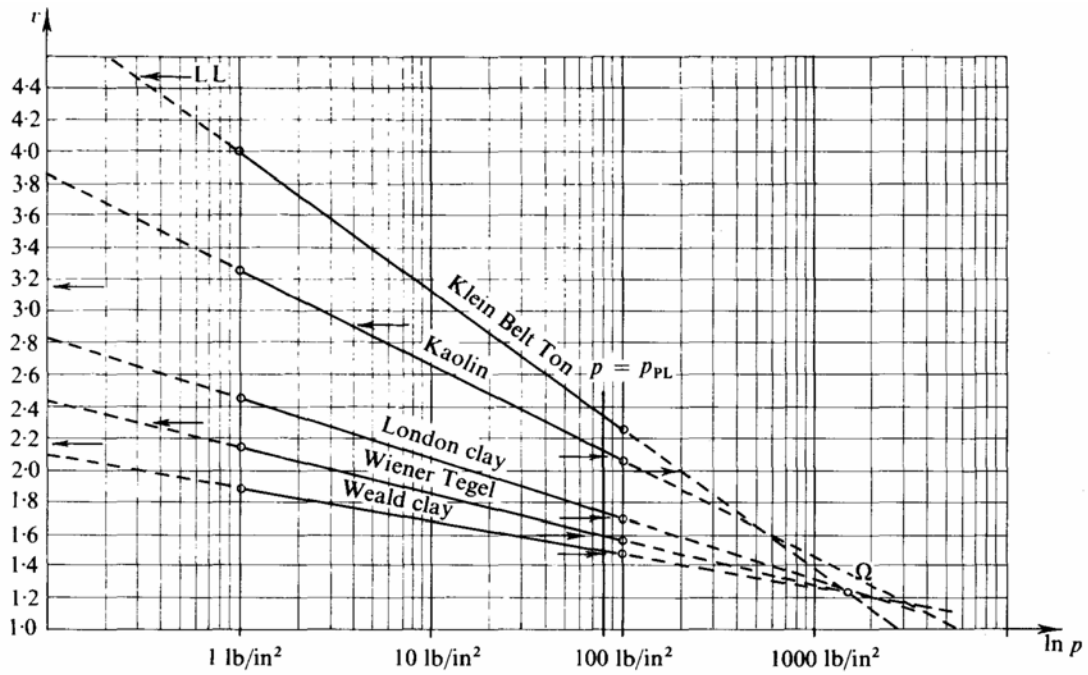


Fig. 2.5 Family of experimental critical state lines [1].

In addition, the points on each critical state line corresponding to the liquid and plastic limits have been marked. Those associated with the plastic limit are all very close to the same effective spherical pressure: $p = p_{pl} = 80 \text{ lb/in}^2$. The pressures p_{ll} associated with the liquid limits show a much wider range of values but this scatter is exaggerated by the logarithmic scale.

These experimental observations have been idealized with all lines passing through Ω , p_{pl} and p_{pl} are assumed to have fixed values. This means that as one can see in Fig. 2.7 (b), where the liquidity index has replaced specific volume as the ordinate, all critical state lines coincide to one unique straight line.

For any one critical state line in Fig. 2.7 (a) one can has:

$$\nu_{pl} - \nu_{\Omega} = \lambda \ln (\Omega / p_{pl}) \dots\dots\dots (2.14)$$

$$\nu_{ll} - \nu_{\Omega} = \lambda \ln (\Omega / p_{ll}) \dots\dots\dots (2.15)$$

$$\Delta \nu_{pl} = \nu_{ll} - \nu_{pl} = \lambda \ln (p_{pl} / p_{ll}) \dots\dots\dots (2.16)$$

Substituting the quoted values for Ω and p_{pl} in the first of these equations we get

$$\nu_{pl} - 1.25 = \lambda \ln (1500 / 80) = 2.93 \lambda \dots\dots\dots (2.17)$$

$$\lambda = 0.341(\nu_{pl} - 1.25) = 0.92(PL - 0.09) \dots\dots\dots (2.18)$$

Similarly, we can predict linear relationship:

$$\lambda = 0.133(\nu_{ll} - 1.25) = 0.36(LL - 0.09) \dots\dots\dots (2.19)$$

Similarly From the idealized situation of Fig. 2.7(a) and (b), one can predict

$$\Gamma = 1.25 + 6.7(PL - 0.09) = 0.65 + 6.7PL \dots\dots\dots (2.20)$$

$$\Gamma = 1.25 + 4.27PI \dots\dots\dots (2.21)$$

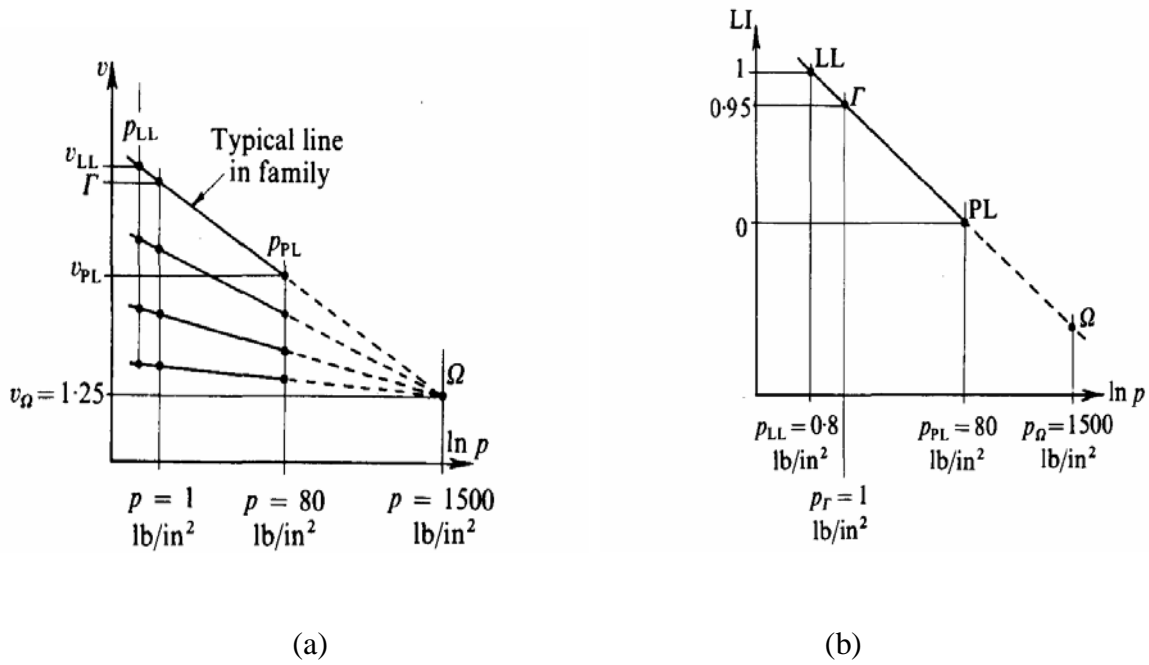


Fig. 2.6 Idealized families of critical state lines [1].

Chapter 3

Laboratory Tests and Results

3.1 General

Soil samples were collected from known areas of Addis Ababa where red clay is found. These are: Addisu Gebeya, Atena Tera, Athari, Awelya, Kolfe and Shegole (see Fig.3.1). One test pit was opened at each site and disturbed samples were taken from two different depths.i.e.1.5 m and 3.0 m. After extracting, the samples were transported to AAiT Geotechnical laboratory. Then the samples were air dried and sieved with different sieve sizes after pulverizing depending on the test requirement.

Soil remolding for the one dimensional consolidation and triaxial compression (isotropic consolidation) tests were done at OMC (optimum moisture content) and MDD (maximum dry density) with standard compacting effort.

Laboratory tests such as specific gravity, particle size analysis, Atterberge limits, and standard compaction were conducted on disturbed samples. Other tests like one dimensional consolidation tests and triaxial compression (isotropic consolidation) were conducted on samples remolded to MDD and OMC.

The summaries of laboratory test results conducted on these samples are presented below. But the detailed laboratory results are attached in appendix A.

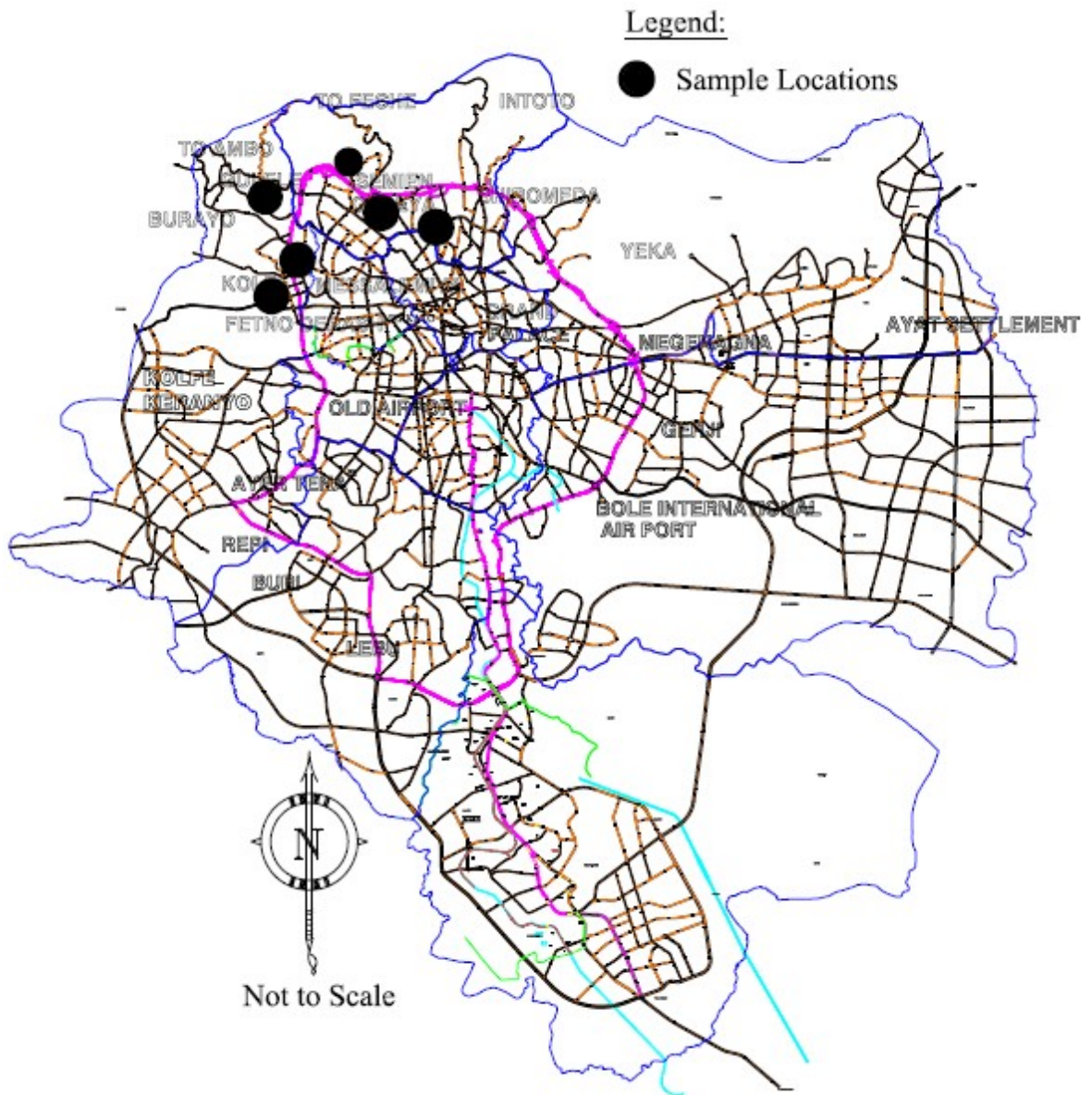


Figure 3.1: Test pit locations.

3.2 Specific Gravity

Test procedure was according to ASTM D 854. Two tests at 1.5 m and 3.0 m are conducted for each six sites. And the results are presented in Tab.3.1.

Table 3.1: Summary of Specific gravity test results

S.No	Site	Sample designation	Depth, m	Specific gravity, Gs
1	Adisu gebeya	TP1-1	1.5	2.73
2		TP1-2	3.0	2.72
3	Atena tera	TP2-1	1.5	2.75
4		TP2-2	3.0	2.76
5	Athari	TP3-1	1.5	2.70
6		TP3-2	3.0	2.71
7	Awelya	TP4-1	1.5	2.76
8		TP4-2	3.0	2.74
9	Kolfe	TP5-1	1.5	2.66
10		TP5-2	3.0	2.74
11	Shegole	TP6-1	1.5	2.74
12		TP6-2	3.0	2.79

3.3 Grain size analysis

To check whether the soil is clay or not, grain size analysis is done on each six sites at a depth of 3.0m. The sample preparation and test procedure was according to ASTM D 421 and ASTM D 422 respectively. Summary of the results are presented Fig.3.2.

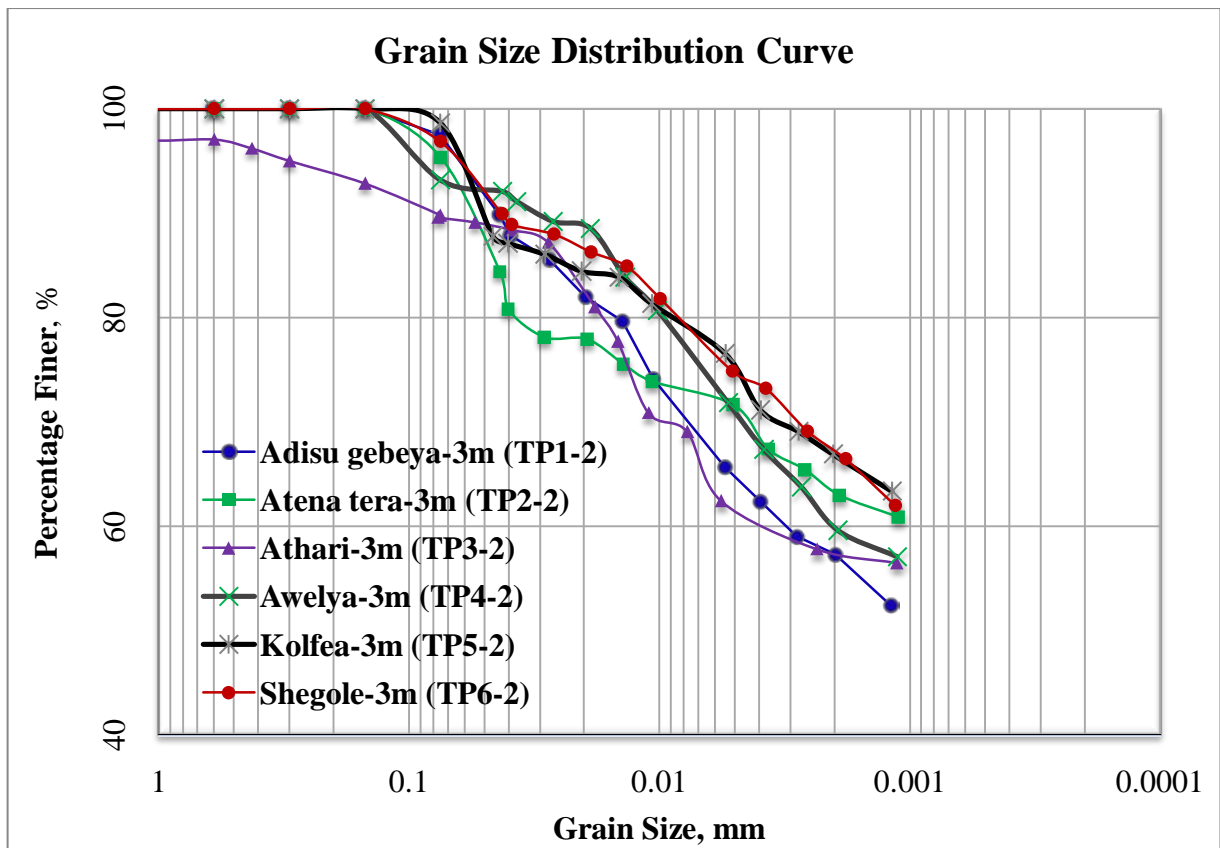


Figure 3.2: Particle Size distribution curves at 3.0 m depth for samples TP1-2, TP2-2, TP3-2, TP4-2, TP5-2 and TP6-2.

Clay fraction is calculated from the grain size analysis by taking the percentage of finer less than 0.005mm size for each test and the results are presented in Tab.3.2.

Table 3.2: Clay fraction

S.No.	Site	Sample designation	Depth (m)	Clay fraction (%)
1	Adisu gebeya	TP1-2	3.0	65.69
2	Atena tera	TP2-2	3.0	71.64
3	Athari	TP3-2	3.0	62.46
4	Awelya	TP4-2	3.0	71.82
5	Kolfe	TP5-2	3.0	76.55
6	Shegole	TP6-2	3.0	74.87

As it is observed from the grain size distribution over 60 % of the material tested consists of clay fraction. The curves do not extend beyond 0.001 mm, since according to ASTM procedure for hydrometer analysis terminate at 24 hrs.

3.4 Atterberge limits

The sample preparation and test procedure is according to ASTM D 421 and ASTM D 4318 respectively. A total of twelve tests, at a depth of 1.5m and 3.0m for each six sites are conducted. The summary of the test results is presented in Table 3.3. The soil is classified Using (USCS) Unified soil classification system (refer Fig. 3.3) below. The detailed test result is attached at appendix A (II).

Table 3.3: Summary of Atterberge Limits test results and soil classification

S.No	Site	Sample designation	Depth (m)	Liquid limit, %	Plastic limit, %	Plasticity index, %	USCS classification
1	Adisu gebeya	TP1-1	1.5	59	31.01	28	CH
2		TP1-2	3.0	59	29.67	29	CH
3	Atena tera	TP2-1	1.5	60	41.16	19	MH
4		TP2-2	3.0	64	43.46	21	MH
5	Athari	TP3-1	1.5	66	36.7	29	MH
6		TP3-2	3.0	70	42.6	27	MH
7	Awelya	TP4-1	1.5	54	29.21	25	CH
8		TP4-2	3.0	51	28.53	22	CH
9	Kolfe	TP5-1	1.5	62	39.02	23	MH
10		TP5-2	3.0	63	39.94	23	MH
11	Shegole	TP6-1	1.5	70	41.145	29	MH
12		TP6-2	3.0	60	41.03	19	MH

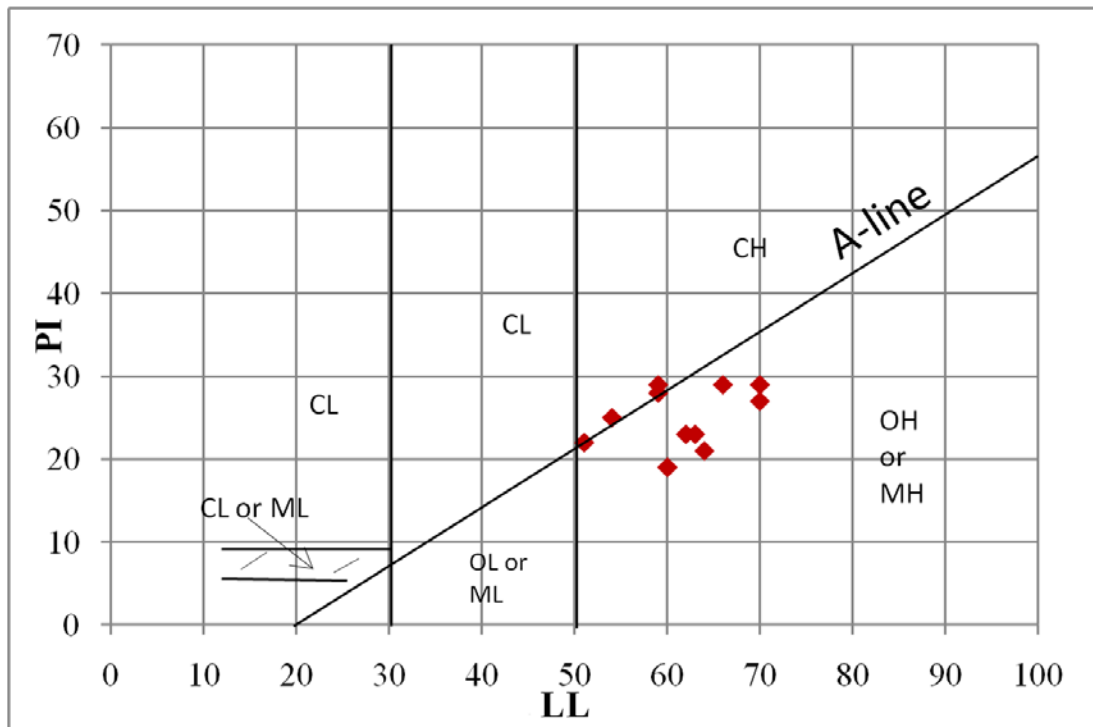


Figure 3.3: Classification of the soil using USCS, plasticity chart [10].

According to USCS classification system, the soils are classified as CH (inorganic clays with high plasticity) and MH (inorganic silts or elastic silts). However, from the percentage of clay fraction; the test results should have been above the A-line. This anomaly had been observed in a number of tests conducted on red clay soils found in Addis Ababa. This raises the question whether the USCS classification is appropriate for these soils.

3.5 Standard compaction

Compaction means pressing the soil particles close to each other by mechanical methods. Air during compaction is expelled from the void space in the soil mass and, therefore, the mass density is increased. Compaction of a soil mass is done to improve its engineering properties. Compaction generally increases the shear strength of the soil, and hence the stability and bearing capacity. It is also useful in reducing the compressibility and permeability of the soil [15].

Two types of compaction tests are routinely performed:

(1) The Standard Proctor Test, and

(2) The Modified Proctor Test.

Each of these tests can be performed in three different methods as outlined in Table 3.4: In the Standard Proctor Test, the soil is compacted by a 5.5 lb hammer falling a distance of one foot into a soil filled mold. The mold is filled with three equal layers of soil, and each layer is subjected to 25 drops of the hammer. The Modified Proctor Test is identical to the Standard Proctor Test except it employs, a 10 lb hammer falling a distance of 18 inches, and uses five equal layers of soil instead of three. There are two types of compaction molds used for testing. The smaller type is 4 inches in diameter and has a volume of about $1/30 \text{ ft}^3$ (944 cm^3), and the larger type is 6 inches in diameter and has a volume of about $1/13.333 \text{ ft}^3$ (2123 cm^3). If the larger mold is used each soil layer must receive 56 blows instead of 25 [16].

Table 3.4: Alternative Proctor Test Methods [16]

	Standard Proctor ASTM 698			Modified Proctor ASTM 1557		
	Method A	Method B	Method C	Method A	Method B	Method C
Material	≤20% Retained on No.4 Sieve	>20% Retained on No.4 ≤20% Retained on 3/8" Sieve	>20% Retained on No.3/8" <30% Retained on 3/4" Sieve	≤20% Retained on No.4 Sieve	>20% Retained on No.4 ≤20% Retained on 3/8" Sieve	>20% Retained on No.3/8" <30% Retained on 3/4" Sieve
For test sample, use soil passing	Sieve No.4	3/8" Sieve	3/4" Sieve	Sieve No.4	3/8" Sieve	3/4" Sieve
Mold size	4"	4"	6"	4"	4"	6"
No. of Layers	3	3	3	5	5	5
No. of blows/layer	25	25	56	25	25	56

Soil placed as engineering fill (embankments, foundation pads, road bases) is compacted to a dense state to obtain satisfactory engineering properties such as, shear strength, compressibility, or permeability. Also, foundation soils are often compacted to improve their engineering properties.

In this thesis standard compaction according to method A is done for all the six sites, Twelve tests (at 1.5m and 3.0m depths each) are conducted. The summary of the test results are presented in Fig.3.4, 3.5 and Table 3.5. The detailed test results are presented in appendix A (III).

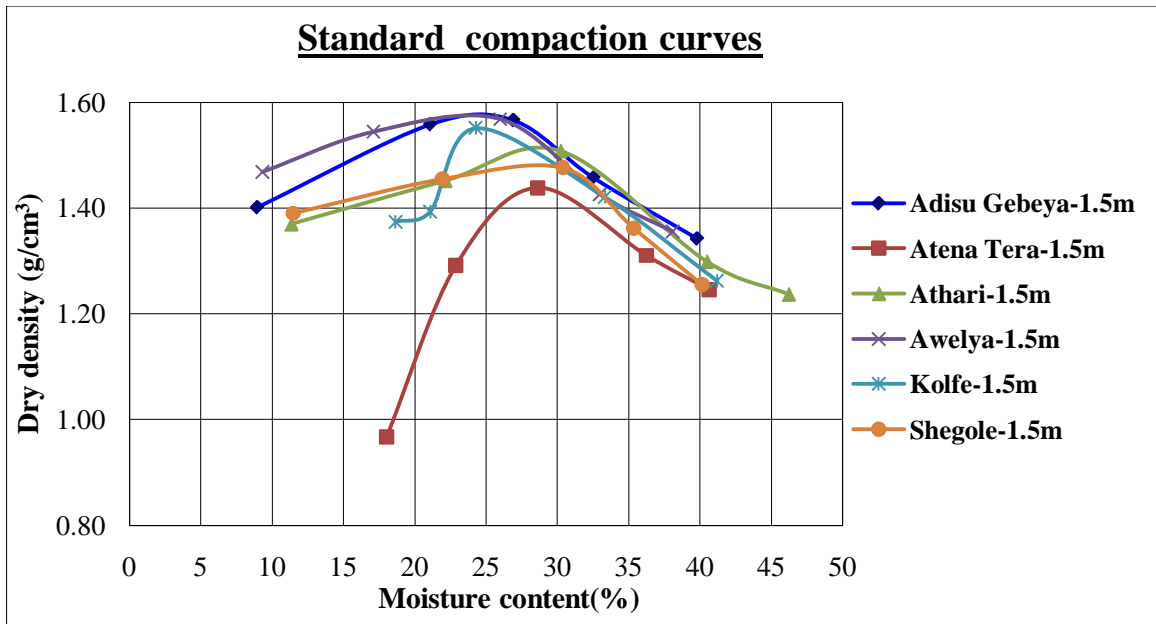


Figure 3.4: Standard compaction curves at 1.5 m depth for samples TP1-1, TP2-1, TP3-1, TP4-1, TP5-1 and TP6-1.

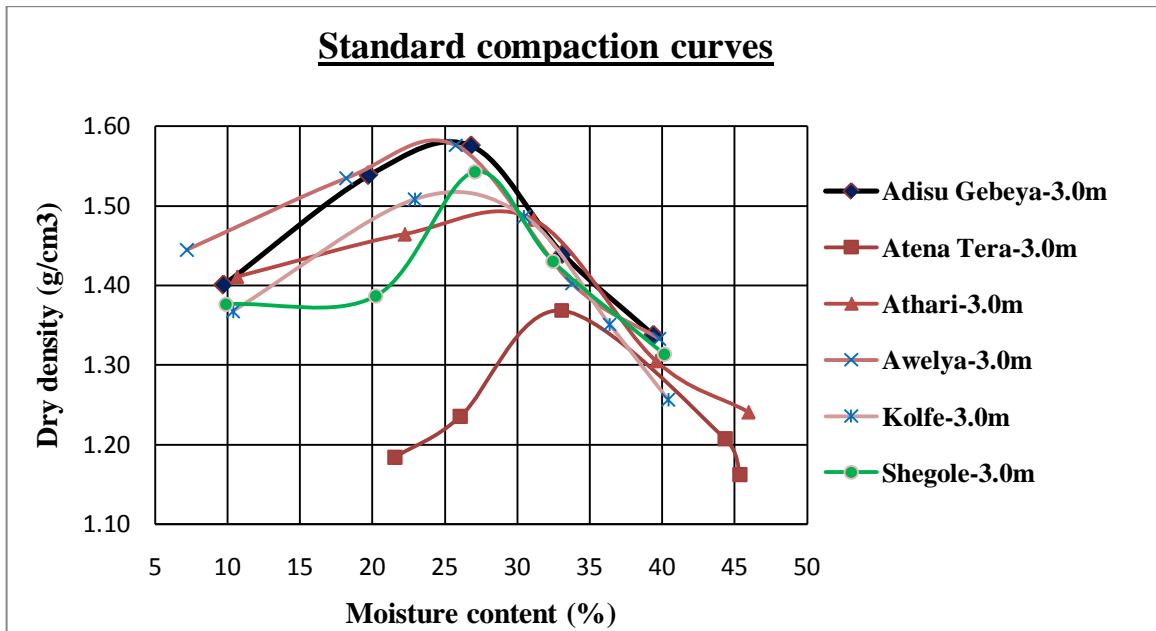


Figure 3.5: Standard compaction curves at 3.0 m depth for samples TP1-2, TP2-2, TP3-2, TP4-2, TP5-2 and TP6-2.

Table 3.5: Summary of standard compaction test results

S.No.	Site	Depth ,m	Sample designation	MDD, g/cm ³	OMC, %
1	Adisu Gebeya	1.5	TP1-1	1.58	25.0
2		3.0	TP1-2	1.58	25.0
3	Atena Tera	1.5	TP2-1	1.44	28.6
4		3.0	TP2-2	1.37	33.06
5	Athari	1.5	TP3-1	1.52	29.0
6		3.0	TP3-2	1.49	29.0
7	Awelya	1.5	TP4-1	1.58	24.0
8		3.0	TP4-2	1.58	24.5
9	Kolfe	1.5	TP5-1	1.55	24.3
10		3.0	TP5-2	1.52	26.0
11	Shegole	1.5	TP6-1	1.48	29.0
12		3.0	TP6-2	1.54	27.1

3.6 One dimensional Consolidation Test

The one dimensional consolidation test is carried out to study the compressibility of the soil using the apparatus called Oedometer. Diameters of 50mm soil samples having height of 20mm were loaded from 50 kPa to 1600 kPa by doubling the loading. For each loading starting from 50 kPa to 1600 kPa the compression was recorded from the dial gage at time intervals of: 0.1, 0.25, 0.5, 1, 2, and 4 ... 1440 minutes.

After remolding the samples to MDD and OMC for all the six sites, twelve oedometer tests (i.e.1.5m and 3.0m depths) are conducted. Then, Compression index (Cc), which is used in developing correlations with index properties, and pre consolidation pressure (Pc) are determined.

ASTM D 2435 procedure is followed while carrying out the tests. The summary of compression index (C_c), pre consolidation pressure (P_c) results for each site is given in Fig.3.6, 3.7, Tab. 3.6. and Tab. 3.7. The detailed test result is presented in appendix A (IV).

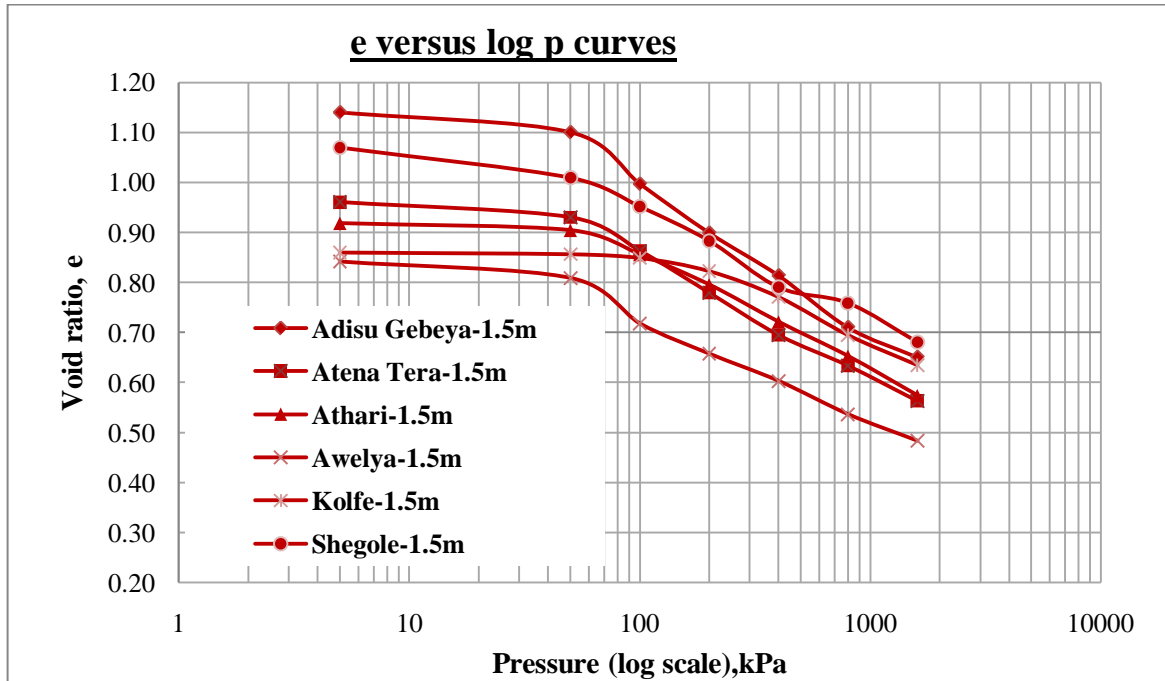


Figure 3.6: e versus log p curves at 1.5 m depth for samples TP1-1, TP2-1, TP3-1, TP4-1, TP5-1 and TP6-1.

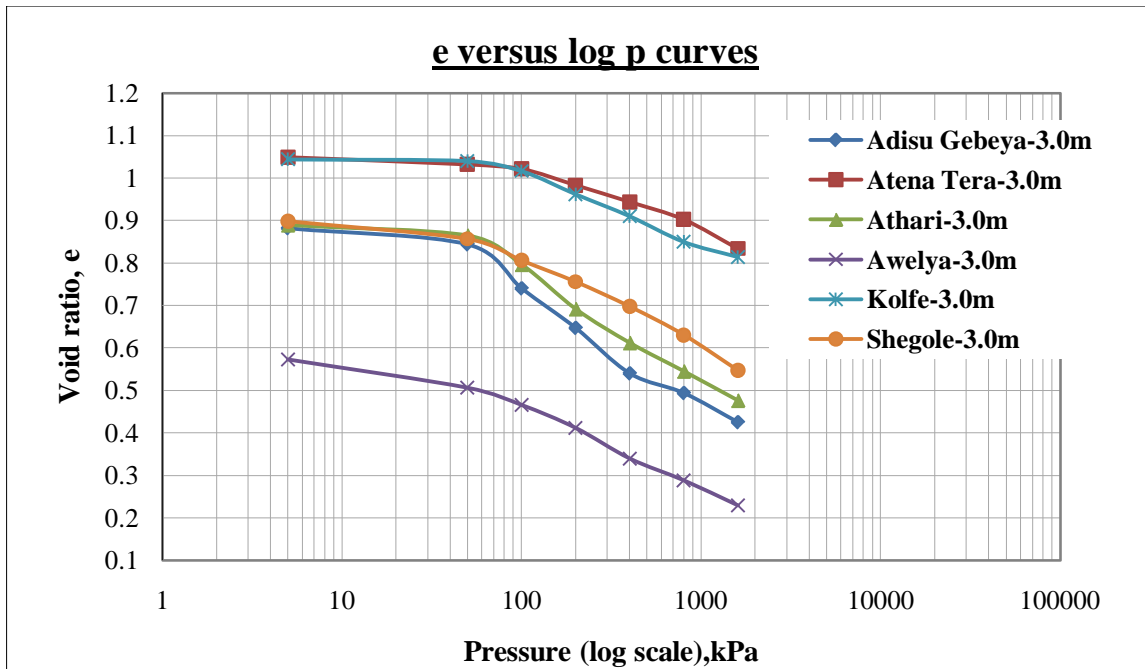


Figure 3.7: e versus log p curves at 3.0 m depth for samples TP1-2, TP2-2, TP3-2, TP4-2, TP5-2 and TP6-2.

Table 3.6: Summary of compression index, C_c test results

S.No.	Site	Depth ,m	Sample designation	C_c
1	Adisu Gebeya	1.5	TP1-1	0.199
2		3.0	TP1-2	0.191
3	Atena Tera	1.5	TP2-1	0.203
4		3.0	TP2-2	0.227
5	Athari	1.5	TP3-1	0.209
6		3.0	TP3-2	0.225
7	Awelya	1.5	TP4-1	0.176
8		3.0	TP4-2	0.180
9	Kolfe	1.5	TP5-1	0.199
10		3.0	TP5-2	0.186
11	Shegole	1.5	TP6-1	0.209
12		3.0	TP6-2	0.180

From the test result it is observed that, compression index (C_c) decreases with an increase in MDD and vice versa.

Table 3.7: Summary of pre consolidation pressure (P_c) test results

S.No.	Site	Depth ,m	Sample designation	P_C (kPa)
1	Adisu Gebeya	3.0	TP1-2	60
2	Atena Tera	3.0	TP2-2	260
3	Athari	3.0	TP3-2	70
4	Awelya	3.0	TP4-2	100
5	Kolfe	3.0	TP5-2	75
6	Shegole	3.0	TP6-2	160

In this study, the pre consolidation pressure (P_c) is the compaction effort while remolding the sample to its MDD and OMC.

3.7 Triaxial compression test (isotropic consolidation)

Consolidation characteristics and the permeability of a soil specimen (undisturbed or reconstituted) can be measured in a triaxial cell. In isotropic condition of triaxial consolidation, where, the specimen is subjected to increments of equal all –round pressures ($\sigma_1 = \sigma_2 = \sigma_3$), the specimen consolidate laterally as well as vertically. In this study, the initial all round pressure applied exceeds the pre consolidation pressure (Table.3.7). The all round confining pressure is applied in increments, each of which is held constant until virtually all the excess pore pressure due to those increments is dissipated. Similarly, three or more increments of pressure are applied to provide three or more stages of consolidation. Each stage is carried out in two phases [6].

(I) The undrained phase, in which the cell confining pressure is increased so that it exceeds the back pressure by an amount equal to the desired effective stress for consolidation, causing the pore pressure to build up and eventually reach a steady value;

(2) The drained phase, in which this excess pore pressure is allowed to dissipate against the back pressure until the pressures virtually equalize (consolidation).



Figure 3.8: Triaxial compression machine.

During the consolidation process, water drains out from one end of the specimen (usually the top), and the volume of expelled water is measured; this is equal to the change in volume of a saturated specimen. Readings of volume change and pore pressure are recorded at suitable intervals of time to enable consolidation curves to be drawn. The relationship between voids ratio and effective isotropic stress can be derived from a series of incremental loadings. Finally from specific volume (ν) versus mean effective stress ($\ln p'$) curve, Γ And λ are determined.

For all six sites, triaxial tests are conducted on samples retrieved at the depth of 3.0m. The summary of the test results are presented Tab. 3.7. The detailed test results and calculations are presented in the appendix-A (V).

Table 3.8: Summary of triaxial test result for different locations

S.N.	Site	Depth ,m	Sample designation	Lambda, λ	Capital gamma, Γ
1	Adisu gebeya	3.0	TP1-2	0.0856	2.2503
2	Atena tera	3.0	TP2-2	0.0749	2.4197
3	Athari	3.0	TP3-2	0.0719	2.2182
4	Awelya	3.0	TP4-2	0.0700	2.1187
5	Kolfe	3.0	TP5-2	0.1036	2.3718
6	Shegole	3.0	TP6-2	0.1052	2.4178

Chapter 4

Regression analysis

4.1. General

Regression analysis is concerned with how the values of Y depend on the corresponding values of X. Y, whose value is to be predicted, is known as dependent variable or response and X, which is used in predicting the value of dependent variable, is called independent or regressor variable. A regression model that contains more than one regressor variable is called multiple regression models. Alternatively, Regression model containing one independent variable or regressor is termed as simple regression model.

Fitting a regression model requires several assumptions. Estimation of the model parameters requires the assumption that, the residuals (actual values less estimated values) corresponding to different observations are uncorrelated random variables with zero mean and constant variance. Tests of hypotheses and interval estimation require that the errors be normally distributed. In addition, one assumes that the order of the model is correct; that is, if one fits a simple linear regression model, one is assuming that the phenomenon actually behaves in a linear or first order manner [5]. During regression analysis, a regression model with higher value of R^2 (coefficient of determination), which quantifies the proportion of the variance of one variable by the other, is usually accepted.

In this study, compression index (λ) and capital gamma (Γ) are the dependent variables where as the LL, PL, and PI are regressor variables. To carry out statistical analysis, Microsoft® excel were used. A total of twelve numbers of samples are used in correlating λ with LL, PL, and PI and six numbers of samples are used in correlating Γ with LL, PL, and PI. While caring out the statistical analysis different regression models are used and those models with a higher value of coefficient of determination are accepted.

4.2 Scatter Plot

In developing correlations, the first step is creating a scatter plot of the data, to visually assess the strength and form of the relationship. In the figures below (Figure 4.1-4.5) the scatter plot of λ with LL, PL, and PI and Γ with LL, PL, and PI are presented.

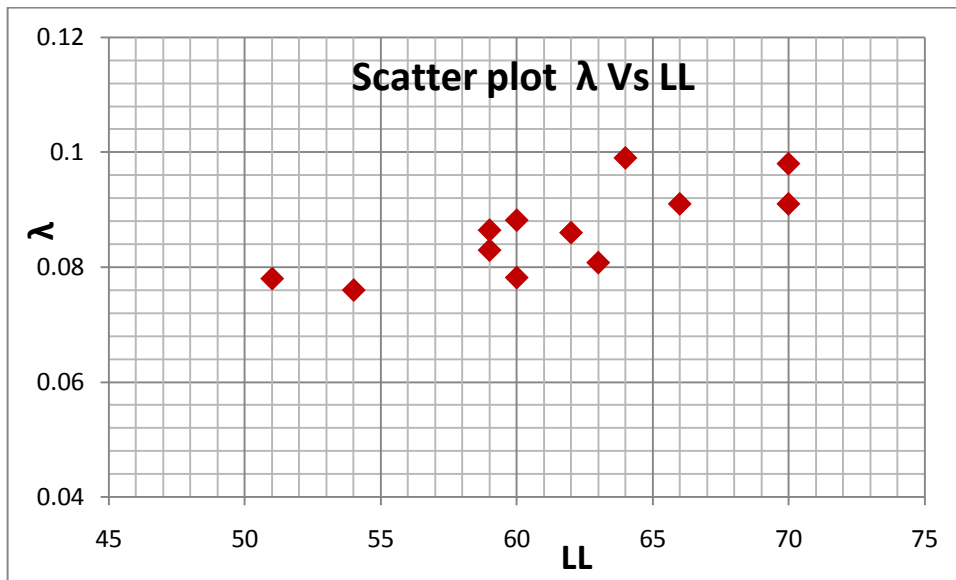


Figure 4.1: Scatter plot of λ versus LL.

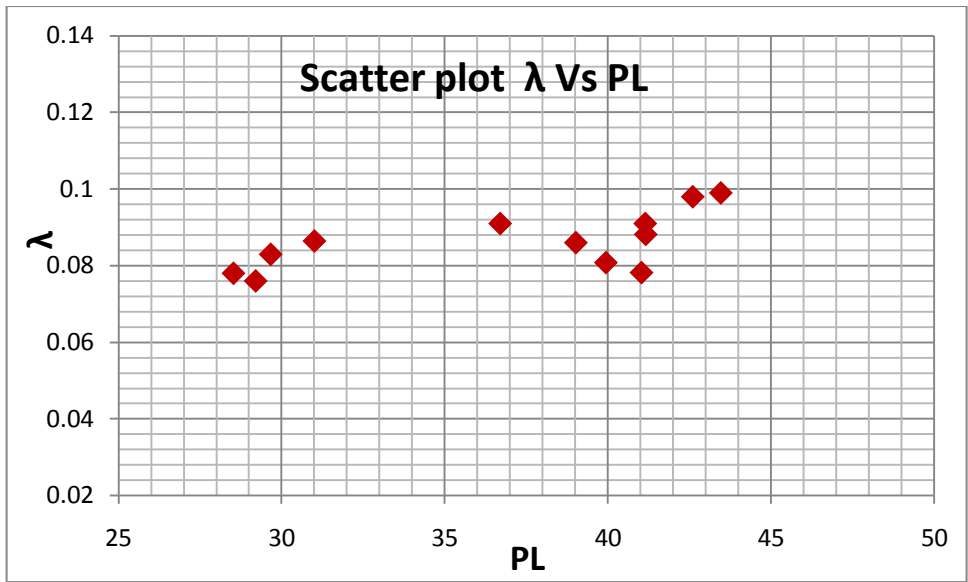


Figure 4.2: Scatter plot of λ versus PL.

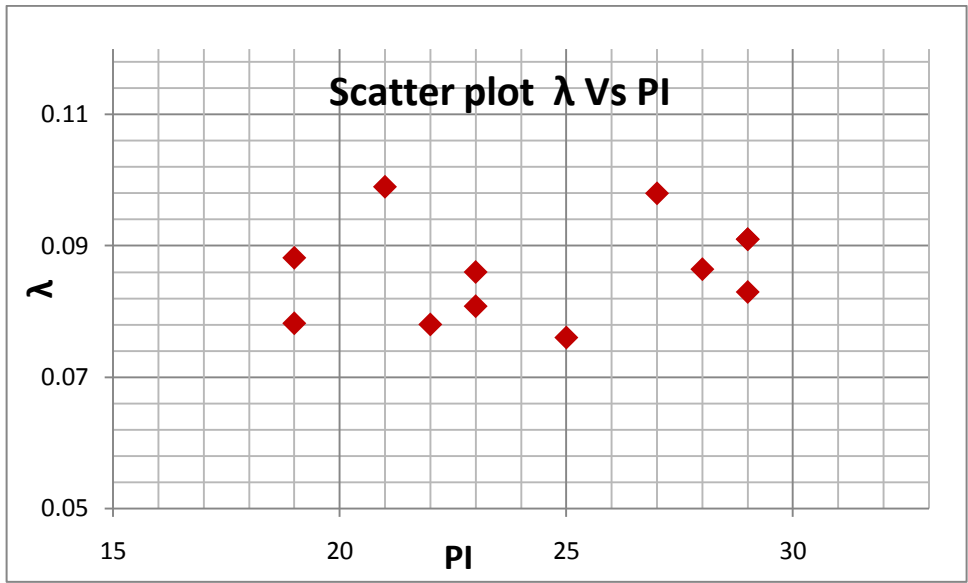


Figure 4.3: Scatter plot of λ versus PI.

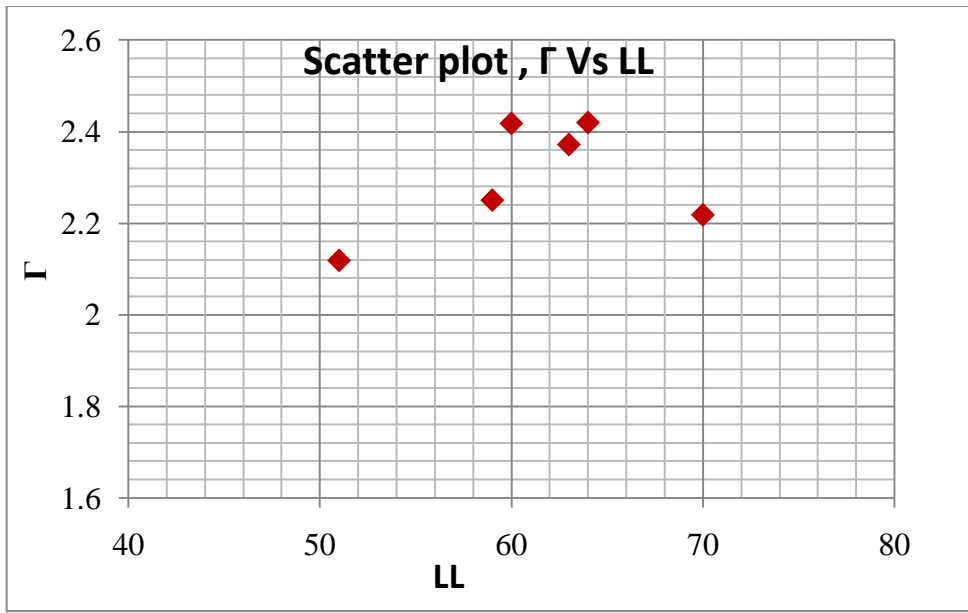


Figure 4.4: Scatter plot of Γ versus LL.

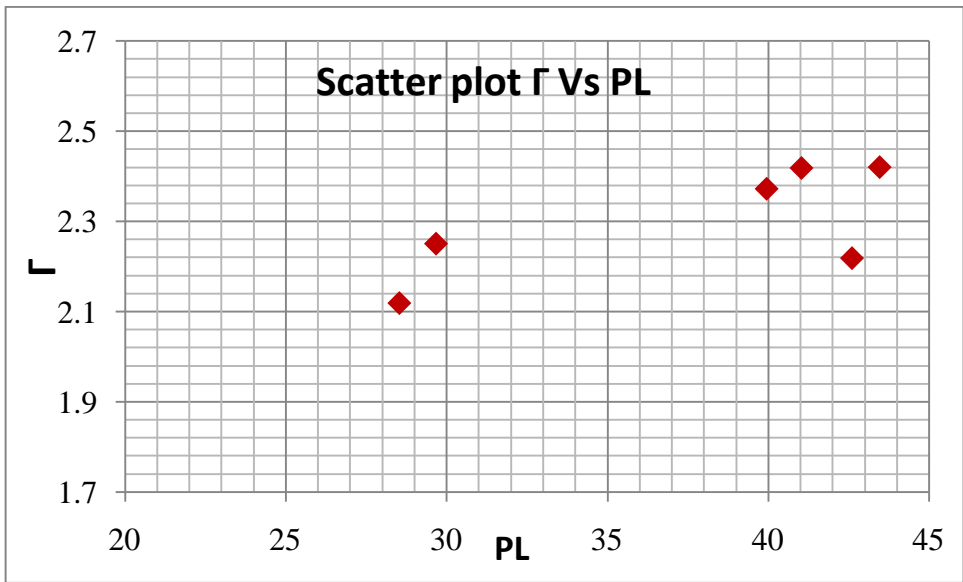


Figure 4.5: Scatter plot of Γ versus PL.

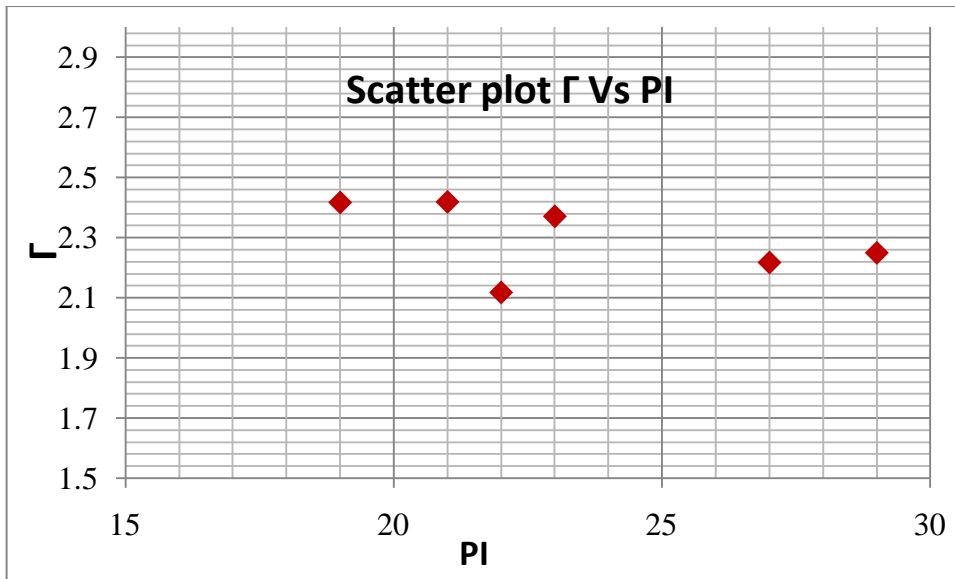


Figure 4.6: Scatter plot of Γ versus PI.

The available test points are not sufficient to give reliable relationships between the independent and dependent variables. Nevertheless different models (linear and non-linear) have been employed to examine the trend of the scatter.

4.3. Correlation between λ and LL, PL and PI

A linear model is used. The correlation coefficient with least standard error is considered, and the following relationships are found:

$$\lambda = 0.001LL + 0.023 \quad R^2 = 0.596 \quad , \quad n = 12$$

$$\lambda = 0.0008PL + 0.056 \quad R^2 = 0.394 \quad , \quad n = 12$$

$$\lambda = 0.0004PI + 0.076 \quad R^2 = 0.05 \quad , \quad n = 12$$

4.4. Correlation between Γ and LL, PL and PI

Linear and non-linear models are used .The correlation coefficient with least standard error is considered, and the following relationships are found:

$$\Gamma = -0.0022LL^2 + 0.27LL - 6.055 \quad R^2 = 0.777 \quad , \quad n = 6$$

$$\Gamma = 0.013PL + 1.81 \quad R^2 = 0.504 \quad , \quad n = 6$$

$$\Gamma = 0.0035PI^2 - 0.187PI + 4.7 \quad R^2 = 0.335 \quad , \quad n = 6$$

Table 4.1: Summary of the regression analysis

S.No.	Model equation	R^2 (coefficient of determination)	No. of samples , n
1	$\lambda = 0.001LL + 0.023$	0.596	12
2	$\lambda = 0.0008PL + 0.056$	0.394	12
3	$\lambda = 0.0004PI + 0.076$	0.05	12
4	$\Gamma = -0.0022LL^2 + 0.27LL - 6.055$	0.777	6
5	$\Gamma = 0.013PL + 1.81$	0.504	6
6	$\Gamma = 0.0035PI^2 - 0.187PI + 4.7$	0.335	6

4.5 Comparison of λ from Oedometer and Triaxial Tests

The value of λ can be determined from Oedometer using the relation shown below [7]. From triaxial test, it is the slope of the line in ν versus $\ln p$ plot.

$$\lambda = \frac{C_c}{2.303}$$

In this study the value of λ found from Oedometer and triaxial tests are almost similar as it is shown in Tab.4.2 below.

Table 4.2: Comparison of value of λ from Oedometer and Triaxial test

S.No.	Site	Depth ,m	Sample designation	Lambda (λ) from oedometer test	Lambda (λ) from triaxial test
1	Adisu gebeya	1.5	TP1-1	0.086	*
2		3.0	TP1-2	0.083	0.0856
3	Atena tera	1.5	TP2-1	0.088	*
4		3.0	TP2-2	0.099	0.0749
5	Athari	1.5	TP3-1	0.091	*
6		3.0	TP3-2	0.098	0.0719
7	Awelya	1.5	TP4-1	0.076	*
8		3.0	TP4-2	0.078	0.0700
9	Kolfe	1.5	TP5-1	0.086	*
10		3.0	TP5-2	0.081	0.1036
11	Shegole	1.5	TP6-1	0.091	*
12		3.0	TP6-2	0.078	0.1052

N.B: * the test is not conducted

Chapter 5

Discussion of test results

The main objective of this study is to develop a model that will allow the prediction of lambda (λ) and capital gamma (Γ) from index test results. The predicted values of λ and Γ depend on the test results.

One dimensional consolidation was done on twelve test samples at loading intensities of 50kPa to 1600kPa. The value of coefficient of compressibility (C_c) ranges from 0.176 to 0.227. The triaxial test also conducted on six remolded soil samples by varying the loading intensities from 300kPa to 780kPa. The value of capital gamma is between 2.1187 and 2.4197. Coefficient of compressibility (C_c) and capital gamma (Γ) values are found to be relatively lower than those obtained for undisturbed soil samples by Jibril [9] as indicated in Table 5.1 and 5.2. The difference arise due to the fact that within the framework of this research, the tests are conducted on remolded soil samples at their Maximum Dry Density and Optimum Moisture Content. The standard compaction test result for the site of Atena Tera at 1.5m depth is found different from the other all sites. Similar result also observed for the same site at 3.0m depth.

The values of lambda (λ) from Oedometer tests on twelve soil samples, varie from 0.076 to 0.099 and from triaxial tests conducted on six soil samples varie from 0.07 to 0.1052. Thus showing that, the values of lambda from Oedometer and triaxial tests are almost similar.

The statistical analysis shows that there is a relatively good correlation between the independent variables (LL, PL and PI) and the dependent variables (Γ , λ). But, Poor correlation is observed between λ and PI. The developed correlations generally show that liquid limit, plastic limit, and plasticity index of soil affect the compression of soil behavior.

A reliable equation for the practice could not be established because the number of test samples was not adequate. More tests could not be conducted due to mechanical problems associated

with the existing equipment. This study however, indicates the existence of a relatively good correlation between index properties (LL, PL and PI) and critical state soil parameters (λ and Γ).

Table 5.1: Values of compression index (C_c) for undisturbed red clay soils of Addis Ababa [9]

S.No.	Name of locality	Test pit	Depth (m)	C_c
1	Addisu Gebeya (Gulele sub-city)	1	1.5	0.183
			2.5	0.219
2	Alem Tsehay Dildy (Gulele sub-city)	1	2.0	0.236
			3.0	0.173
3	Atari (Gulele sub-city)	1	2.0	0.186
			3.0	0.174
4	Kalae (Kolfе sub-city)	1	1.5	0.176
			2.5	0.146
5	Kolfе (Kolfе sub-city)	1	2.0	0.226
			3.0	0.189
6	Shogele (Gulele sub-city)	1	1.0	0.193
			3.0	0.262
7	Traffic seffer (Kolfе sub-city)	1	2.0	0.179
			3.0	0.229
8	Rufael (Gulele sub-city)	1	2.0	0.182
			3.0	0.196
9	Semen Mazegaja (Gulele sub-city)	1	1.5	0.143
			2.5	0.159
10	Asko (Kolfе sub-city)	1	2.0	0.199
			3.0	0.252

Table 5.2: Values of capital gamma (Γ) for undisturbed red clay soils of Addis Ababa [9]

S. No.	Name of locality	Depth (m)	Capital gamma
1	Alem Tsehay dildy (Gulele sub-city)	3.0	2.256
2	Atari (Gulele sub-city)	3.0	2.558
3	Kalae (Kolfe sub-city)	2.5	2.129
4	Kolfe (Kolfe sub-city)	2.0	2.525
5	Shogole (Gulele sub-city)	1.0	2.434
6	Traffic Seffer (Kolfe sub-city)	2.0	2.285
7	Semen Mazegaja (Gulele sub-city)	1.5	1.927
8	Asko (Kolfe sub-city)	3.0	2.572

Chapter 6

Conclusions and Recommendations

6.1. Conclusions

- From the statistical analysis, one observes a relatively good indicative correlation between Γ and liquid limit (LL), Γ and plastic limit (PL) and Γ and plasticity index (PI). A similar trend is observed between λ and liquid limit (LL) and λ and plastic limit (PL).
- From the developed correlations one would be in a position to determine the critical state soil parameters from the index properties for Remolded Red Clay Soils of Addis Ababa.

6.2. Recommendations

- In this research it is observed that, there is a relationship between critical state soil parameters and index properties for remolded red clay soils of Addis Ababa. To get reliable correlation it is necessary to increase the number of test samples and also the coverage of sites in Addis Ababa where red clay is found.
- In this research, the soil is remolded according to the standard compaction test by considering its applicability to the construction of low to medium traffic roads and small story buildings in the city. For high intensity loads such as high traffic roads and high rise buildings, one should conduct the investigation by remolding the soil according to the modified compaction test.

References

- [1] Schofield, A. and Wroth, P. (1968). *Critical State Soil Mechanics*. Mc Graw – Hill.
- [2] Getaneh Weldemedhin. (2010). *A study on shear strength characteristics of Addis Ababa red clay soil for unsaturated case*. A thesis presented to School of Graduate Studies, Addis Ababa University.
- [3] Chen F.H. (1975). *Foundations on Expansive Soils*. Elsevier Science Publishers, Amsterdam.
- [4] Bowles, J. E. (1984). *Physical and Geo-Technical properties of soils*. The McGraw-Hill Companies, New York.
- [5] Douglas C. M. and George C. Runger, *Applied Statistics and Probability for Engineers*, John Wiley & Sons, Inc.USA,third edition ,2003
- [6] Head K.H. (1998). *Manual of Soil Laboratory Testing, V.3,Effective Stress Tests, Second Edition*.
- [7] Budhu, M. (2000). *Soil Mechanics & Foundations*. New York, NY: John Wiley & Sons, Inc.
- [8] Bankole, A. (1996). *Critical State Behaviour of an Agriculatural Soil*. Ph.D. Thesis Submitted to College of Graduate Studies and Research, Saskatchewan University, Agricultural & Bio resource Engineering Department, Canada.
- [9] Jibril Jemal. (2011). *Correlation between critical state soil parameters and index properties of undisturbed red clay soils in Addis Ababa*. A thesis presented to School of Graduate Studies, Addis Ababa University.
- [10] ASTM (2004). *Standard Test Method for Soil and Rock*, Annual Book of ASTM Standards, Philadelphia, U.S.A.

- [11] Merihun Lukas. (2010). *A Study on the Effect of Remolding on the Mechanical Behavior of Addis Ababa Red Clay Soils*. M.Sc. Thesis Presented to School of Graduate Studies, Addis Ababa University, Civil Engineering Department, Addis Ababa.
- [12] Das, B.M (1997), *Advanced Soil Mechanics*, Taylor and Francis, USA.
- [13] Alemayehu Teferra. and Mesfin Leikun, (1999). *Soil Mechanics*, AAU. Printing Press, Addis Ababa.
- [14] Atkinson, J. and Bransby, P.(1982). *An Introduction to Critical State Soil Mechanics*. United Kingdom, UK: McGraw-HILL Book Company.
- [15] Arora, K.R., *Soil Mechanics and Foundation Engineering*, Standard publishers and distributors, Delhi, 1997.
- [16] Krishna, R., *Engineering Properties of Soils Based on Laboratory Testing*, UIC.
- [17] Samuel Taddese. (1989). Investigation into Some of the Engineering Properties of Addis Ababa Red Clay Soil. M.Sc. Thesis Presented to School of Graduate Studies, Addis Ababa University, Civil Engineering Department, Addis Ababa.

Appendix –A:
(Laboratory Test Results)

The various laboratory experimental tests that were performed on the soil samples were recorded and presented as follows.

I. Grain size analysis test Results

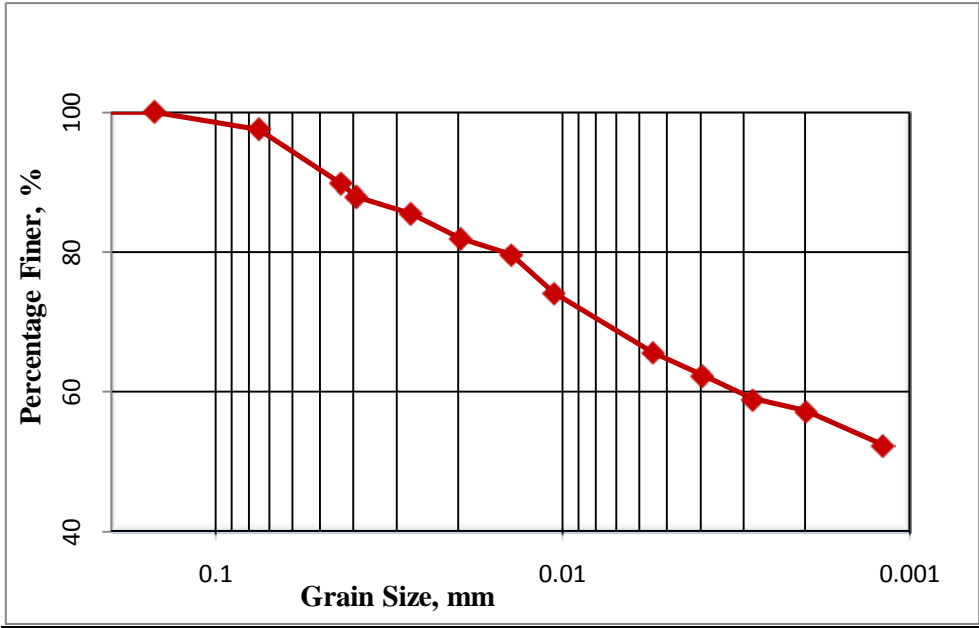


Figure AI-1: Particle Size distribution curve for Addisu gebeya site, sample TP1-2.

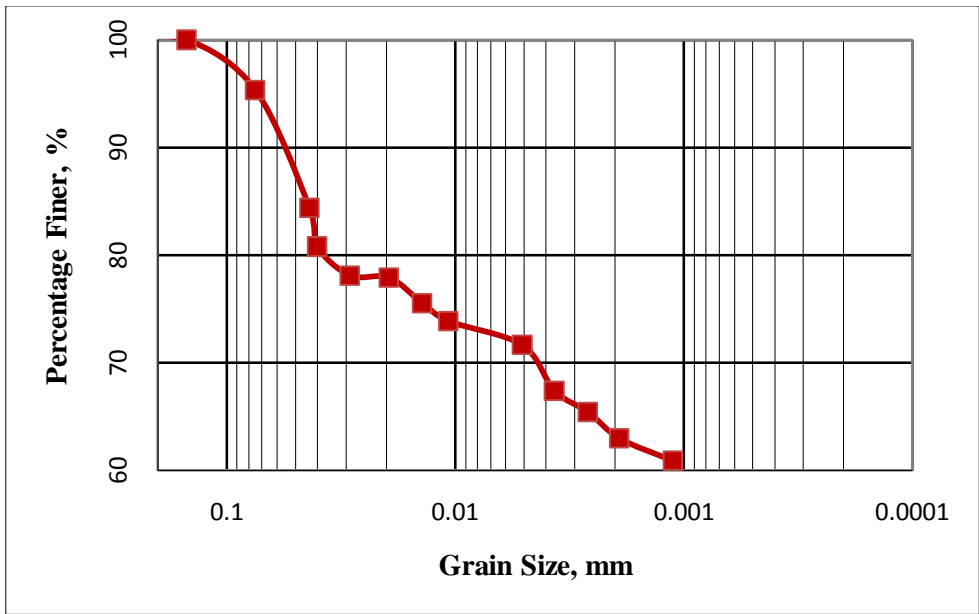


Figure AI-2: Particle Size distribution curve for Atena Tera site, sample TP2-2.

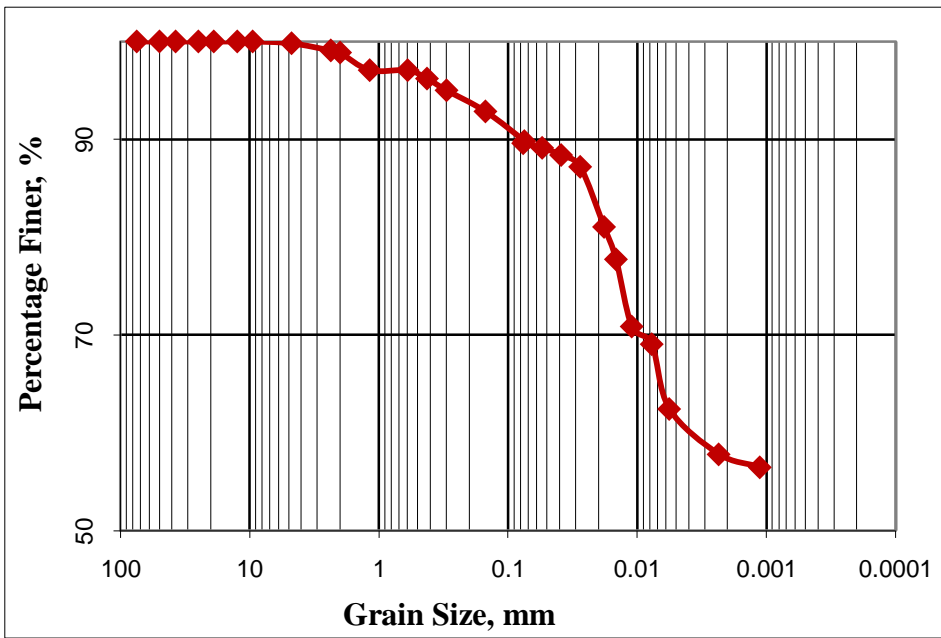


Figure AI-3: Particle Size distribution curve for Athari site, sample TP3-2.

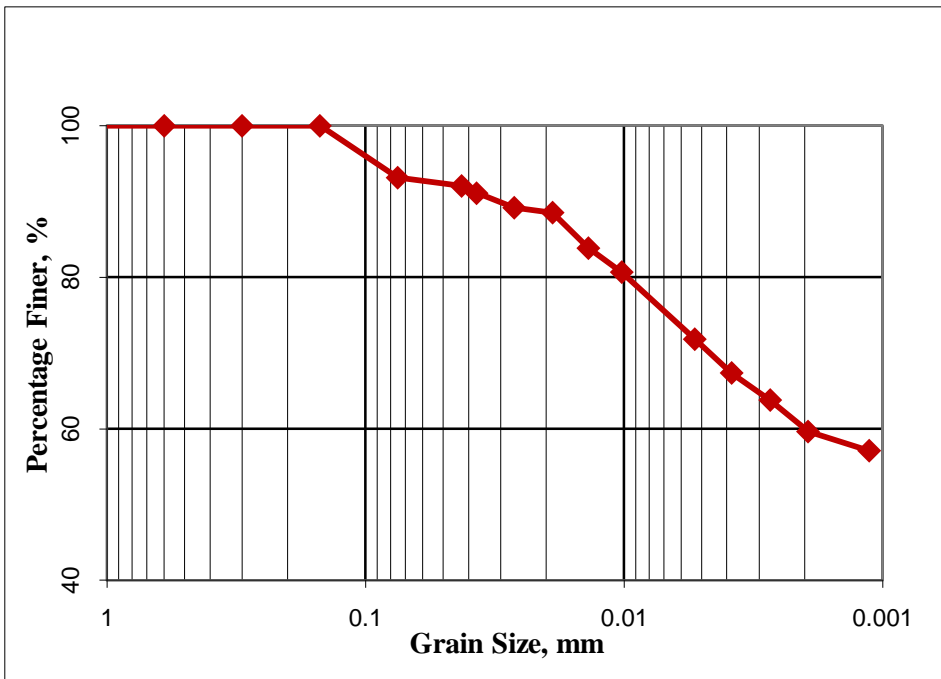


Figure AI-4: Particle Size distribution curve for Awelya site, sample TP4-2.

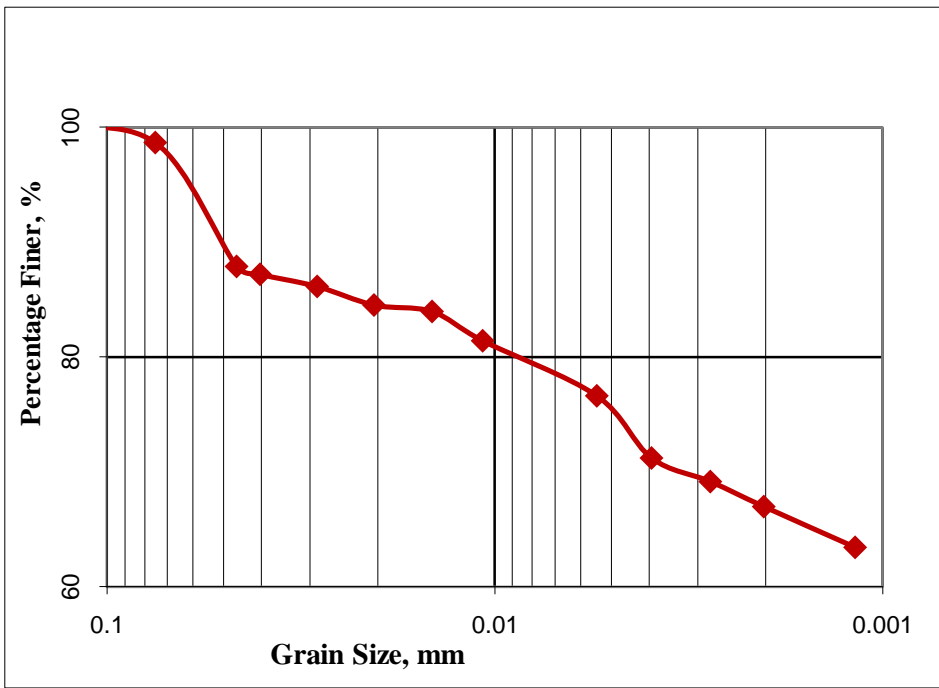


Figure AI-5: Particle Size distribution curve for Kolfe site, sample TP5-2.

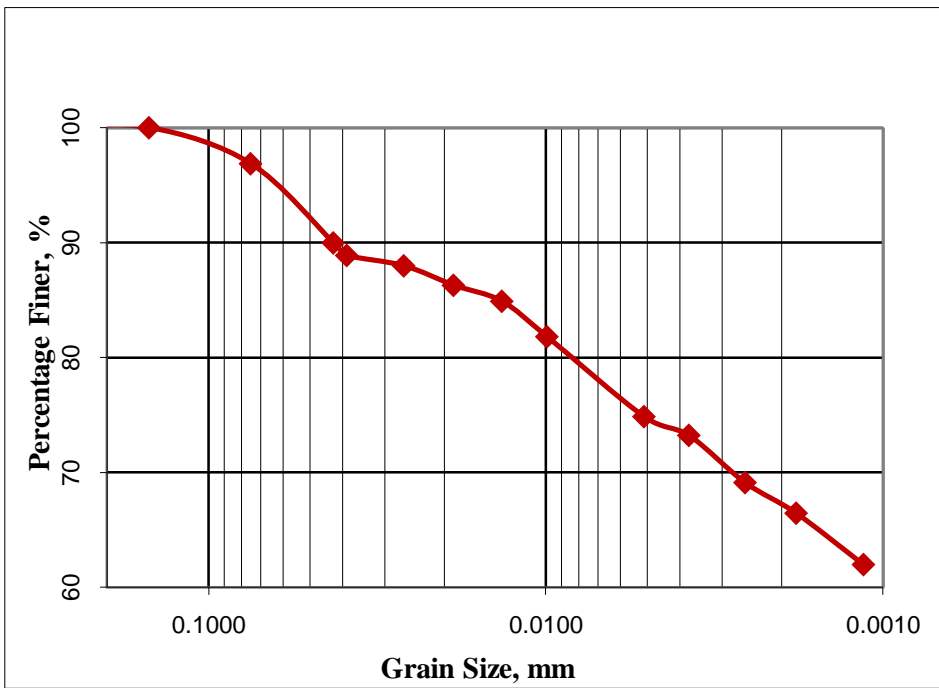


Figure AI-6: Particle Size distribution curve for Shegole site, sample TP6-2.

II. Atterberge limits test Results

Table AII-1: Liquid limit and plastic limit test result analysis for TP-1-1

Trial No	Liquid Limit				Plastic Limit		
	1	2	3	4	1	2	3
Container No	D5	2	D22	GHI	C8	12	47
Mass of container, g	15.69	15.65	15.75	15.59	13.69	15.88	15.68
Mass of container + Wet soil, g	45.24	50.39	41.43	42.59	18.82	20.92	21.05
Mass of container + Dry soil, g	34.24	36.75	31.98	32.59	17.59	19.72	19.80
Mass of water, g	11.00	13.65	9.46	10.00	1.23	1.20	1.24
Mass of dry soil, g	18.55	21.10	16.23	17.00	3.89	3.84	4.12
Water content, %	59.33	64.68	58.26	58.80	31.61	31.30	30.12
No of blows	21	16	28	24	-----	-----	-----

Liquid Limit, % = 59 Plastic Limit, % = 31.0114 PI, % = 28

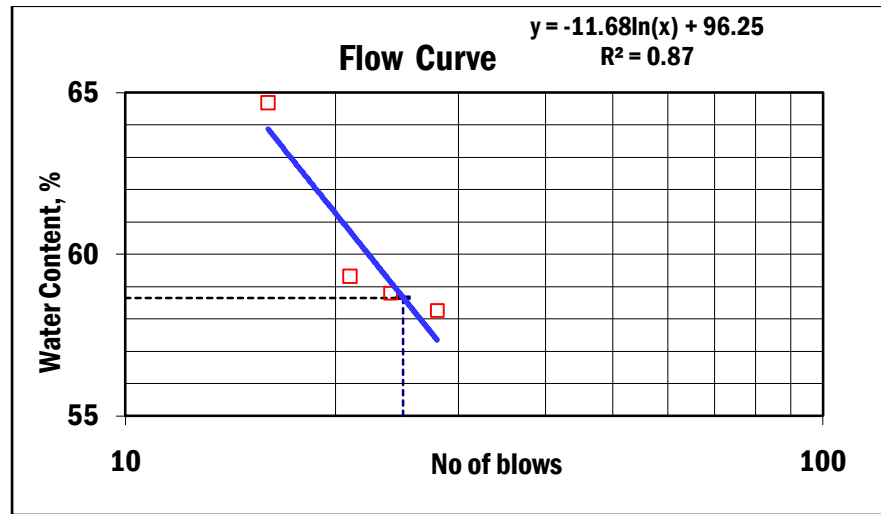


Figure AII-1: Flow curve analysis for TP1-1.

Table AII-2: Liquid limit and plastic limit test result analysis for TP-1-2

Trial No	Liquid Limit				Plastic Limit		
	1	2	3	4	1	2	3
Container No	C-13	A2	A-1	D-23	C31	D25	70
Mass of container, g	14.29	15.65	11.50	15.37	14.06	15.88	15.73
Mass of container + Wet soil, g	47.06	41.29	48.01	54.39	20.12	19.28	21.32
Mass of container + Dry soil, g	34.75	31.82	33.73	40.10	18.74	18.48	20.06
Mass of water, g	12.30	9.47	14.28	14.29	1.37	0.80	1.26
Mass of dry soil, g	20.46	16.17	22.23	24.73	4.68	2.60	4.33
Water content, %	60.12	58.57	64.24	57.79	29.32	30.66	29.03
No of blows	20	26	16	28	-----	-----	-----

Liquid Limit, % = 59 Plastic Limit, % = 29.6695 PI, % = 29

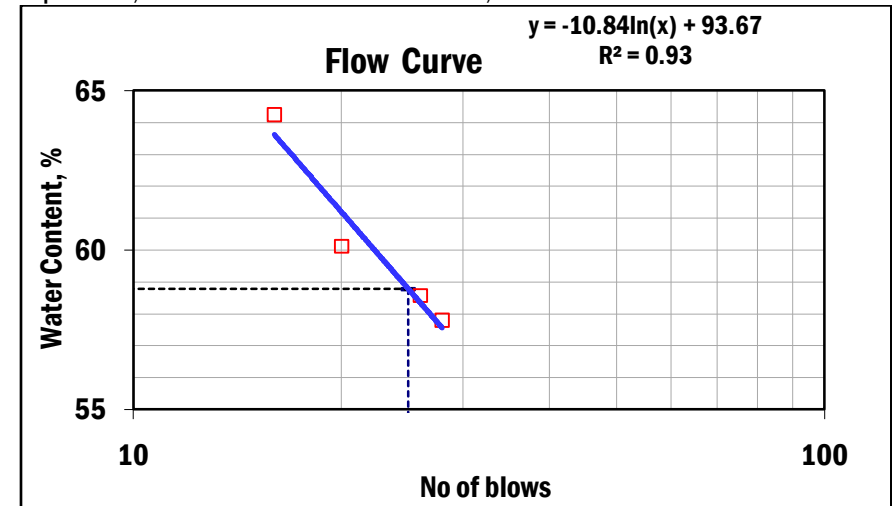


Figure AII-2: Flow curve analysis for TP1-2.

Table AII-3: Liquid limit and plastic limit test result analysis for TP-2-1

Trial No	Liquid Limit				Plastic Limit	
	1	2	3	4	1	2
Container No	E2	5.2	2.1	D20	D4	B1
Mass of container, g	15.67	15.57	15.63	15.50	15.98	15.96
Mass of container + Wet soil, g	47.11	42.18	40.65	33.46	20.25	22.36
Mass of container + Dry soil, g	34.76	31.96	31.58	26.91	19.00	20.50
Mass of water, g	12.35	10.22	9.07	6.55	1.25	1.86
Mass of dry soil, g	19.09	16.39	15.95	11.41	3.02	4.54
Water content, %	64.69	62.33	56.87	57.46	41.37	40.95
No of blows	15	24	34	26	-----	-----

Liquid Limit, % = 60 Plastic Limit, % = 41.16 PI, % = 19

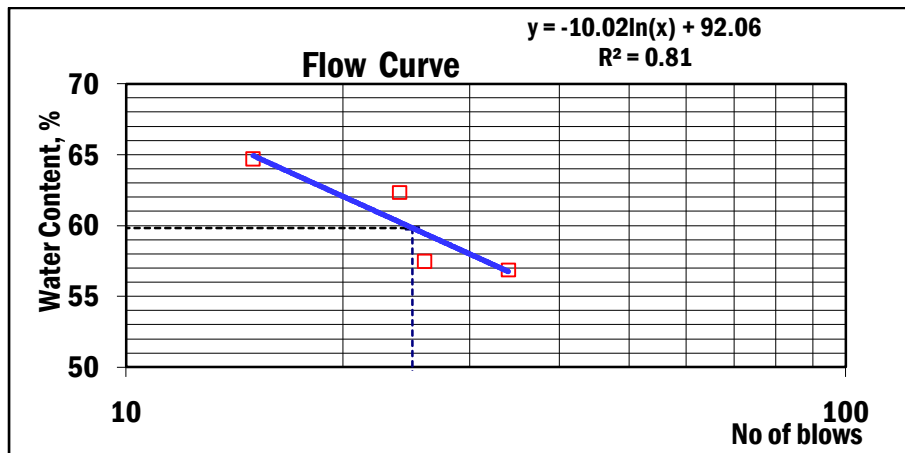


Figure AII-3: Flow curve analysis for TP2-1.

Table AII-4: Liquid limit and plastic limit test result analysis for TP-2-2

Trial No	Liquid Limit				Plastic Limit	
	1	2	3	4	1	2
Container No	E1	E3	22	54	C18	D5
Mass of container, g	15.63	15.83	15.55	15.88	13.62	15.86
Mass of container + Wet soil, g	44.31	41.11	46.45	46.79	17.58	20.34
Mass of container + Dry soil, g	33.27	31.21	33.96	34.36	16.38	18.98
Mass of water, g	11.04	9.90	12.49	12.43	1.20	1.36
Mass of dry soil, g	17.64	15.39	18.41	18.48	2.76	3.12
Water content, %	62.58	64.34	67.87	67.25	43.32	43.59
No of blows	28	23	18	16	-----	-----

Liquid Limit, % = 64 Plastic Limit, % = 43.46 PI, % = 21

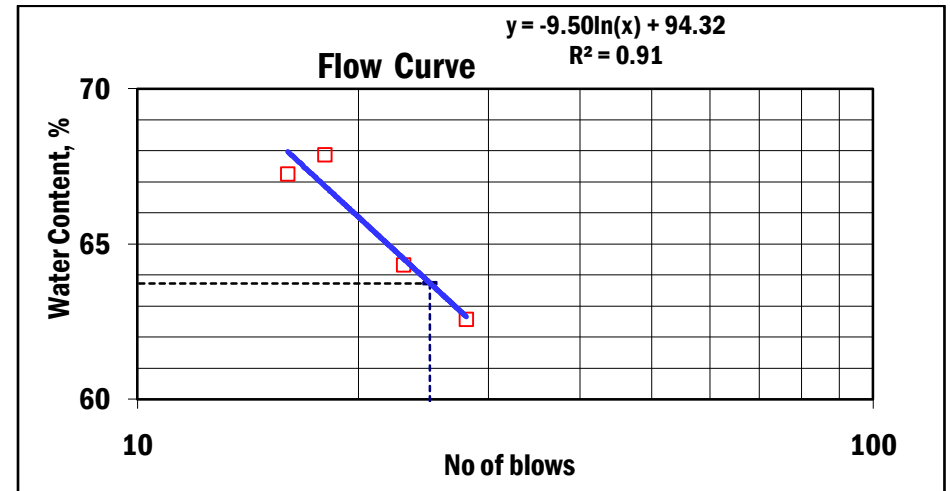


Figure AII-4: Flow curve analysis for TP2-2.

Table AII-5: Liquid limit and plastic limit test result analysis for TP-3-1

Trial No	Liquid Limit				Plastic Limit	
	1	2	3	4	1	2
Container No	36	30	24	4	67	68
Mass of container, g	13.89	15.67	15.65	15.67	15.50	15.50
Mass of container + Wet soil, g	43.42	42.56	49.48	30.54	25.00	25.00
Mass of container + Dry soil, g	31.40	31.83	35.97	24.77	22.45	22.45
Mass of water, g	12.02	10.73	13.52	5.77	2.55	2.55
Mass of dry soil, g	17.51	16.16	20.32	9.10	6.95	6.95
Water content, %	68.64	66.40	66.54	63.40	36.69	36.69
No of blows	15	23	20	35	-----	-----

Liquid Limit, % = 66 Plastic Limit, % = 36.7 PI, % = 29

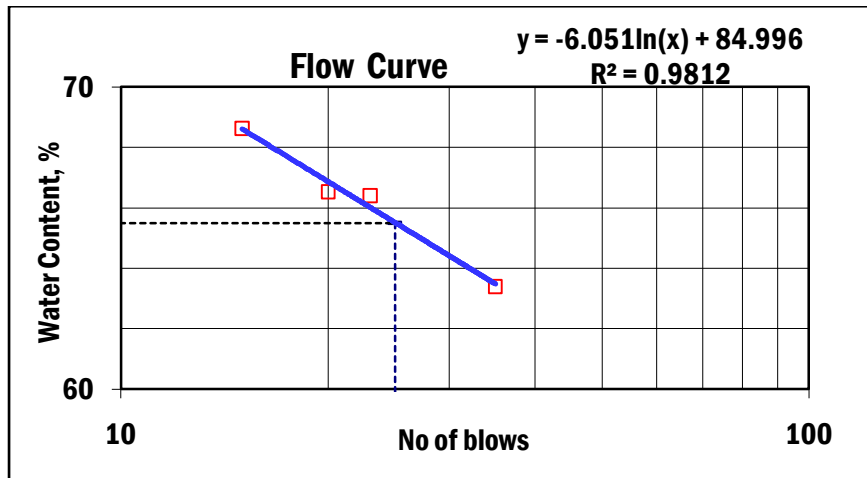


Figure AII-5: Flow curve analysis for TP3-1.

Table AII-6: Liquid limit and plastic limit test result analysis for TP-3-2

Trial No	Liquid Limit				Plastic Limit	
	1	2	3	4	1	2
Container No	A1	70	D-5	D-33	7	A34
Mass of container, g	15.18	15.72	15.70	15.51	15.56	15.67
Mass of container + Wet soil, g	41.09	36.05	45.37	40.00	21.80	22.46
Mass of container + Dry soil, g	30.50	27.64	33.23	29.90	19.93	20.44
Mass of water, g	10.60	8.41	12.14	10.10	1.87	2.02
Mass of dry soil, g	15.31	11.92	17.53	14.39	4.37	4.77
Water content, %	69.21	70.55	69.25	70.19	42.79	42.35
No of blows	30	17	27	23	-----	-----

Liquid Limit, % = 70.0 Plastic Limit, % = 42.6 PI, % = 27

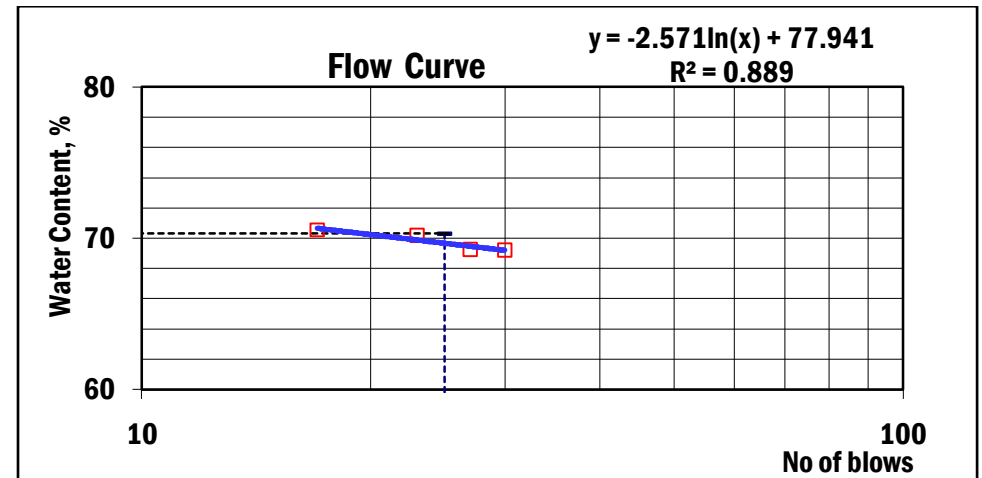


Figure AII-6: Flow curve analysis for TP3-2.

Table AII-7: Liquid limit and plastic limit test result analysis for TP4-1

Trial No	Liquid Limit				Plastic Limit		
	1	2	3	4	1	2	3
Container No	GHI	D-23	108	53	79	D22	A-1
Mass of container, g	15.59	15.37	15.62	15.56	15.51	15.75	11.50
Mass of container + Wet soil, g	44.24	42.93	45.50	45.67	18.08	18.52	16.64
Mass of container + Dry soil, g	33.88	33.08	35.32	34.85	17.48	17.88	15.53
Mass of water, g	10.36	9.85	10.18	10.83	0.60	0.63	1.11
Mass of dry soil, g	18.29	17.71	19.70	19.29	1.98	2.13	4.03
Water content, %	56.65	55.62	51.70	56.11	30.38	29.76	27.52
No of blows	19	25	29	21	-----	-----	-----

Liquid Limit, % = 54 Plastic Limit, % = 29.2173 PI, % = 25

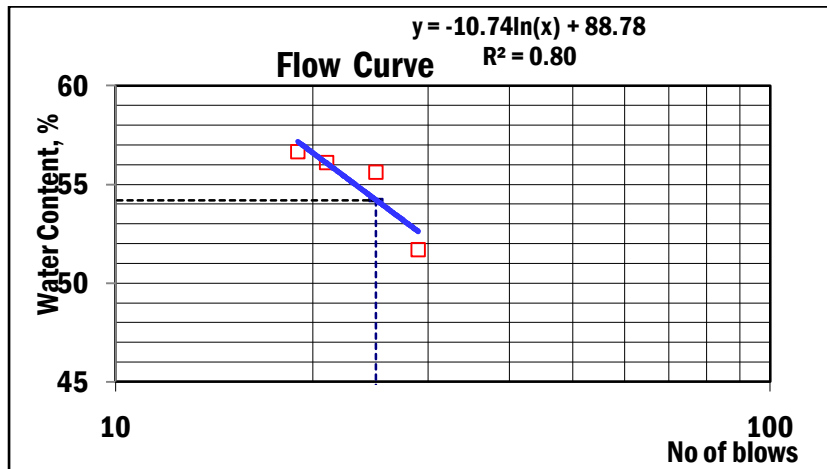


Figure AII-7: Flow curve analysis for TP4-1.

Table AII-8: Liquid limit and plastic limit test result analysis for TP4-2

Trial No	Liquid Limit				Plastic Limit		
	1	2	3	4	1	2	3
Container No	A1	45	D25	D5	D9	86	59
Mass of container, g	15.50	15.45	15.87	15.69	15.85	15.57	15.32
Mass of container + Wet soil, g	42.57	42.84	40.39	41.72	21.82	20.34	21.60
Mass of container + Dry soil, g	33.50	33.60	32.09	32.92	20.48	19.31	20.19
Mass of water, g	9.07	9.24	8.30	8.80	1.34	1.04	1.41
Mass of dry soil, g	18.00	18.16	16.22	17.23	4.63	3.73	4.87
Water content, %	50.38	50.88	51.17	51.07	28.89	27.74	28.96
No of blows	35	28	17	22	-----	-----	-----

Liquid Limit, % = 51 Plastic Limit, % = 28.5312 PI, % = 22

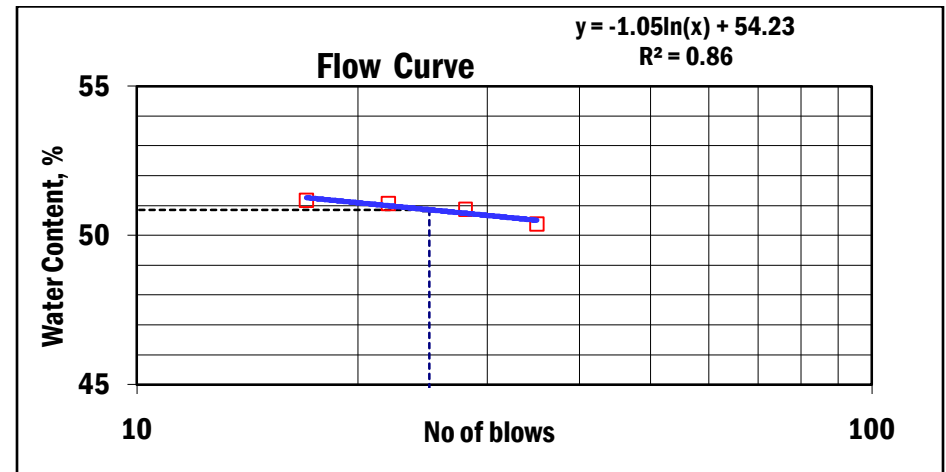


Figure AII-8: Flow curve analysis for TP4-2.

Table AII-9: Liquid limit and plastic limit test result analysis for TP5-1

Trial No	Liquid Limit				Plastic Limit		
	1	2	3	4	1	2	3
Container No	24	5	A29	2	102	19	H3
Mass of container, g	15.65	13.86	15.33	15.65	15.67	11.69	14.05
Mass of container + Wet soil, g	46.01	43.91	44.89	45.71	19.83	15.55	19.43
Mass of container + Dry soil, g	34.46	32.42	33.39	34.12	18.67	14.48	17.90
Mass of water, g	11.56	11.49	11.50	11.59	1.16	1.07	1.53
Mass of dry soil, g	18.81	18.57	18.06	18.48	2.99	2.79	3.85
Water content, %	61.45	61.86	63.72	62.71	38.87	38.53	39.66
No of blows	33	29	16	23	-----	-----	-----

Liquid Limit, % = 62 Plastic Limit, % = 39.0211 PI, % = 23

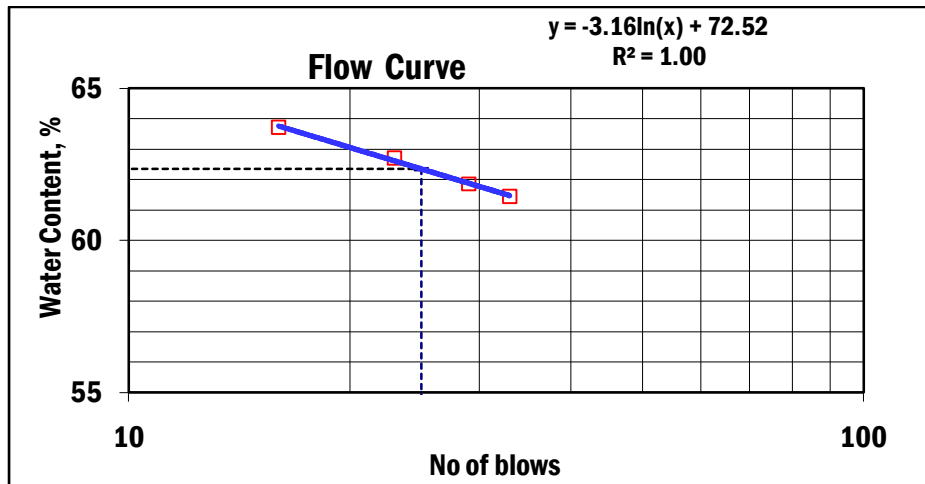


Figure AII-9: Flow curve analysis for TP5-1.

Table AII-10: Liquid limit and plastic limit test result analysis for TP5-2

Trial No	Liquid Limit				Plastic Limit		
	1	2	3	4	1	2	3
Container No	A25	A19	79	E3	69	62	A31
Mass of container, g	15.72	15.57	15.50	15.83	15.74	15.63	15.79
Mass of container + Wet soil, g	43.19	48.85	48.83	44.65	23.02	23.84	22.72
Mass of container + Dry soil, g	32.81	36.03	35.61	33.38	20.88	21.43	20.86
Mass of water, g	10.38	12.82	13.23	11.27	2.13	2.42	1.86
Mass of dry soil, g	17.09	20.45	20.10	17.55	5.15	5.80	5.07
Water content, %	60.72	62.68	65.79	64.23	41.43	41.72	36.69
No of blows	33	26	16	21	-----	-----	-----

Liquid Limit, % = 63 Plastic Limit, % = 39.9456 PI, % = 23

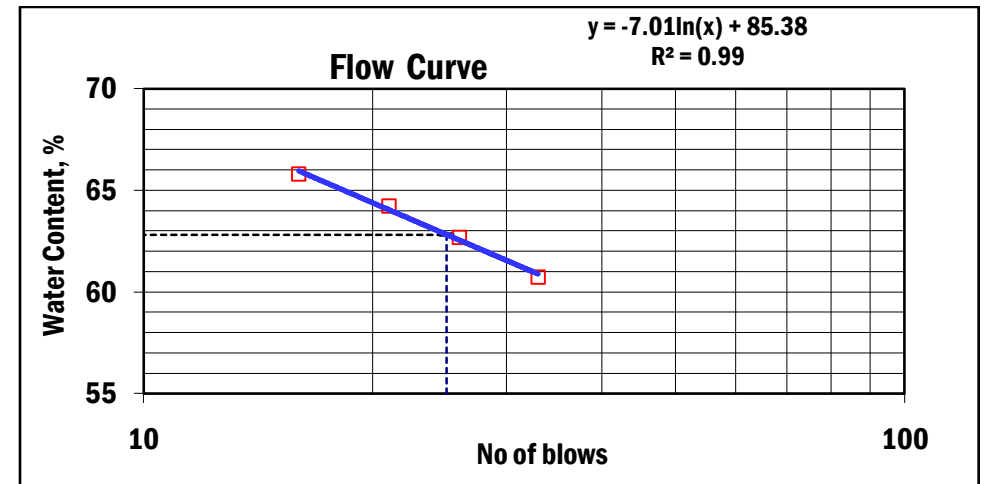


Figure AII-10: Flow curve analysis for TP5-2.

Table AII-11: Liquid limit and plastic limit test result analysis for TP6-1

Trial No	Liquid Limit				Plastic Limit		
	1	2	3	4	1	2	3
Container No	12	C31	D9	2.1	23	51	53
Mass of container, g	15.85	14.04	15.81	15.63	15.64	15.83	13.72
Mass of container + Wet soil, g	51.38	42.78	39.75	45.61	22.27	21.72	21.59
Mass of container + Dry soil, g	36.93	30.95	29.74	33.18	20.36	19.98	19.31
Mass of water, g	14.45	11.84	10.01	12.43	1.91	1.74	2.28
Mass of dry soil, g	21.08	16.90	13.93	17.55	4.72	4.15	5.59
Water content, %	68.56	70.03	71.86	70.83	40.60	42.06	40.77
No of blows	30	26	17	22	-----	-----	-----

Liquid Limit, % = 70 Plastic Limit, % = 41.1454 PI, % = 29

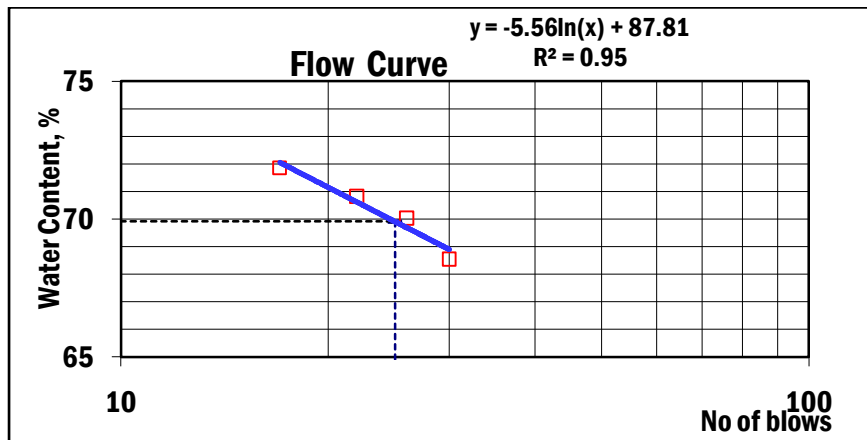


Figure AII-11: Flow curve analysis for TP6-1.

Table AII-12: Liquid limit and plastic limit test result analysis for TP6-2

Trial No	Liquid Limit				Plastic Limit		
	1	2	3	4	1	2	3
Container No	DEF	A34	53	5	85	22	Y
Mass of container, g	15.64	15.63	15.56	13.86	15.84	21.06	15.70
Mass of container + Wet soil, g	46.71	53.75	42.04	43.41	24.22	27.54	20.75
Mass of container + Dry soil, g	34.97	39.77	31.70	32.40	21.77	25.67	19.27
Mass of water, g	11.74	13.98	10.34	11.01	2.45	1.87	1.47
Mass of dry soil, g	19.33	24.14	16.14	18.54	5.93	4.61	3.58
Water content, %	60.76	57.90	64.03	59.38	41.33	40.57	41.19
No of blows	23	31	16	27	-----	-----	-----

Liquid Limit, % = 60 Plastic Limit, % = 41.0303 PI, % = 19

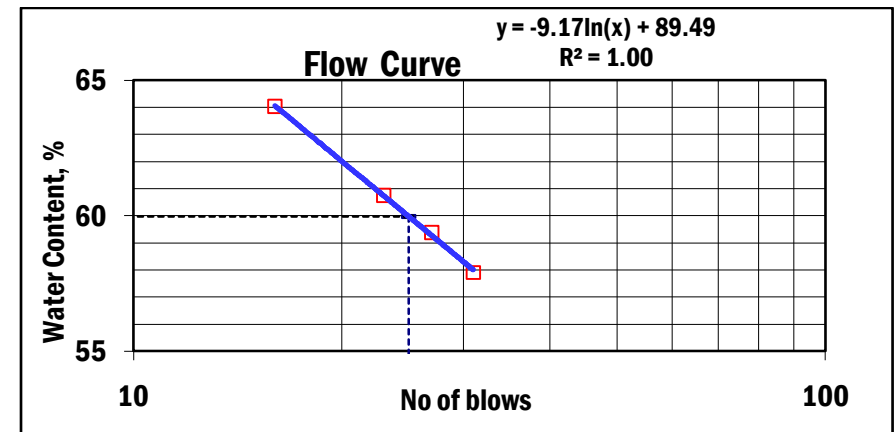


Figure AII-12: Flow curve analysis for TP6-1.

III. Standard Compaction test Results

Table AIII-1: Standard compaction result for Adisu gebeya site, TP1-1

Dry density determination

Determination No.	1	2	3	4	5
Mass of Mold, g	5630	5630	5630	5630	5630
Mass of mold+ Compacted Soil, g	7071	7411	7506	7453	7401
Mass of Compacted soil, g	1441	1781	1876	1823	1771
Volume of Mold,cm3	944	944	944	944	944
Bulk density, g/cm3	1.53	1.89	1.99	1.93	1.88
Dry density, g/cm3	1.40	1.56	1.57	1.46	1.34
Moisture Content Determination	1	2	3	4	5
Container No	22	47	62	6	cmc-3
Mass of container, g	5	5	5	5	5
Mass of container + wet soil, g	212	206	222	225	272
Mass of container + Dry soil, g	195	171	176	171	196
Mass of Water, g	17	35	46	54	76
Mass of Dry soil, g	190	166	171	166	191
Water content, %	8.95	21.08	26.90	32.53	39.79

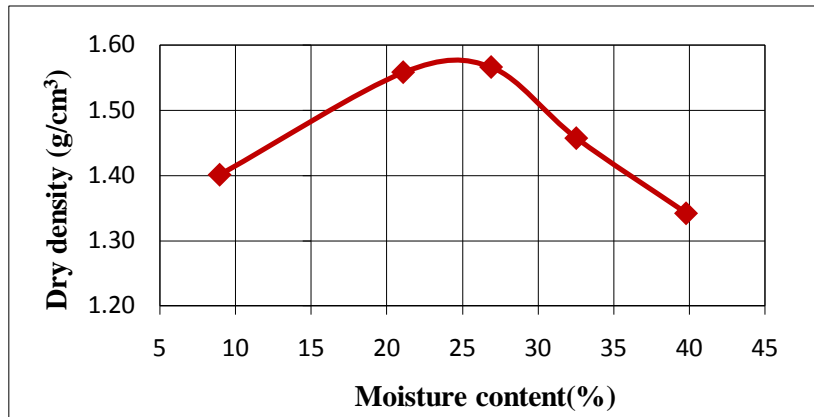


Figure AIII-1: OMC Vs OMC for Adisu gebeya site, TP1-1

Table AIII-2: Standard compaction result for Adisu gebeya site, TP1-2

Dry density determination

Determination No.	1	2	3	4	5
Mass of Mold, g	5630	5630	5630	5630	5630
Mass of mold+ Compacted Soil, g	7081	7369	7516	7439	7390
Mass of Compacted soil, g	1451	1739	1886	1809	1760
Volume of Mold,cm3	944	944	944	944	944
Bulk density, g/cm3	1.54	1.84	2.00	1.92	1.86
Dry density, g/cm3	1.40	1.54	1.58	1.44	1.34
Moisture Content Determination	1	2	3	4	5
Container No	28	19	31	cmc-4	10
Mass of container, g	5	5	5	5	5
Mass of container + wet soil, g	208	193	180	234	235
Mass of container + Dry soil, g	190	162	143	177	170
Mass of Water, g	18	31	37	57	65
Mass of Dry soil, g	185	157	138	172	165
Water content, %	9.73	19.75	26.81	33.14	39.39

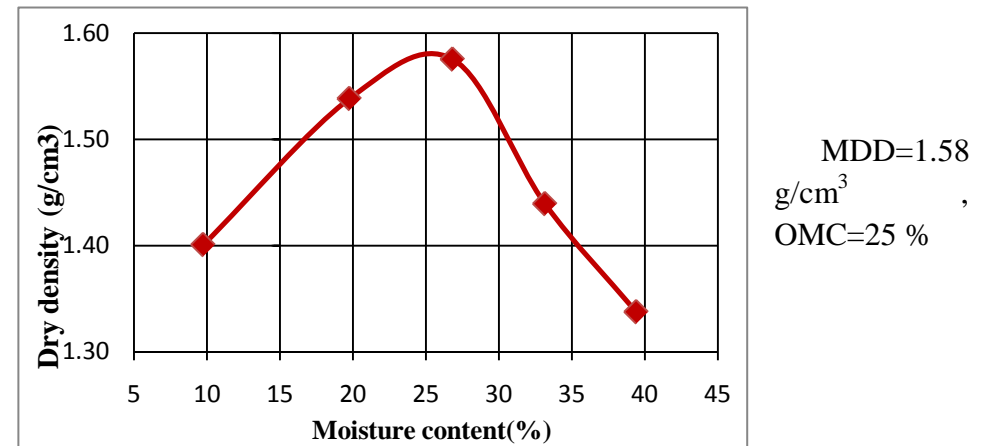
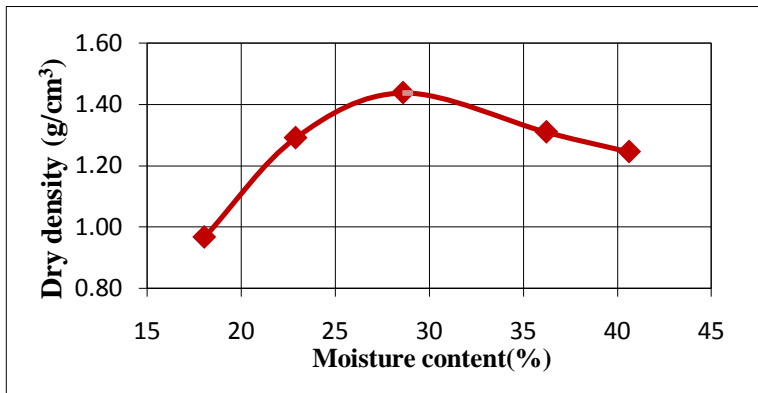


Figure AIII-2: OMC Vs OMC for Adisu gebeya site, TP1-2.

Table AIII-3: Standard compaction result for Atena tera site, TP2-1

Dry density determination

Determination No.	2	2	3	4	5
Mass of Mold, g	5630	5630	5630	5630	5630
Mass of mold+ Compacted Soil, g	6708	7128	7376	7315	7284
Mass of Compacted soil, g	1078	1498	1746	1685	1654
Volume of Mold,cm3	944	944	944	944	944
Bulk density, g/cm3	1.14	1.59	1.85	1.78	1.75
Dry density, g/cm3	0.97	1.29	1.44	1.31	1.25
Moisture Content Determination					
	1	2	3	4	5
Container No	5	53	8	A1	42
Mass of container, g	13.89	15.59	15.68	15.81	15.44
Mass of container + wet soil, g	39.09	34.64	49.72	43.64	63.45
Mass of container + Dry soil, g	35.24	31.09	42.15	36.24	49.58
Mass of Water, g	3.85	3.548	7.571	7.399	13.87
Mass of Dry soil, g	21.35	15.50	26.47	20.43	34.14
Water content, %	18.03	22.89	28.60	36.22	40.62



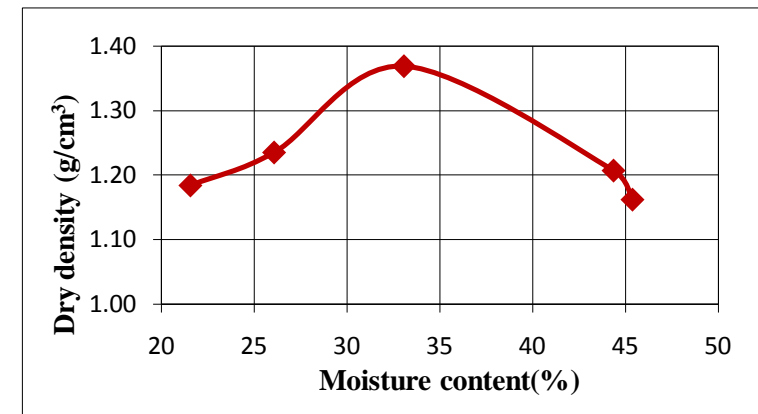
MDD=1.44
g/cm³ ,
OMC=28.6 %

Figure AIII-3: OMC Vs OMC for Atena tera site, TP2-1.

Table AIII-4: Standard compaction result for Atena tera site, TP2-2

Dry density determination

Determination No.	1	2	3	4	5
Mass of Mold, g	5630	5630	5630	5630	5630
Mass of mold+ Compacted Soil, g	6989	7100	7349	7275	7225
Mass of Compacted soil, g	1359	1470	1719	1645	1595
Volume of Mold,cm3	944	944	944	944	944
Bulk density, g/cm3	1.44	1.56	1.82	1.74	1.69
Dry density, g/cm3	1.18	1.24	1.37	1.21	1.16
Moisture Content Determination					
	1	2	3	4	5
Container No	A1	5.1	D33	36	23
Mass of container, g	15.304	15.456	15.54	15.64	15.685
Mass of container + wet soil, g	36.656	36.344	37.45	49.179	37.31
Mass of container + Dry soil, g	32.869	32.025	32.007	38.876	30.562
Mass of Water, g	3.787	4.319	5.443	10.303	6.748
Mass of Dry soil, g	17.564	16.569	16.467	23.236	14.87
Water content, %	21.56	26.07	33.06	44.34	45.36



MDD= 1.37
g/cm³ and
OMC=33.06
%

Figure AIII-4: OMC Vs OMC for Atena tera site, TP2-4.

Table AIII-5: Standard compaction result for Athari site, TP3-1

Dry density determination

Determination No.	1	2	3	4	5
Mass of Mold, g	5630	5630	5630	5630	5630
Mass of mold+ Compacted Soil, g	7070	7304	7484	7353	7338
Mass of Compacted soil, g	1440	1674	1854	1723	1708
Volume of Mold,cm3	944	944	944	944	944
Bulk density, g/cm3	1.53	1.77	1.96	1.83	1.81
Dry density, g/cm3	1.37	1.45	1.51	1.30	1.24
Moisture Content Determination					
	1	2	3	4	5
Container No	9.0	36.0	41.0	62.0	8.0
Mass of container, g	5.0	5.0	5.0	5.0	5.0
Mass of container + wet soil, g	172.0	154.0	186.0	182.0	198.0
Mass of container + Dry soil, g	155.0	127.0	144.0	131.0	137.0
Mass of Water, g	17.0	27.0	42.0	51.0	61.0
Mass of Dry soil, g	150.0	122.0	139.0	126.0	132.0
Water content, %	11.3	22.1	30.2	40.5	46.2

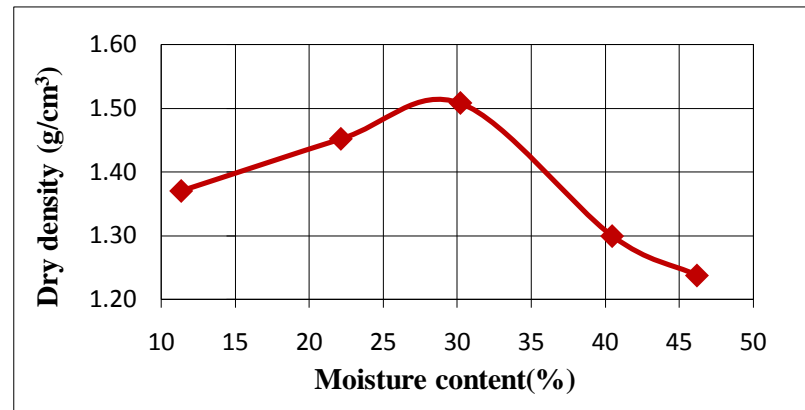


Figure AIII-5: OMC Vs OMC for Athari site, TP3-1.

Table AIII-6: Standard compaction result for Athari site, TP3-2

Dry density determination

Determination No.	1	2	3	4	5
Mass of Mold, g	5630	5630	5630	5630	5630
Mass of mold+ Compacted Soil, g	7104	7320	7466	7350	7340
Mass of Compacted soil, g	1474	1690	1836	1720	1710
Volume of Mold,cm3	944	944	944	944	944
Bulk density, g/cm3	1.56	1.79	1.94	1.82	1.81
Dry density, g/cm3	1.41	1.46	1.48	1.31	1.24
Moisture Content Determination					
	1	2	3	4	5
Container No	28	10	38	cmc 1	30
Mass of container, g	5	5	5	5	5
Mass of container + wet soil, g	192	203	182	199	221
Mass of container + Dry soil, g	174	167	140	144	153
Mass of Water, g	18	36	42	55	68
Mass of Dry soil, g	169	162	135	139	148
Water content, %	10.65	22.22	31.11	39.57	45.95

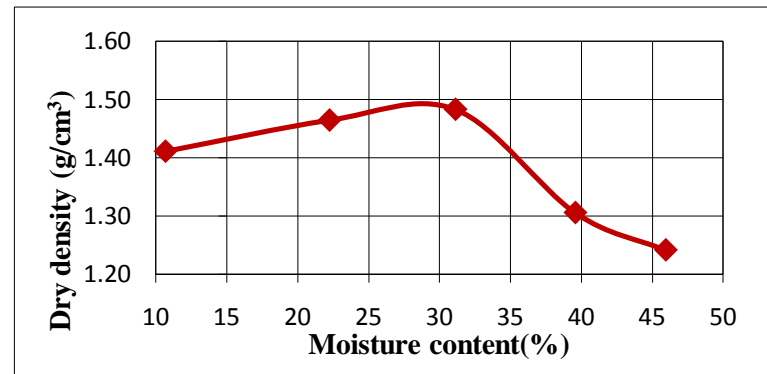


Figure AIII-6: OMC Vs OMC for Athari site, TP3-2.

Table AIII-7: Standard compaction result for Awelya site, TP4-1

Dry density determination

Determination No.	1	2	3	4	5
Mass of Mold, g	5630	5630	5630	5630	5630
Mass of mold+ Compacted Soil, g	7145	7337	7495	7420	7397
Mass of Compacted soil, g	1515	1707	1865	1790	1767
Volume of Mold,cm3	944	944	944	944	944
Bulk density, g/cm3	1.60	1.81	1.98	1.90	1.87
Dry density, g/cm3	1.47	1.54	1.57	1.43	1.36
Moisture Content Determination					
	1	2	3	4	5
Container No	10	22	29	88	38
Mass of container, g	5	5	5	5	5
Mass of container + wet soil, g	181	183	165	243	208
Mass of container + Dry soil, g	166	157	132	184	152
Mass of Water, g	15	26	33	59	56
Mass of Dry soil, g	161	152	127	179	147
Water content, %	9	17	26	33	38

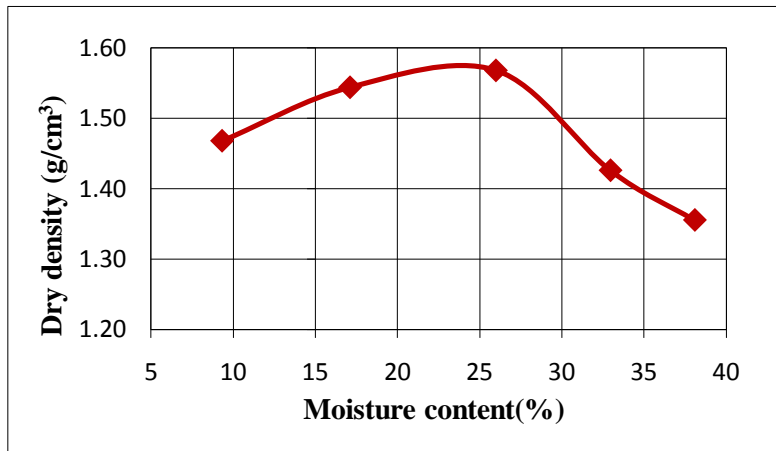


Figure AIII-7: OMC Vs OMC for Awelya site, TP4-1.

Table AIII-8: Standard compaction result for Awelya site, TP4-2

Dry density determination

Determination No.	1	2	3	4	5
Mass of Mold, g	5630	5630	5630	5630	5630
Mass of mold+ Compacted Soil, g	7092	7342	7501	7401	7389
Mass of Compacted soil, g	1462	1712	1871	1771	1759
Volume of Mold,cm3	944	944	944	944	944
Bulk density, g/cm3	1.55	1.81	1.98	1.88	1.86
Dry density, g/cm3	1.44	1.53	1.58	1.40	1.33
Moisture Content Determination					
	1	2	3	4	5
Container No	44	19	CMC4	28	16
Mass of container, g	5	5	5	5	5
Mass of container + wet soil, g	154	187	171	207	293
Mass of container + Dry soil, g	144	159	137	156	211
Mass of Water, g	10	28	34	51	82
Mass of Dry soil, g	139	154	132	151	206
Water content, %	7.19	18.18	25.76	33.77	39.81

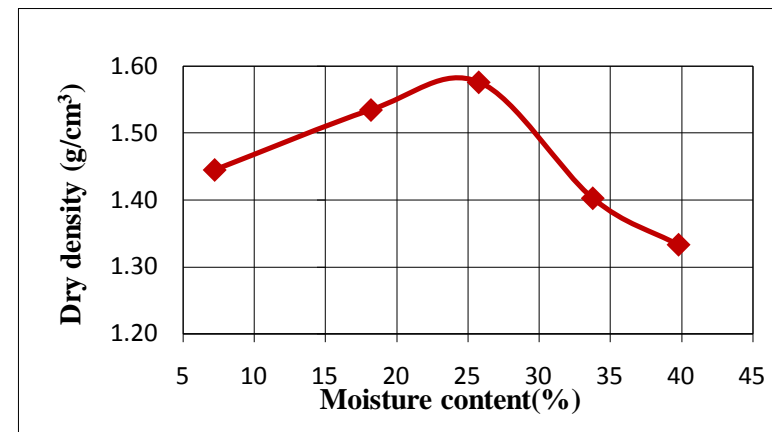
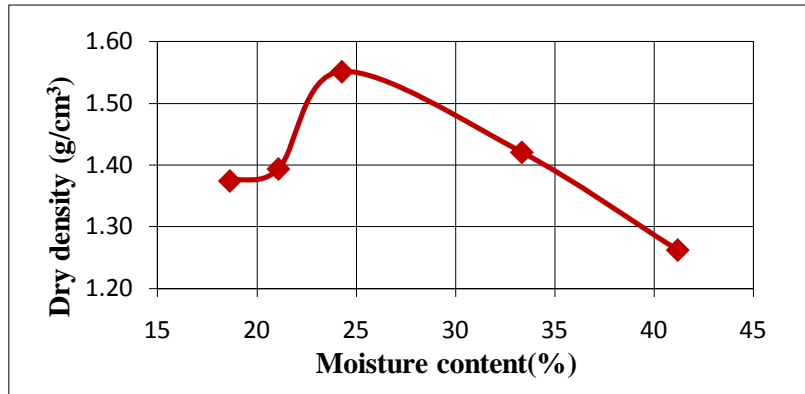


Figure AIII-8: OMC Vs OMC for Awelya site, TP4-2.

Table AIII-9: Standard compaction result for Kolfe site, TP5-1

Dry density determination

Determination No.	1	2	3	4	5
Mass of Mold, g	5630	5630	5630	5630	5630
Mass of mold+ Compacted Soil, g	7169	7223	7450	7418	7312
Mass of Compacted soil, g	1539	1593	1820	1788	1682
Volume of Mold, cm ³	944	944	944	944	944
Bulk density, g/cm ³	1.63	1.69	1.93	1.89	1.78
Dry density, g/cm ³	1.37	1.39	1.55	1.42	1.26
Moisture Content Determination					
	1	2	3	4	5
Container No	22	cmc-3	41	16	36
Mass of container, g	5	5	5	5	5
Mass of container + wet soil, g	215	206	220	205	245
Mass of container + Dry soil, g	182	171	178	155	175
Mass of Water, g	33	35	42	50	70
Mass of Dry soil, g	177	166	173	150	170
Water content, %	18.64	21.08	24.28	33.33	41.18



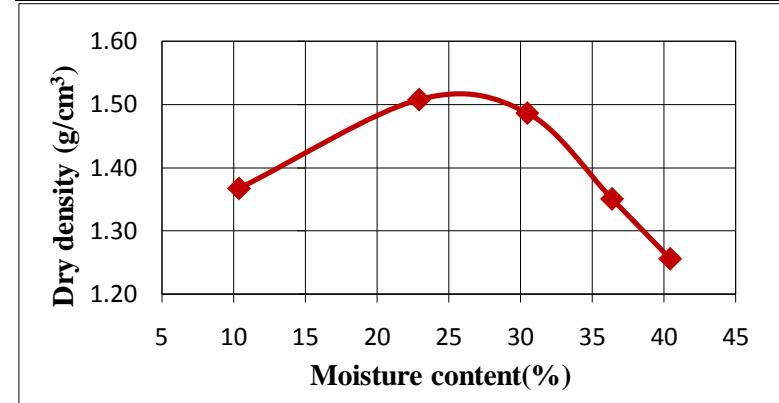
MDD=1.55
g/cm³ ,
OMC=24.3%

Figure AIII-9: OMC Vs OMC for Kolfe site, TP5-1.

Table AIII-10: Standard compaction result for Kolfe site, TP5-2

Dry density determination

Determination No.	1	2	3	4	5
Mass of Mold, g	5630	5630	5630	5630	5630
Mass of mold+ Compacted Soil, g	7055	7380	7461	7369	7295
Mass of Compacted soil, g	1425	1750	1831	1739	1665
Volume of Mold, cm ³	944	944	944	944	944
Bulk density, g/cm ³	1.51	1.85	1.94	1.84	1.76
Dry density, g/cm ³	1.37	1.51	1.49	1.35	1.26
Moisture Content Determination					
	1	2	3	4	5
Container No	41	77	42	16	36
Mass of container, g	5	5	5	5	5
Mass of container + wet soil, g	207	198	202	200	210
Mass of container + Dry soil, g	188	162	156	148	151
Mass of Water, g	19	36	46	52	59
Mass of Dry soil, g	183	157	151	143	146
Water content, %	10.38	22.93	30.46	36.36	40.41



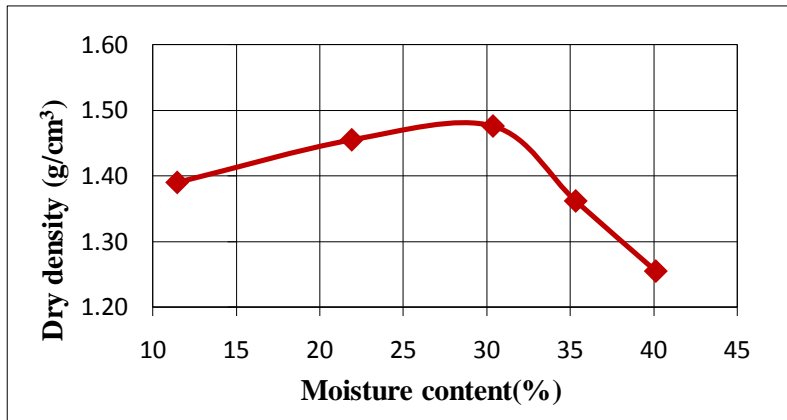
MDD=1.52
g/cm³ ,
OMC=26 %

Figure AIII-10: OMC Vs OMC for Kolfe site, TP5-2.

Table AIII-11: Standard compaction result for Shegole site, TP6-1

Dry density determination

Determination No.	1	2	3	4	5
Mass of Mold, g	5630	5630	5630	5630	5630
Mass of mold+ Compacted Soil, g	7093	7305	7447	7370	7290
Mass of Compacted soil, g	1463	1675	1817	1740	1660
Volume of Mold,cm3	944	944	944	944	944
Bulk density, g/cm3	1.55	1.77	1.92	1.84	1.76
Dry density, g/cm3	1.39	1.46	1.48	1.36	1.25
Moisture Content Determination					
	1	2	3	4	5
Container No	78	28	8	77	10
Mass of container, g	5	5	5	5	5
Mass of container + wet soil, g	209	233	211	208	225
Mass of container + Dry soil, g	188	192	163	155	162
Mass of Water, g	21	41	48	53	63
Mass of Dry soil, g	183	187	158	150	157
Water content, %	11.48	21.93	30.38	35.33	40.13



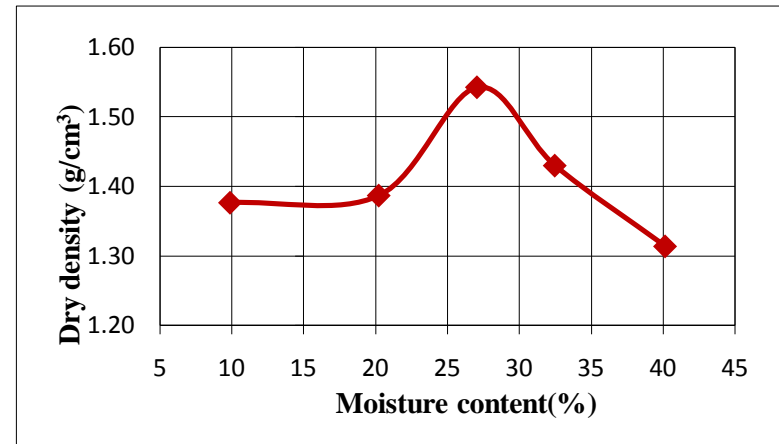
MDD=1.48
g/cm³ ,
OMC=29 %

Figure AIII-11: OMC Vs OMC for Shegole site, TP6-1.

Table AIII-12: Standard compaction result for Shegole site, TP6-2

Dry density determination

Determination No.	1	2	3	4	5
Mass of Mold, g	5630	5630	5630	5630	5630
Mass of mold+ Compacted Soil, g	7058	7204	7480	7418	7368
Mass of Compacted soil, g	1428	1574	1850	1788	1738
Volume of Mold,cm3	944	944	944	944	944
Bulk density, g/cm3	1.51	1.67	1.96	1.89	1.84
Dry density, g/cm3	1.38	1.39	1.54	1.43	1.31
Moisture Content Determination					
	1	2	3	4	5
Container No	cmc 5	62	cm 1	31	29
Mass of container, g	5	5	5	5	5
Mass of container + wet soil, g	216	213	221	209	211
Mass of container + Dry soil, g	197	178	175	159	152
Mass of Water, g	19	35	46	50	59
Mass of Dry soil, g	192	173	170	154	147
Water content, %	9.90	20.23	27.06	32.47	40.14



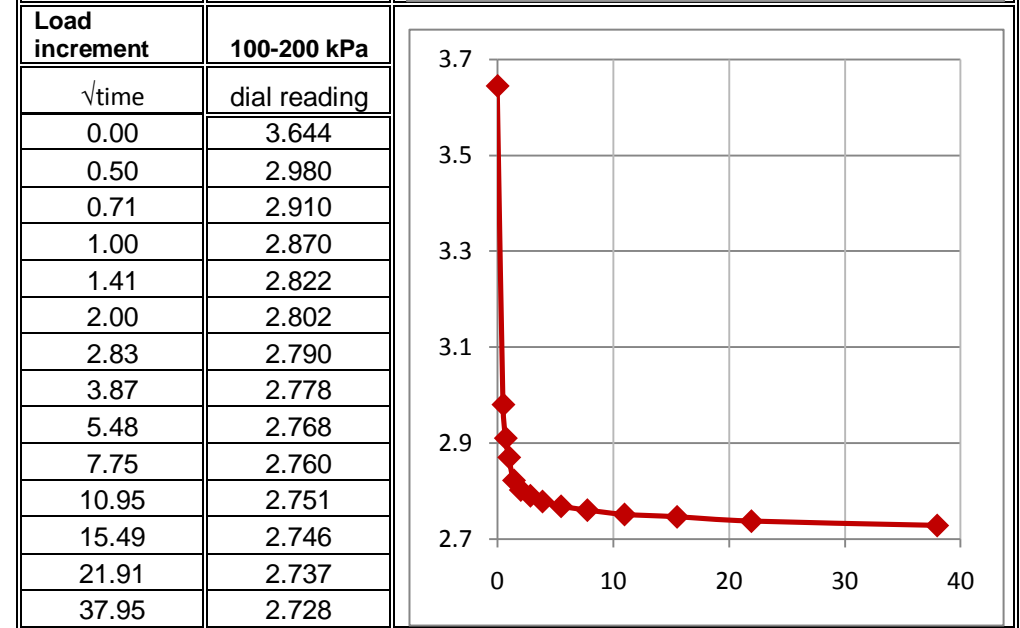
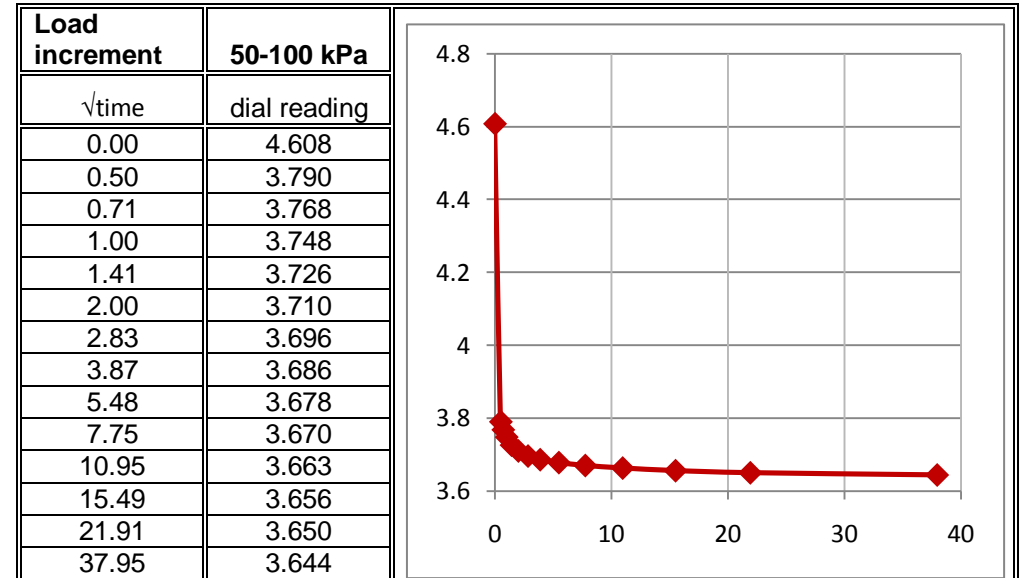
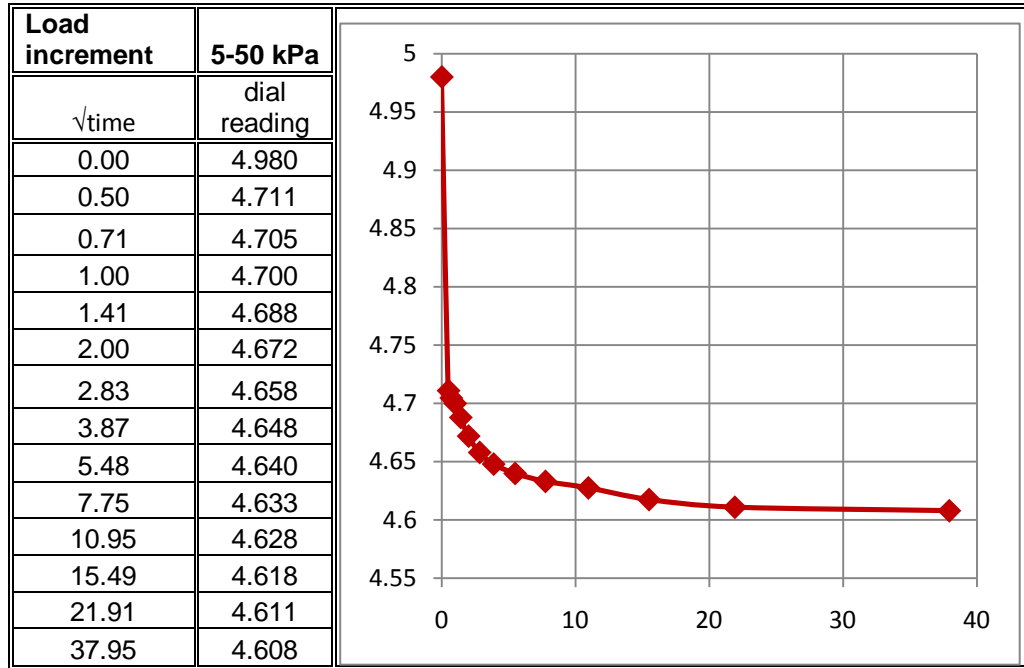
MDD=1.54
g/cm³ ,
OMC=27.1
%

Figure AIII-12: OMC Vs OMC for Shegole site, TP6-2.

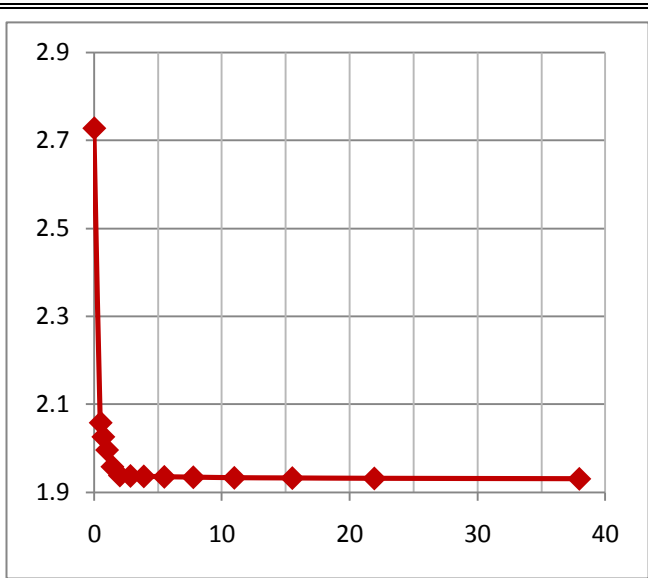
IV. One dimensional consolidation test Results

Deformation versus dial reading for different loading

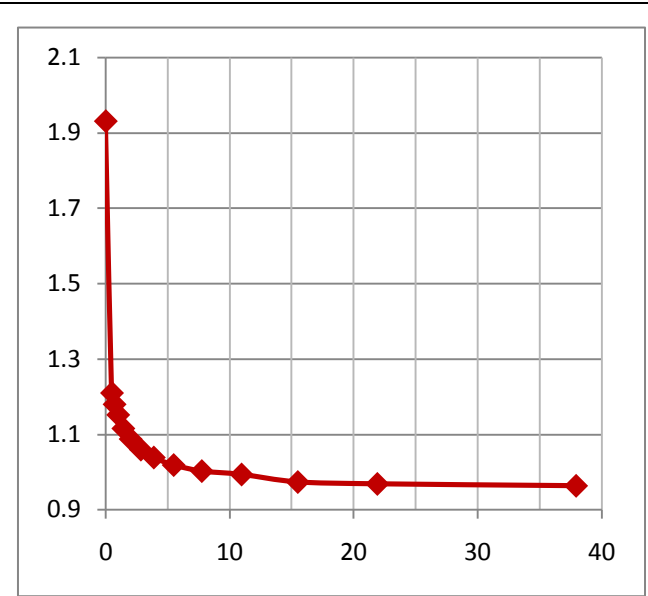
Sample No.	TP1-1	Location: Addisu Gebeya	
Sample Depth, m:	1.50		
[A] In the beginning of the test		[B] In the end of the test	
Sample type :	Disturbed	Final Moisture Content, %	28.71
Ring Area, cm ² :	19.625	Dry specimen wt (ms), gm:	50.03
Height of sample, mm:	20	Dry density, g/cm ³	1.65
Seating Load, Kpa	5	Height of Solids(Hs), mm	9.33
Initial Void Ratio, eo:	1.14	Final Void Ratio, ef:	0.67
Initial moisture content, %	25.00		
Specific Gravity:	2.73		
Wet density, g/cm ³	2.01		



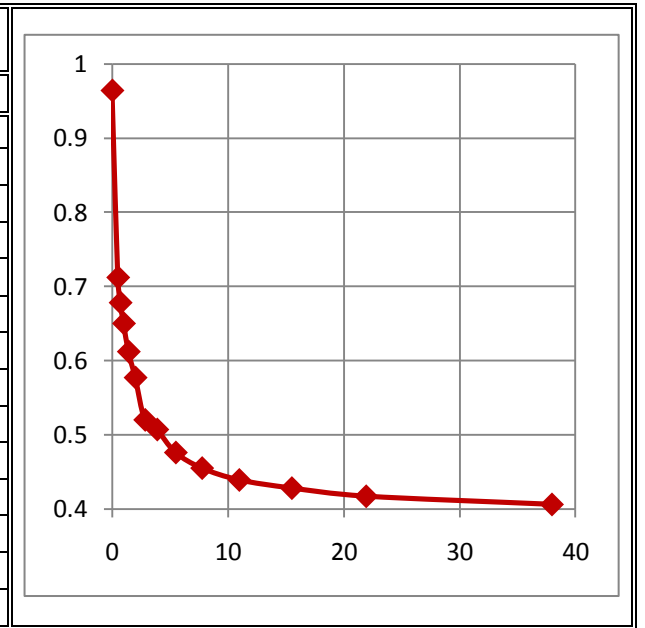
Load increment	200-400 kPa
$\sqrt{\text{time}}$	dial reading
0.00	2.728
0.71	2.026
1.00	1.996
1.41	1.958
2.00	1.938
2.83	1.937
3.87	1.936
5.48	1.935
7.75	1.934
10.95	1.933
15.49	1.932
21.91	1.931
37.95	1.930



Load increment	400-800 kPa
$\sqrt{\text{time}}$	dial reading
0.00	1.930
0.50	1.210
0.71	1.180
1.00	1.152
1.41	1.116
2.00	1.088
2.83	1.060
3.87	1.039
5.48	1.019
7.75	1.003
10.95	0.994
15.49	0.974
21.91	0.969
37.95	0.964

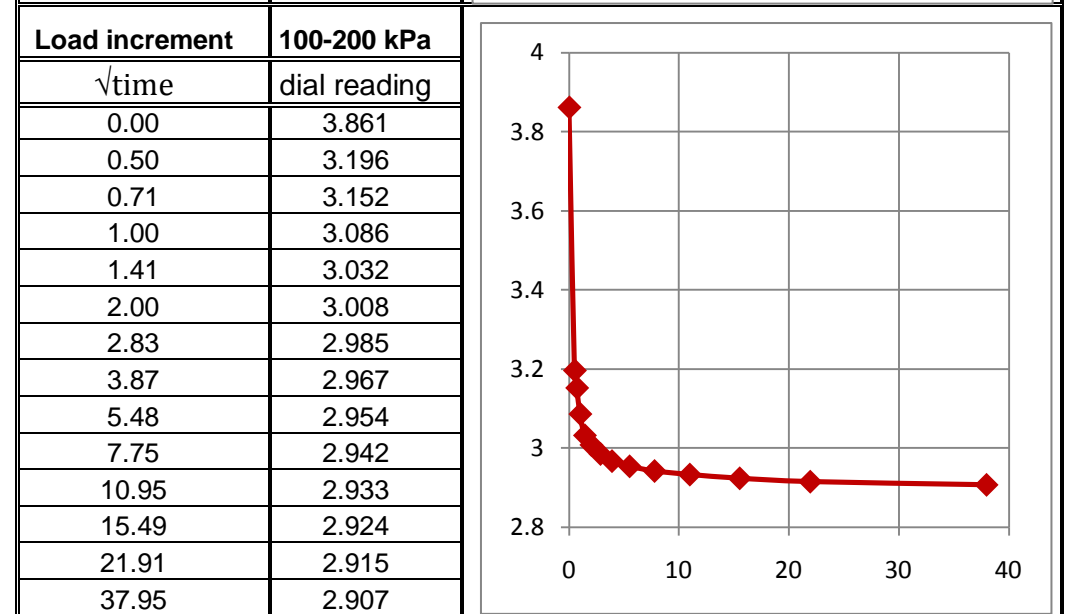
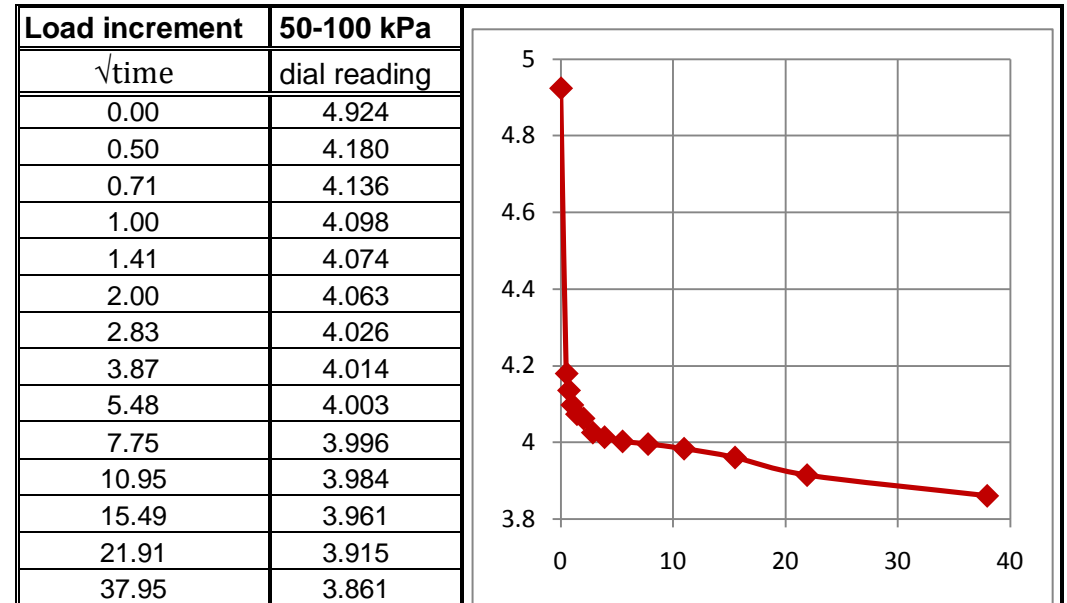
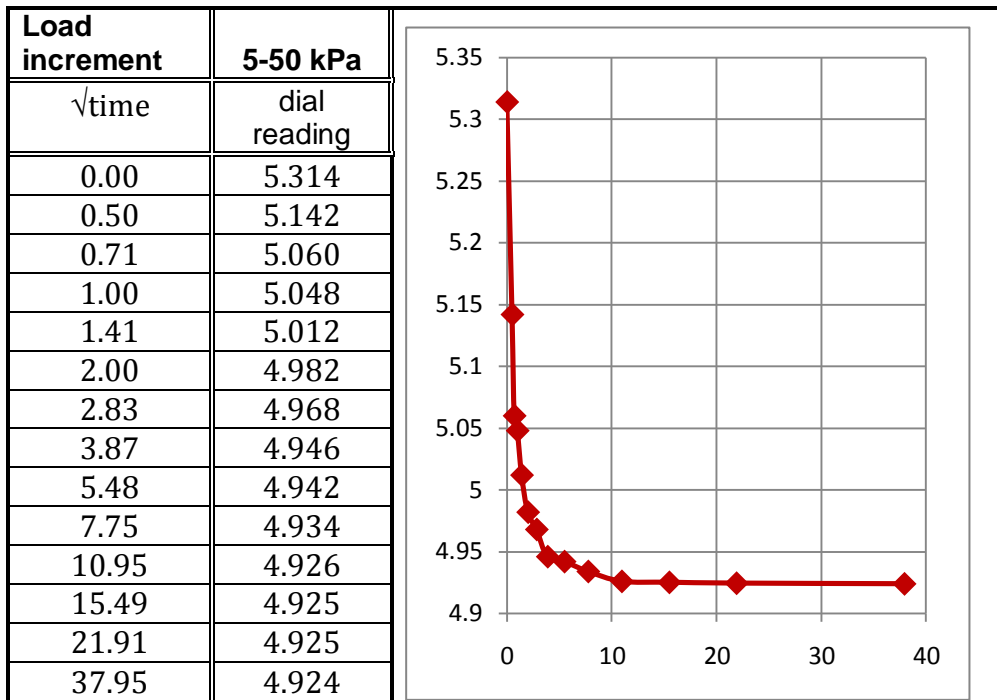


Load increment	800-1600 kPa
$\sqrt{\text{time}}$	dial reading
0.00	0.964
0.50	0.712
0.71	0.678
1.00	0.650
1.41	0.612
2.00	0.577
2.83	0.520
3.87	0.507
5.48	0.476
7.75	0.455
10.95	0.439
15.49	0.428
21.91	0.417
37.95	0.406

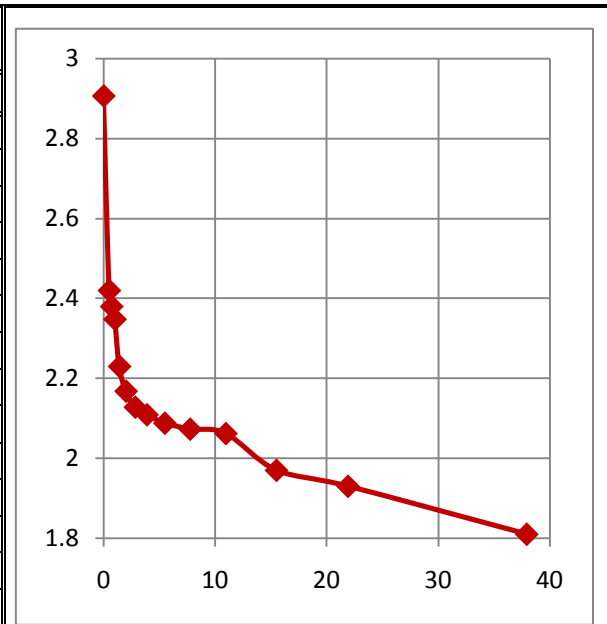


Sample No.	TP1-2	Location:	Addisu Gebeya
Sample Depth, m:	3.00		
[A] In the beginning of the test		[B] In the end of the test	
Sample type :	Disturbed	Final Moisture Content,%	55.80
Ring Area,cm2:	19.625	Dry specimen wt (ms), gm:	54.80
Height of sample,mm:	20	Dry density,g/cm3	1.02
Seating Load,Kpa	5	Height of Solids(Hs), mm	10.27
Initial Void Ratio, eo:	0.88	Final Void Ratio, ef:	0.43
Initial moisture content,%	25.00		
Specific Gravity:	2.72		
Wet density,g/cm3	1.59		

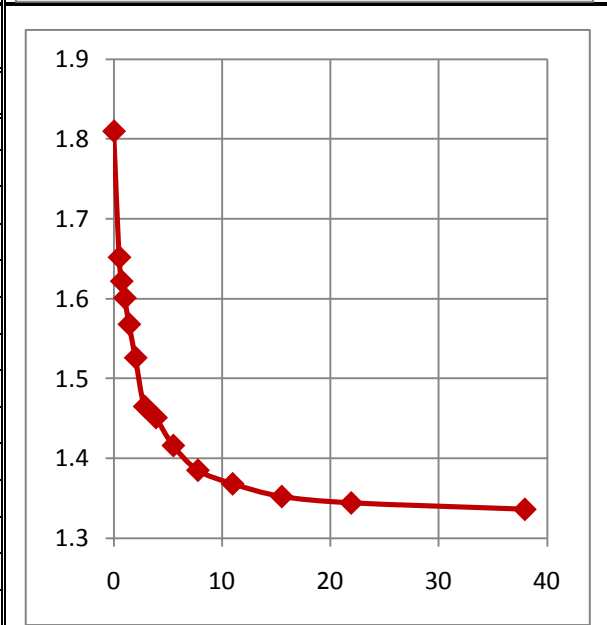
I. Deformation versus dial reading for different loading



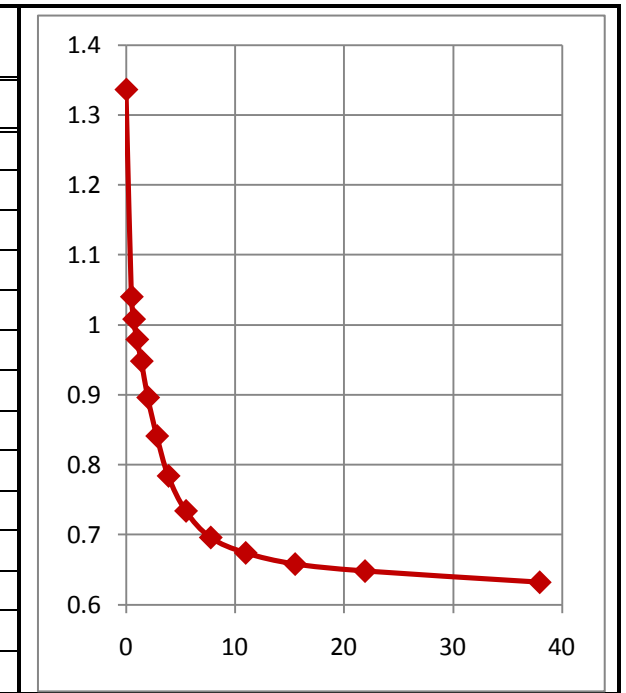
Load increment	200-400 kPa
$\sqrt{\text{time}}$	dial reading
0.00	2.907
0.50	2.420
0.71	2.380
1.00	2.348
1.41	2.230
2.00	2.168
2.83	2.128
3.87	2.109
5.48	2.088
7.75	2.073
10.95	2.062
15.49	1.970
21.91	1.930
37.95	1.810



Load increment	400-800 kPa
$\sqrt{\text{time}}$	dial reading
0.00	1.810
0.50	1.652
0.71	1.622
1.00	1.601
1.41	1.568
2.00	1.526
2.83	1.465
3.87	1.451
5.48	1.416
7.75	1.385
10.95	1.368
15.49	1.352
21.91	1.344
37.95	1.336

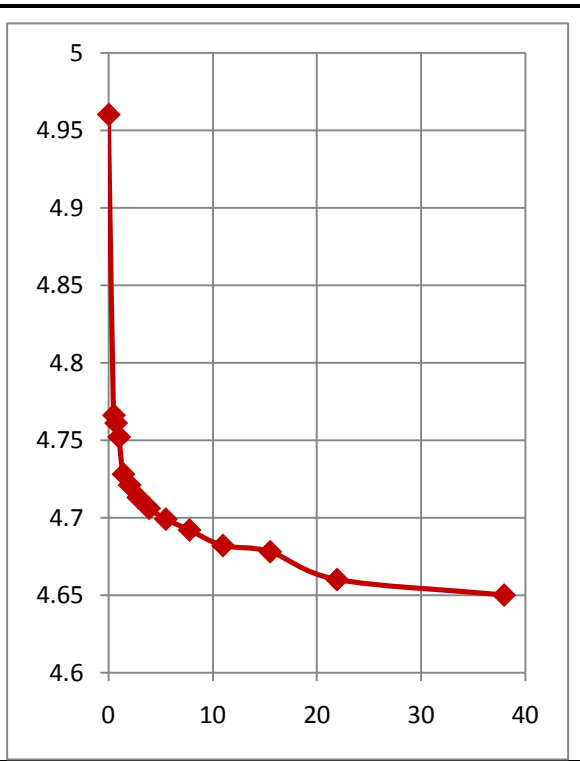


Load increment	800-1600 kPa
$\sqrt{\text{time}}$	dial reading
0.00	1.336
0.50	1.040
0.71	1.008
1.00	0.979
1.41	0.948
2.00	0.896
2.83	0.841
3.87	0.784
5.48	0.734
7.75	0.696
10.95	0.674
15.49	0.658
21.91	0.648
37.95	0.632

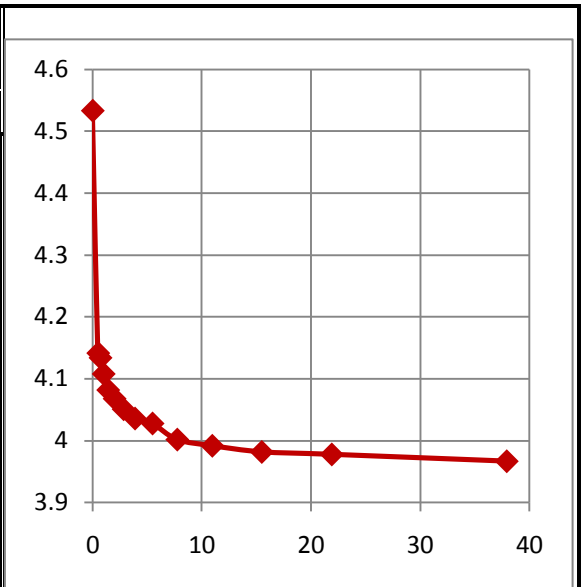


Sample No.	TP2-1	Location: 'Atena Tera	
Sample Depth, m:	1.50		
[A] In the beginning of the test		[B] In the end of the test	
Sample type :	Disturbed	Final Moisture Content, %	55.80
Ring Area, cm ² :	19.625	Dry specimen wt (ms), gm:	54.80
Height of sample, mm:	20	Dry density, g/cm ³	1.02
Seating Load, Kpa	5	Height of Solids(Hs), mm	10.27
Initial Void Ratio, eo:	0.96	Final Void Ratio, ef:	0.43
Initial moisture content, %	28.60		
Specific Gravity:	2.75		
Wet density, g/cm ³	1.85		

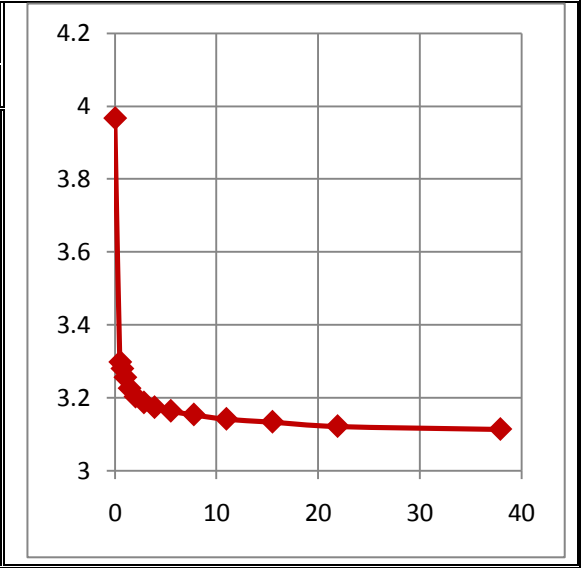
Load increment	5-50 kPa
$\sqrt{\text{time}}$	dial reading
0.00	4.960
0.50	4.766
0.71	4.761
1.00	4.752
1.41	4.728
2.00	4.721
2.83	4.713
3.87	4.706
5.48	4.699
7.75	4.692
10.95	4.682
15.49	4.678
21.91	4.660
37.95	4.650

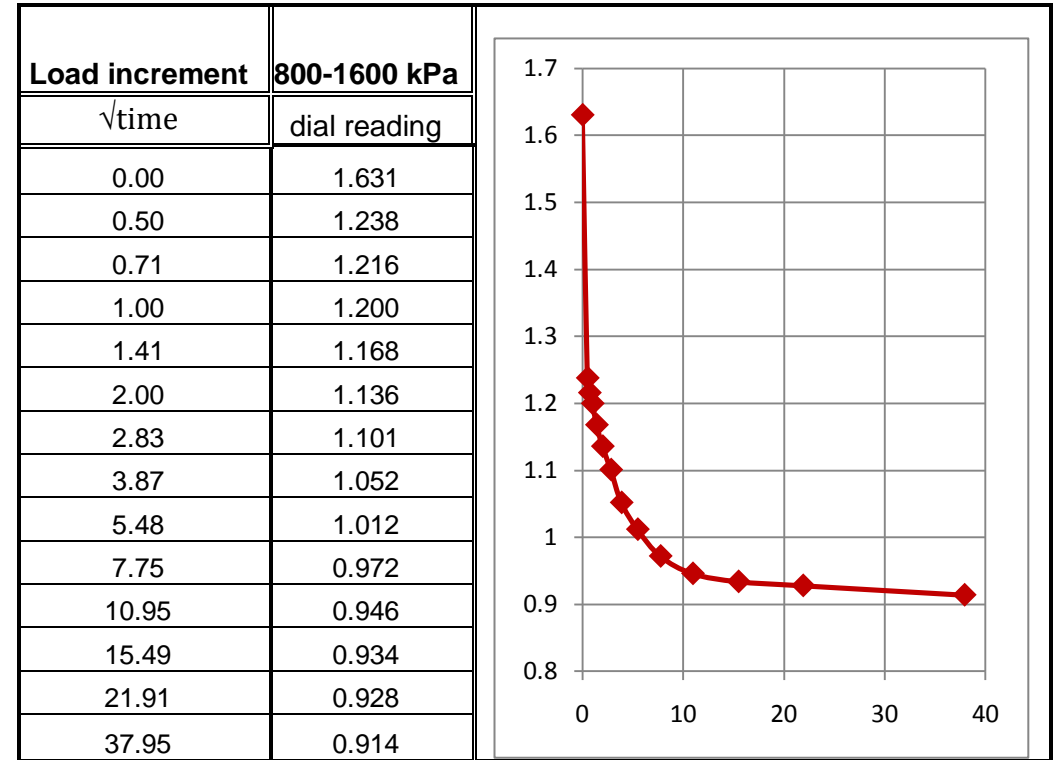
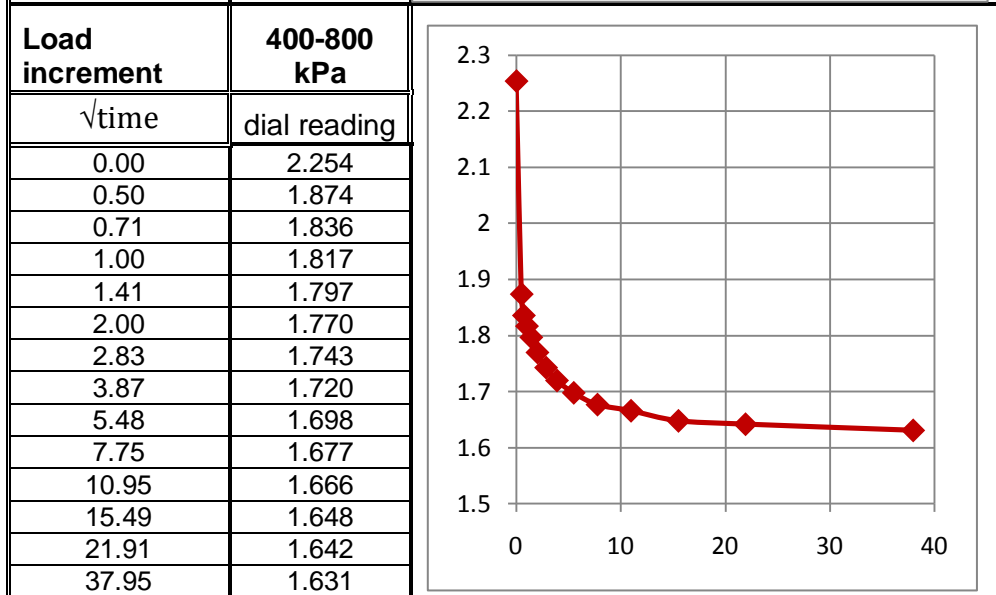
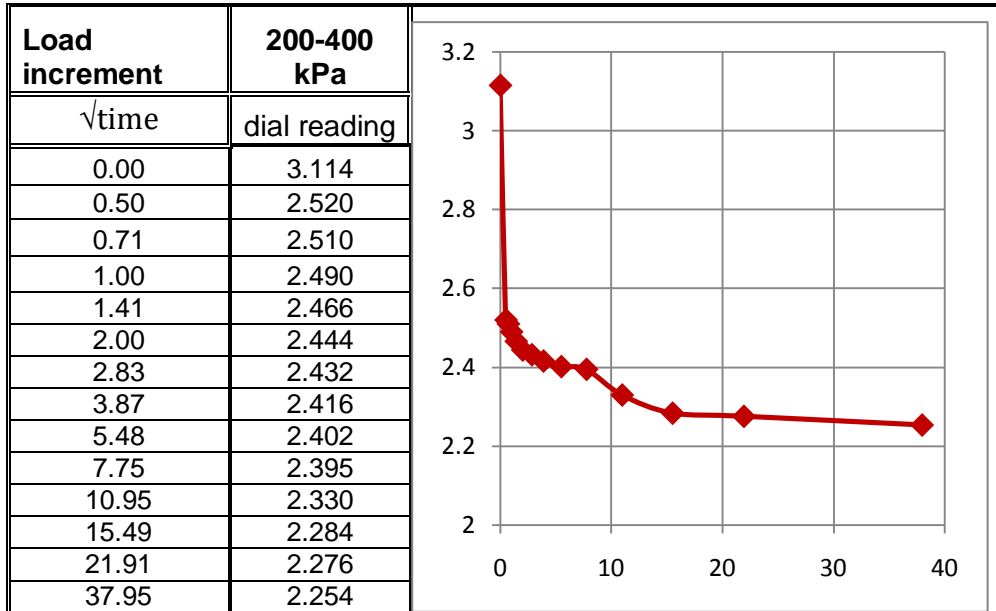


Load increment	50-100 kPa
$\sqrt{\text{time}}$	dial reading
0.00	4.533
0.50	4.142
0.71	4.134
1.00	4.108
1.41	4.082
2.00	4.068
2.83	4.051
3.87	4.036
5.48	4.028
7.75	4.002
10.95	3.992
15.49	3.982
21.91	3.978
37.95	3.967

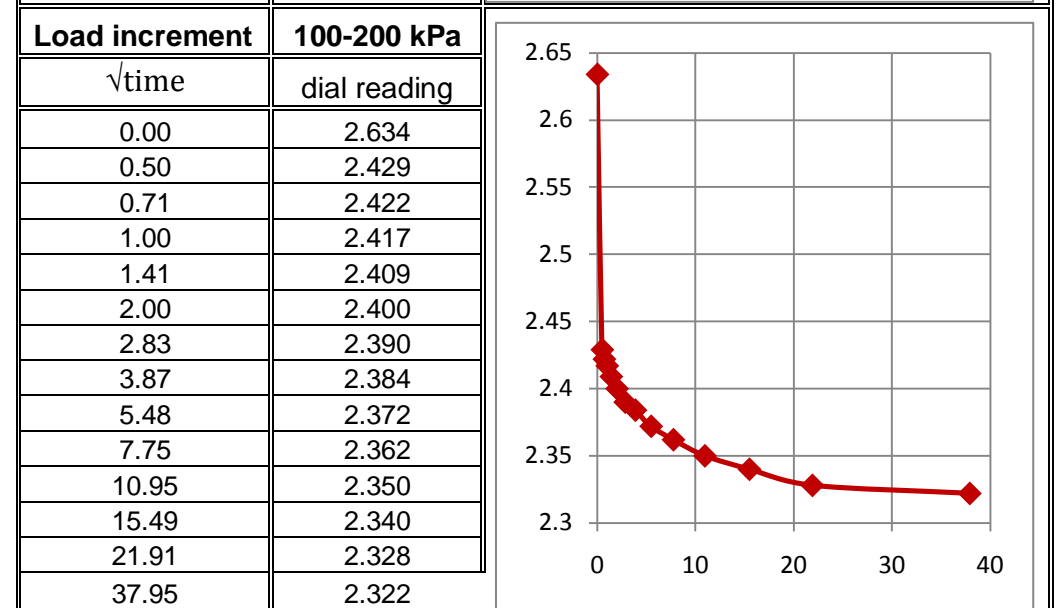
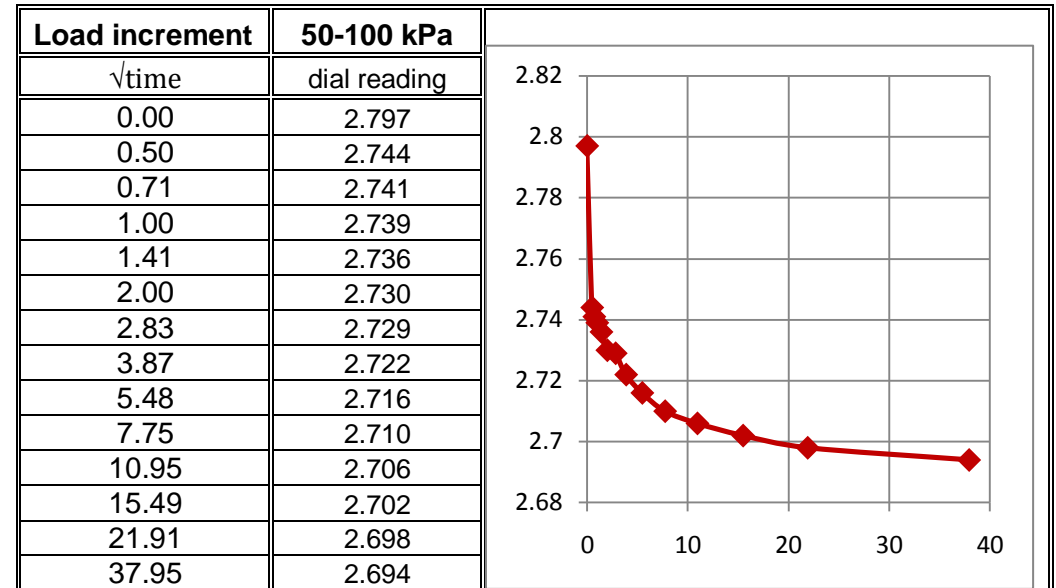
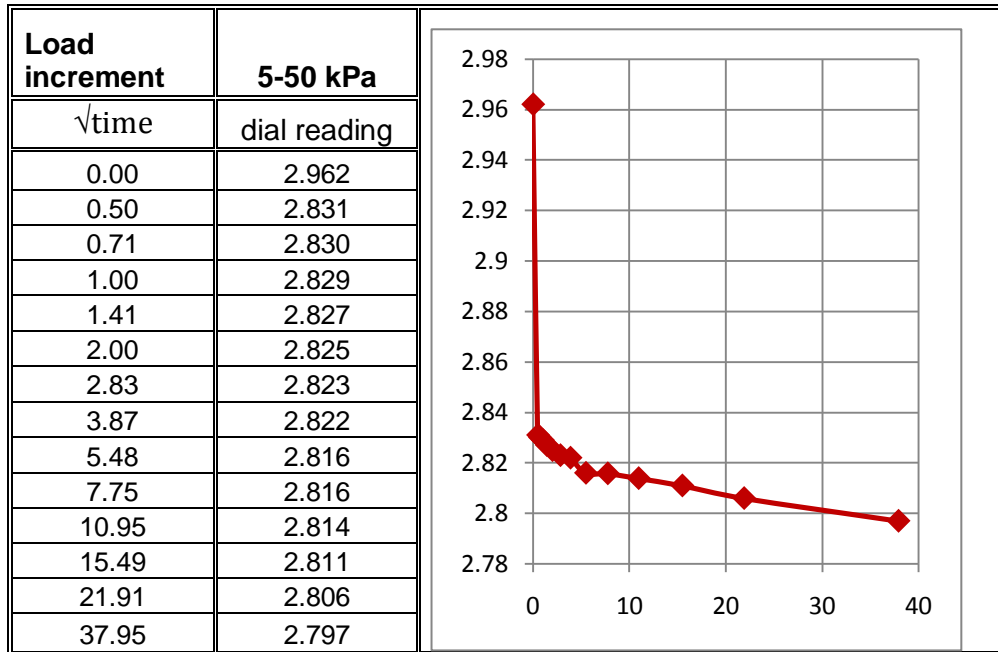


Load increment	100-200 kPa
$\sqrt{\text{time}}$	dial reading
0.00	3.967
0.50	3.298
0.71	3.280
1.00	3.256
1.41	3.226
2.00	3.203
2.83	3.187
3.87	3.174
5.48	3.164
7.75	3.154
10.95	3.142
15.49	3.134
21.91	3.122
37.95	3.114

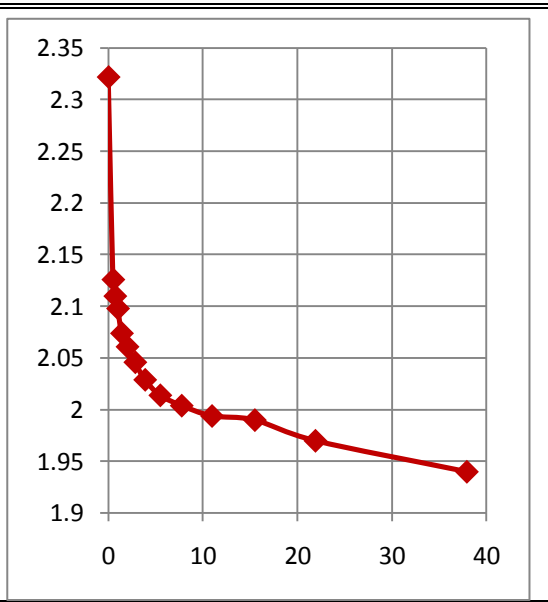




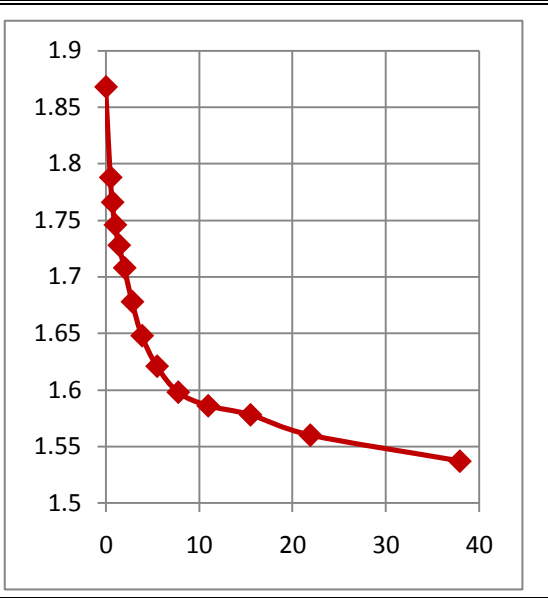
Sample No.	TP2-2	Location: Atena Tera	
Sample Depth, m:	3.00		
[A] In the beginning of the test		[B] In the end of the test	
Sample type :	Disturbed	Final Moisture Content,%	34.07
Ring Area,cm ² :	19.625	Dry specimen wt (ms), gm:	52.70
Height of sample,mm:	20	Dry density,g/cm ³	0.90
Seating Load,Kpa	5	Height of Solids(Hs), mm	9.74
Initial Void Ratio, eo:	1.05	Final Void Ratio, ef:	0.83
Initial moisture content,%	33.06		
Specific Gravity:	2.76		
Wet density,g/cm ³	1.82		



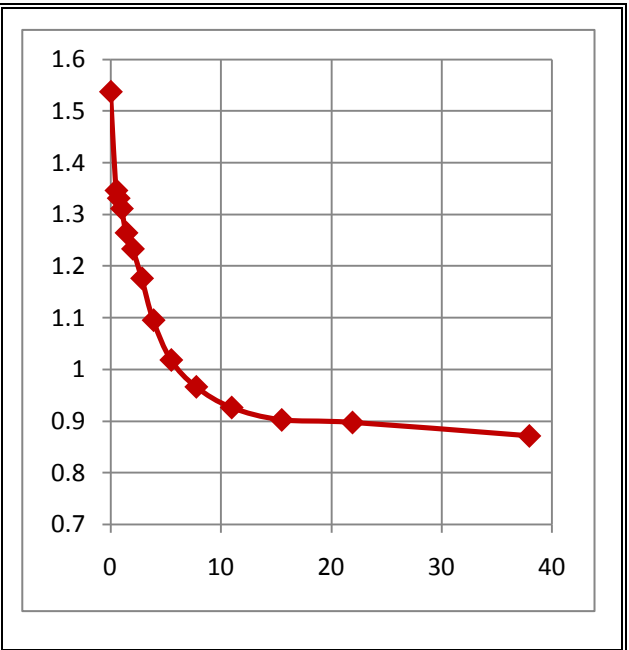
Load increment	200-400 kPa
$\sqrt{\text{time}}$	dial reading
0.00	2.322
0.50	2.126
0.71	2.110
1.00	2.098
1.41	2.074
2.00	2.061
2.83	2.046
3.87	2.029
5.48	2.014
7.75	2.004
10.95	1.994
15.49	1.990
21.91	1.970
37.95	1.940



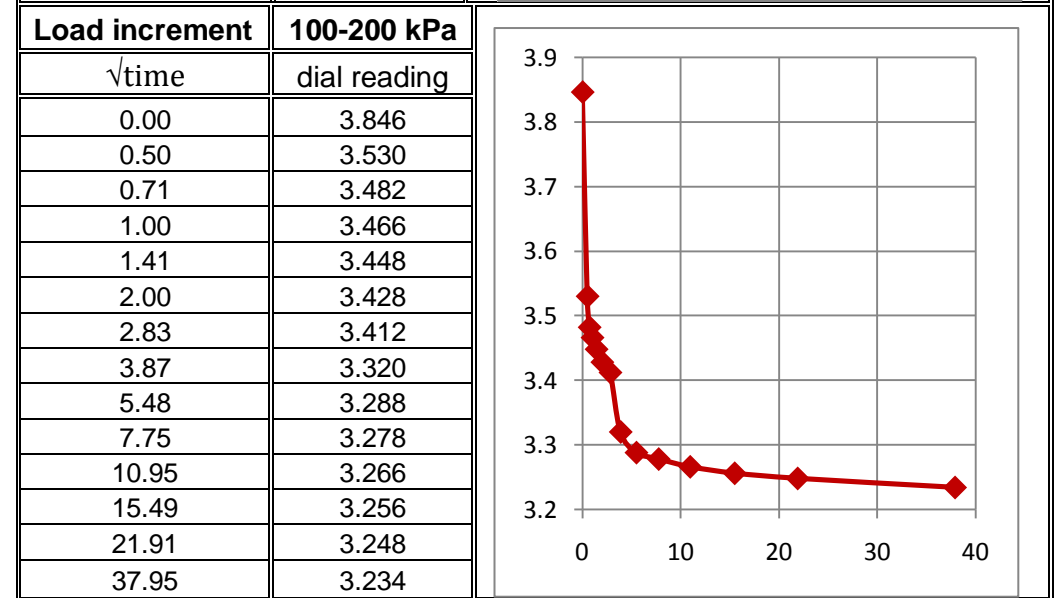
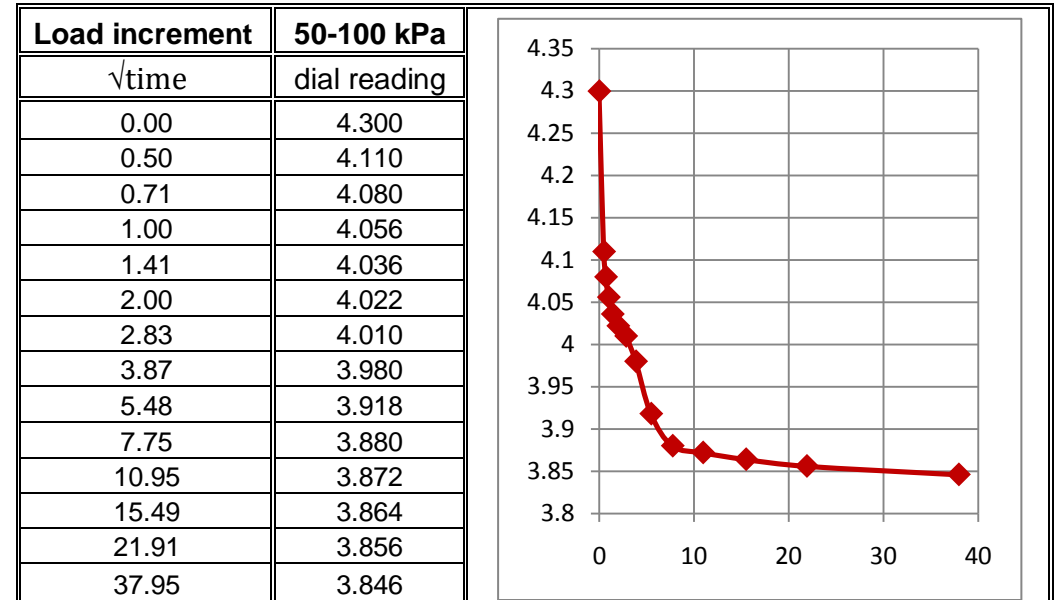
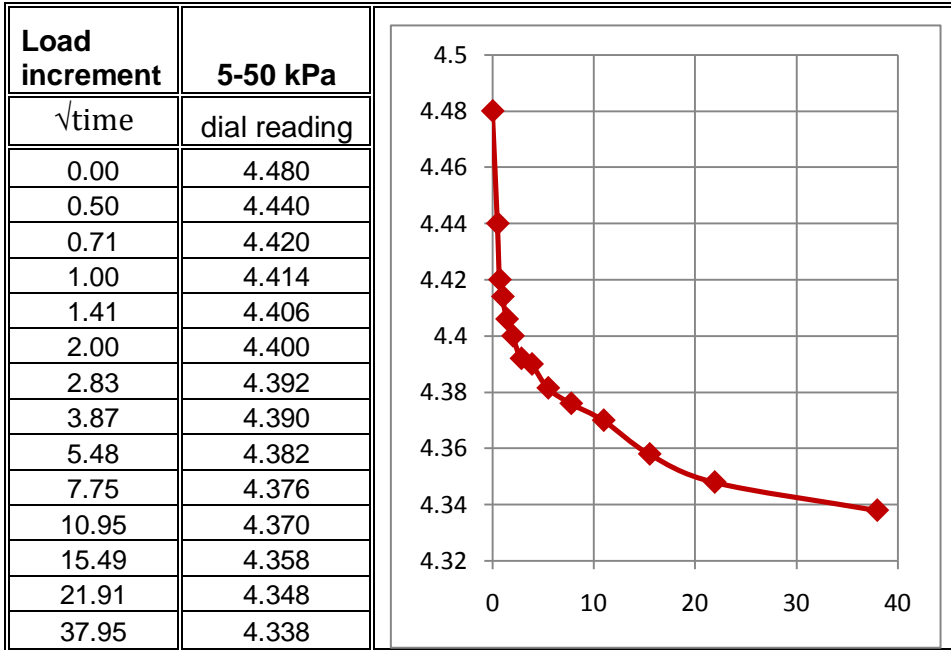
Load increment	400-800 kPa
$\sqrt{\text{time}}$	dial reading
0.00	1.868
0.50	1.788
0.71	1.766
1.00	1.746
1.41	1.728
2.00	1.708
2.83	1.678
3.87	1.648
5.48	1.621
7.75	1.598
10.95	1.586
15.49	1.578
21.91	1.560
37.95	1.537



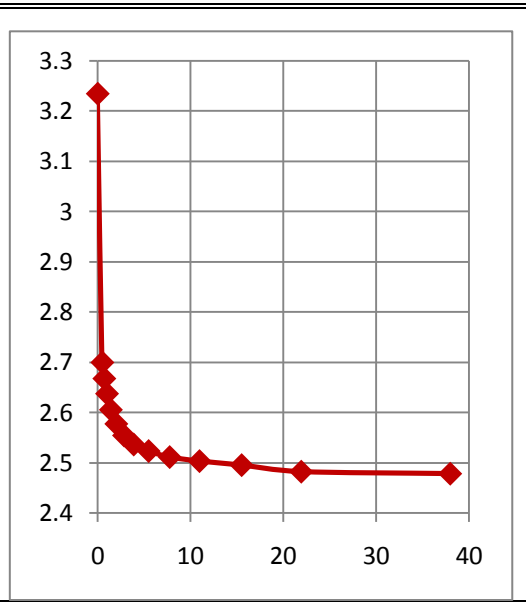
Load increment	800-1600 kPa
$\sqrt{\text{time}}$	dial reading
0.00	1.537
0.50	1.346
0.71	1.331
1.00	1.311
1.41	1.264
2.00	1.233
2.83	1.176
3.87	1.095
5.48	1.018
7.75	0.966
10.95	0.926
15.49	0.902
21.91	0.897
37.95	0.871



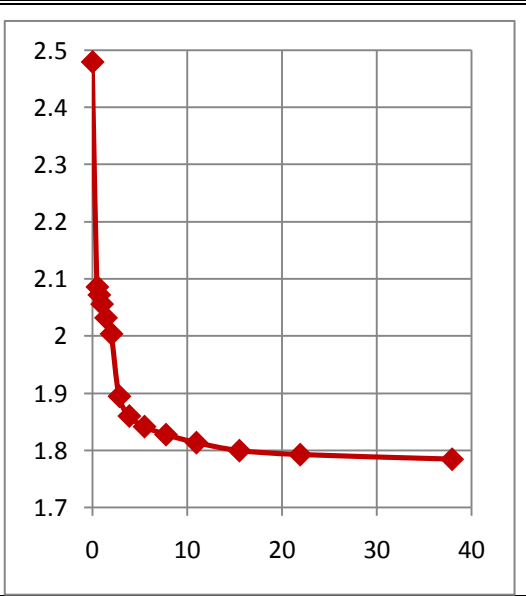
Sample No.:	TP3-1	Location:	Athari
Sample Depth, m:	1.50		
[A] In the beginning of the test		[B] In the end of the test	
Sample type:	Disturbed	Final Moisture Content, %	31.66
Ring Area, cm ² :	19.625	Dry specimen wt (ms), gm:	53.71
Height of sample, mm:	20	Dry density, g/cm ³	0.90
Seating Load, Kpa	5	Height of Solids(Hs), mm	10.16
Initial Void Ratio, eo:	0.92	Final Void Ratio, ef:	0.57
Initial moisture content, %	29.00		
Specific Gravity:	2.70		
Wet density, g/cm ³	1.96		



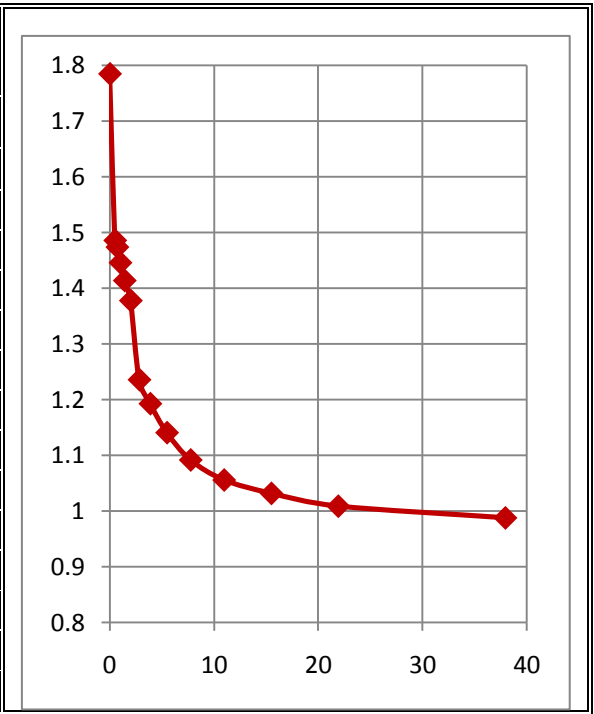
Load increment	200-400 kPa
$\sqrt{\text{time}}$	dial reading
0.00	3.234
0.50	2.700
0.71	2.668
1.00	2.638
1.41	2.606
2.00	2.578
2.83	2.555
3.87	2.537
5.48	2.524
7.75	2.512
10.95	2.504
15.49	2.496
21.91	2.483
37.95	2.479



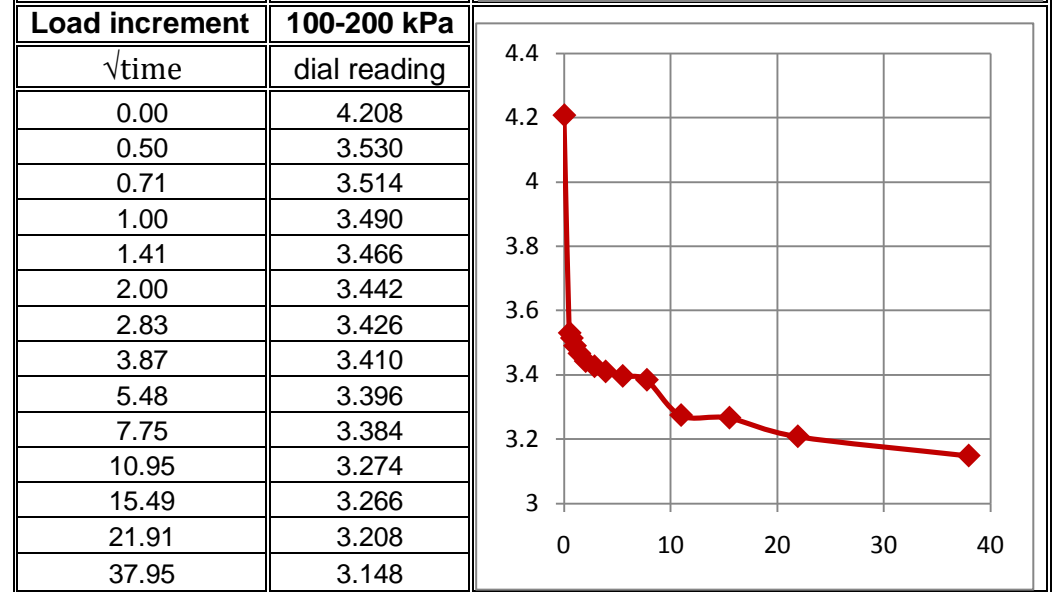
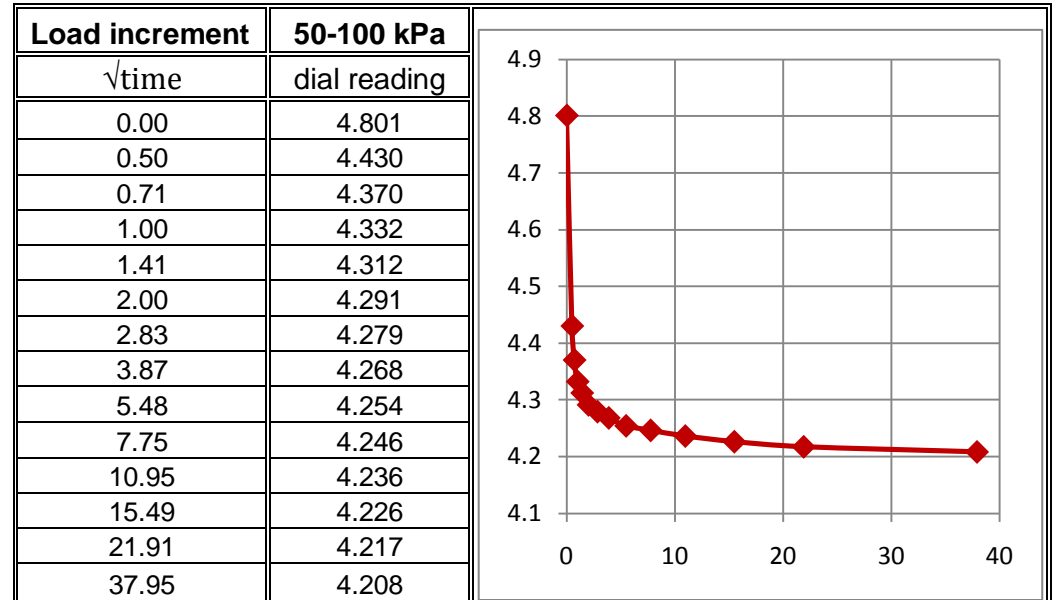
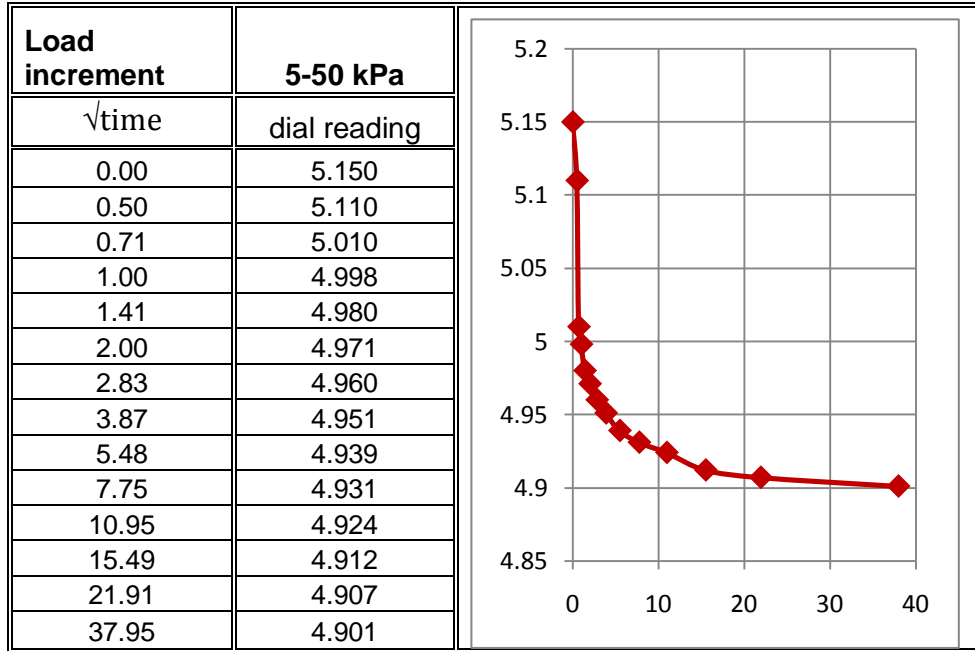
Load increment	400-800 kPa
$\sqrt{\text{time}}$	dial reading
0.00	2.479
0.50	2.086
0.71	2.072
1.00	2.056
1.41	2.032
2.00	2.004
2.83	1.895
3.87	1.861
5.48	1.842
7.75	1.828
10.95	1.814
15.49	1.800
21.91	1.793
37.95	1.785

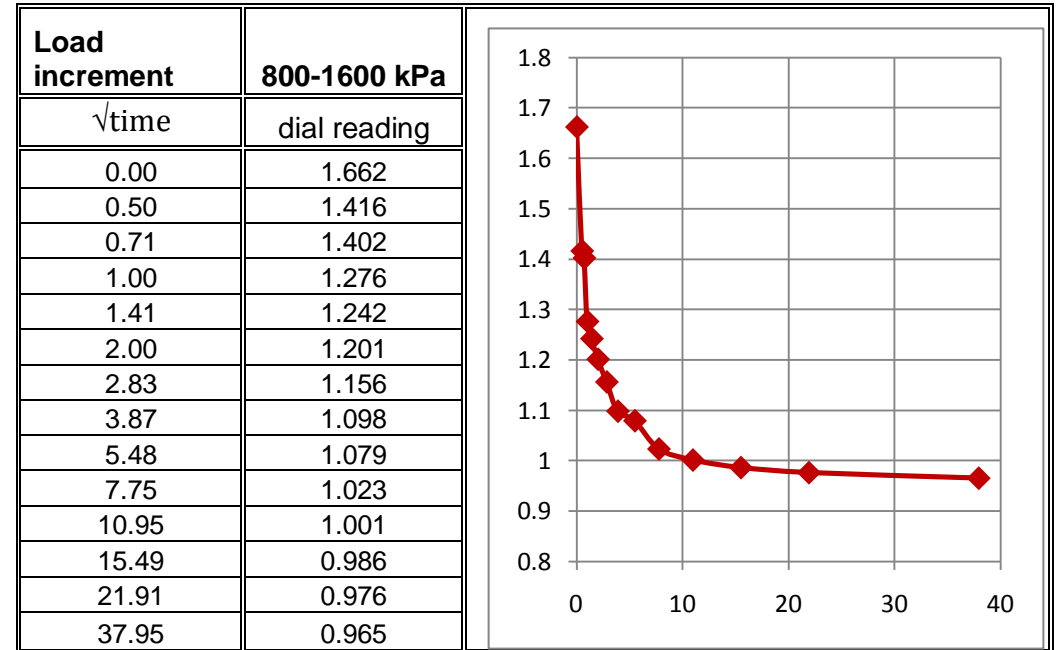
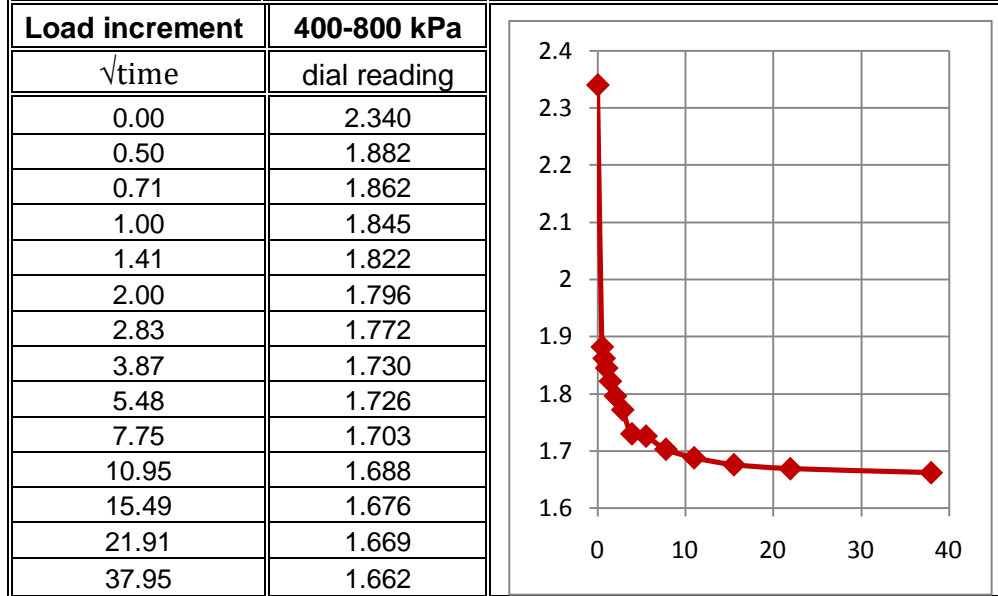
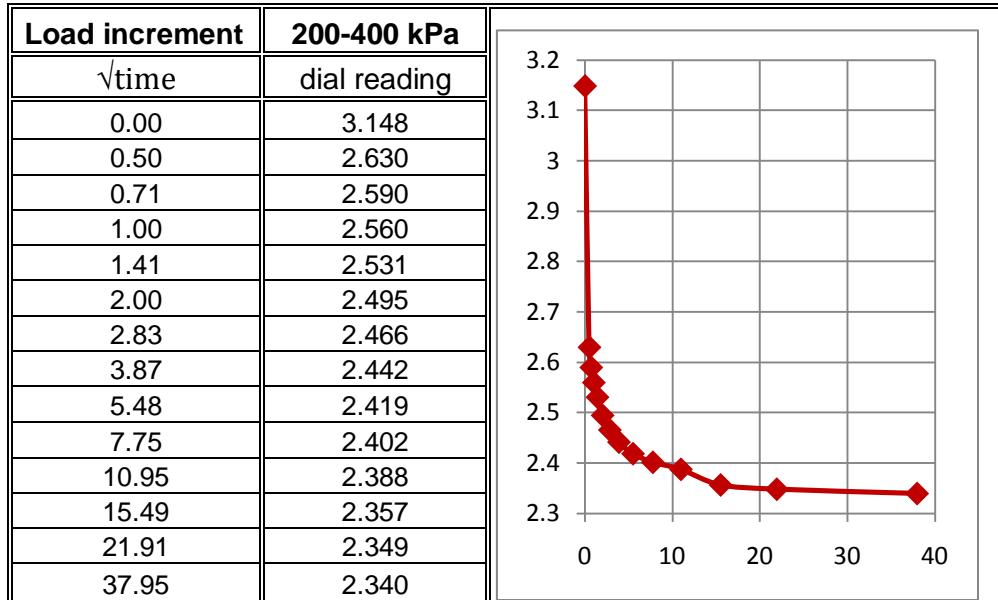


Load increment	800-1600 kPa
$\sqrt{\text{time}}$	dial reading
0.00	1.785
0.50	1.486
0.71	1.474
1.00	1.446
1.41	1.414
2.00	1.378
2.83	1.236
3.87	1.193
5.48	1.141
7.75	1.092
10.95	1.056
15.49	1.032
21.91	1.009
37.95	0.988

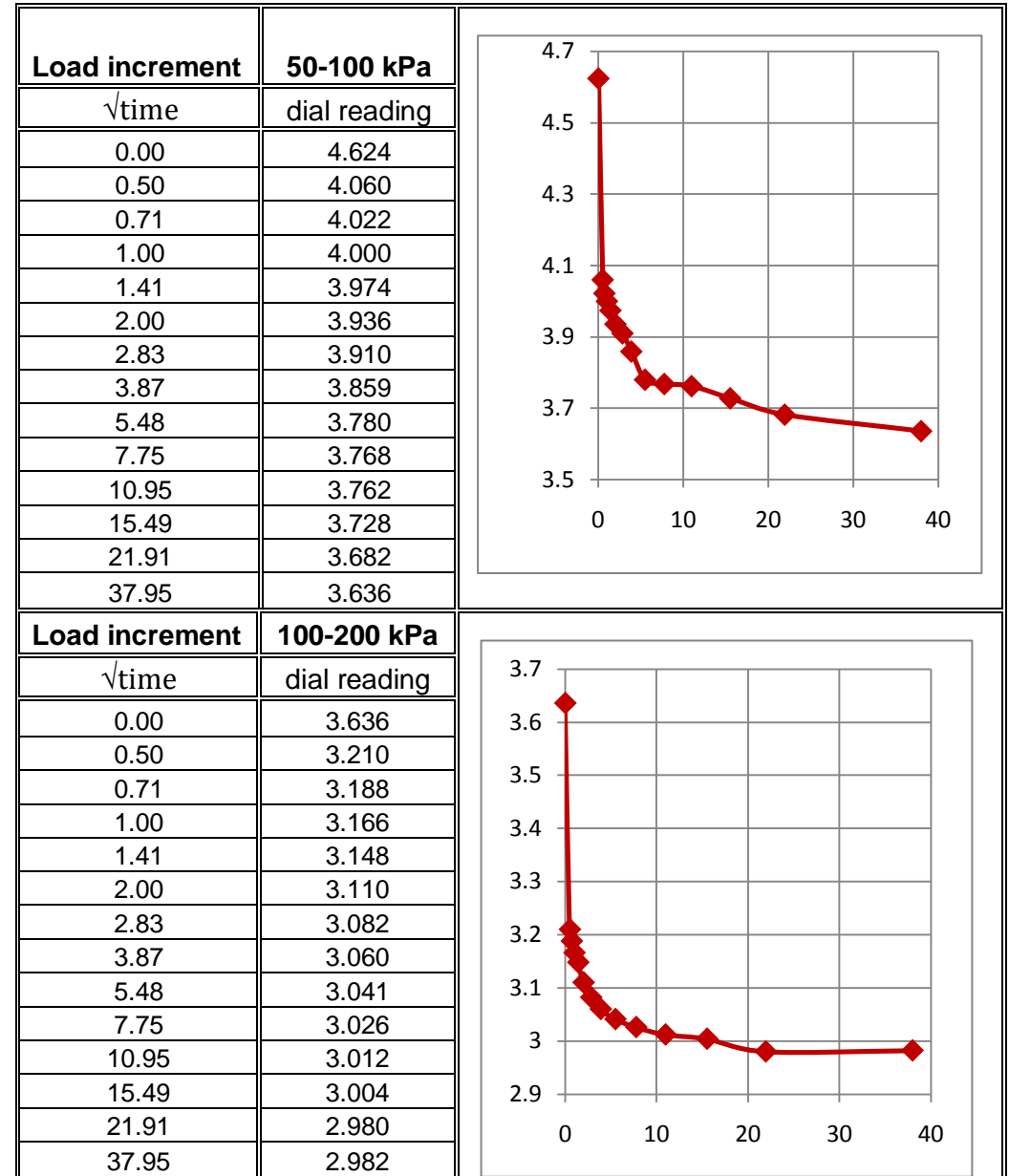
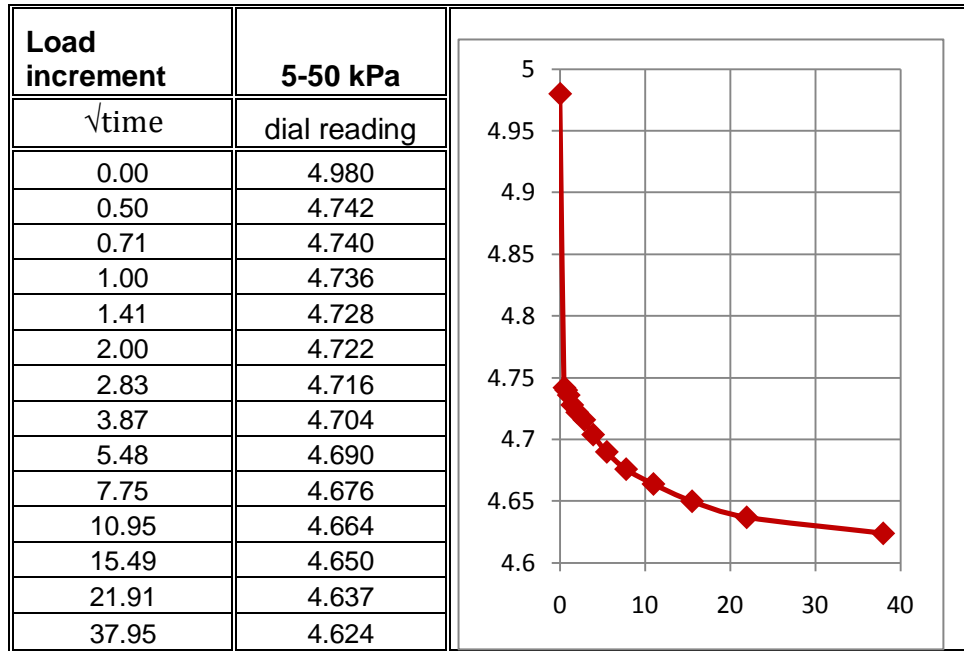


Sample No.:	TP3-2	Location: Athari	
Sample Depth, m:	3.00		
[A] In the beginning of the test		[B] In the end of the test	
Sample type :	Disturbed	Final Moisture Content, %	28.74
Ring Area, cm ² :	19.625	Dry specimen wt (ms), gm:	54.02
Height of sample, mm:	20	Dry density, g/cm ³	1.17
Seating Load, Kpa	5	Height of Solids(Hs), mm	10.14
Initial Void Ratio, eo:	0.89	Final Void Ratio, ef:	0.48
Initial moisture content, %	31.00		
Specific Gravity:	2.71		
Wet density, g/cm ³	1.92		

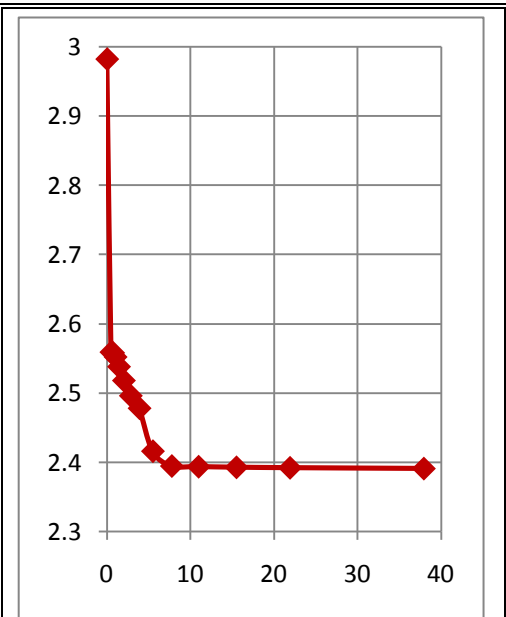




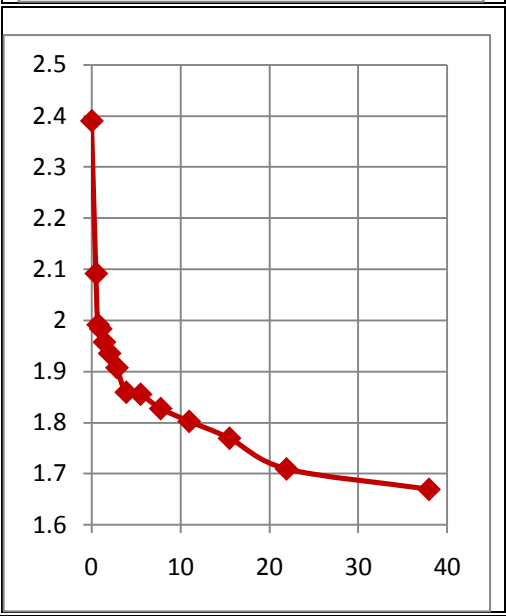
Sample No.	TP4-1	Location: Awelya	
Sample Depth, m:	1.50		
[A] In the beginning of the test		[B] In the end of the test	
Sample type :	Disturbed	Final Moisture Content, %	28.33
Ring Area, cm ² :	19.625	Dry specimen wt (ms), gm:	58.73
Height of sample, mm:	20	Dry density, g/cm ³	0.76
Seating Load, Kpa	5	Height of Solids(Hs), mm	10.85
Initial Void Ratio, e _o :	0.84	Final Void Ratio, e _f :	0.48
Initial moisture content, %	24.00		
Specific Gravity:	2.76		
Wet density, g/cm ³	1.96		



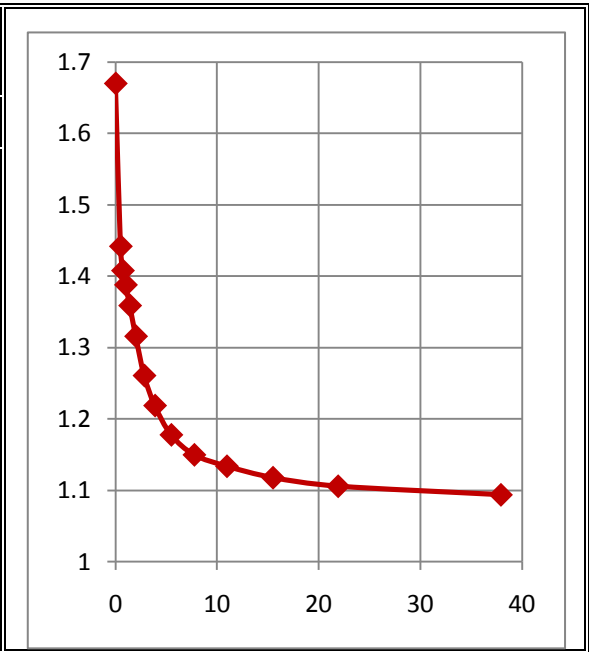
Load increment	200-400 kPa
$\sqrt{\text{time}}$	dial reading
0.00	2.982
0.50	2.559
0.71	2.558
1.00	2.552
1.41	2.538
2.00	2.518
2.83	2.496
3.87	2.478
5.48	2.416
7.75	2.395
10.95	2.394
15.49	2.393
21.91	2.392
37.95	2.391



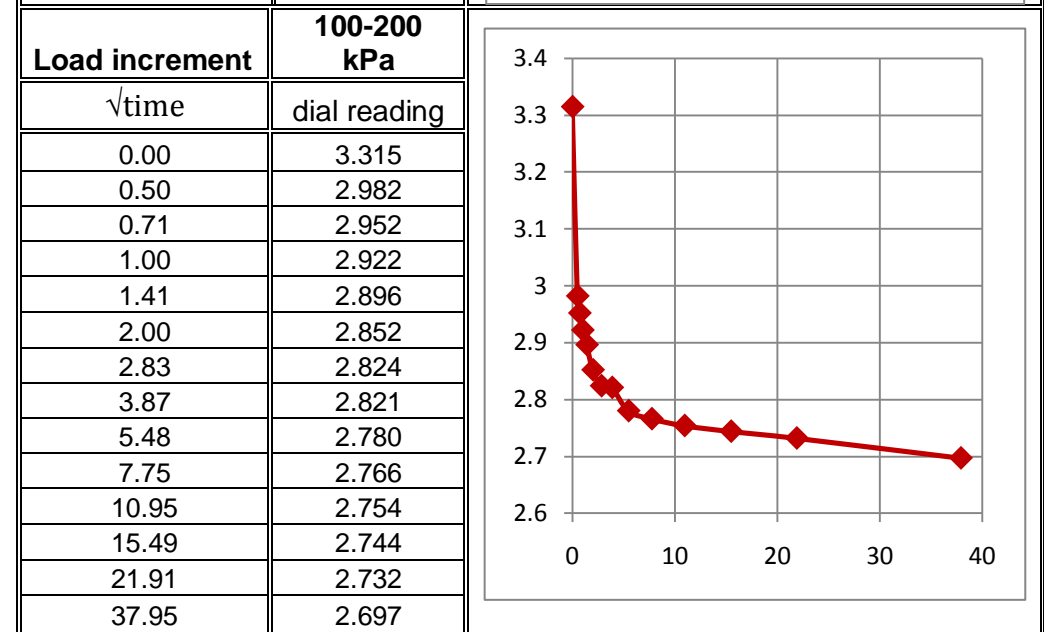
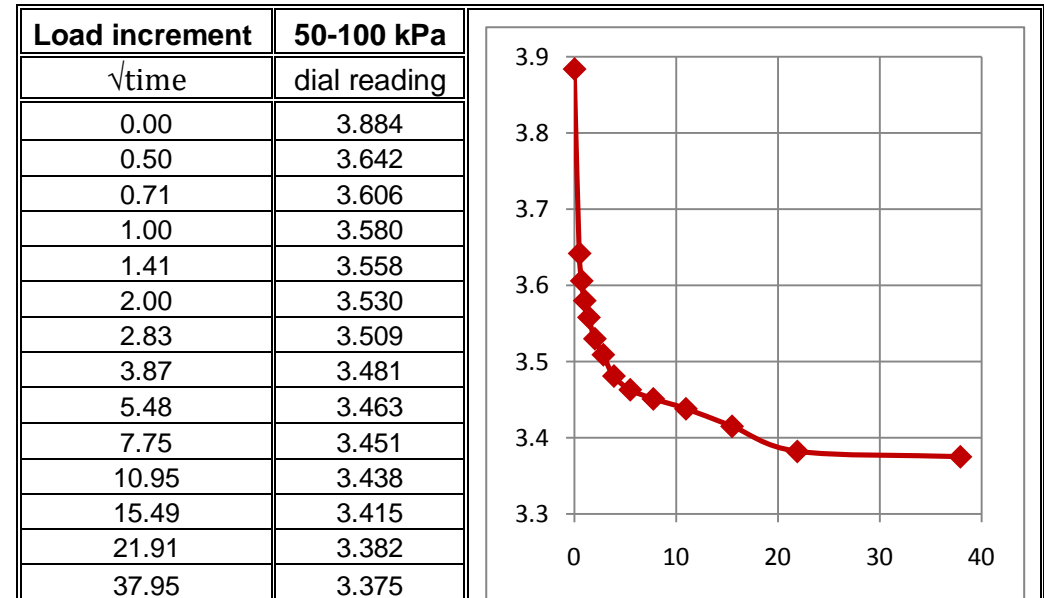
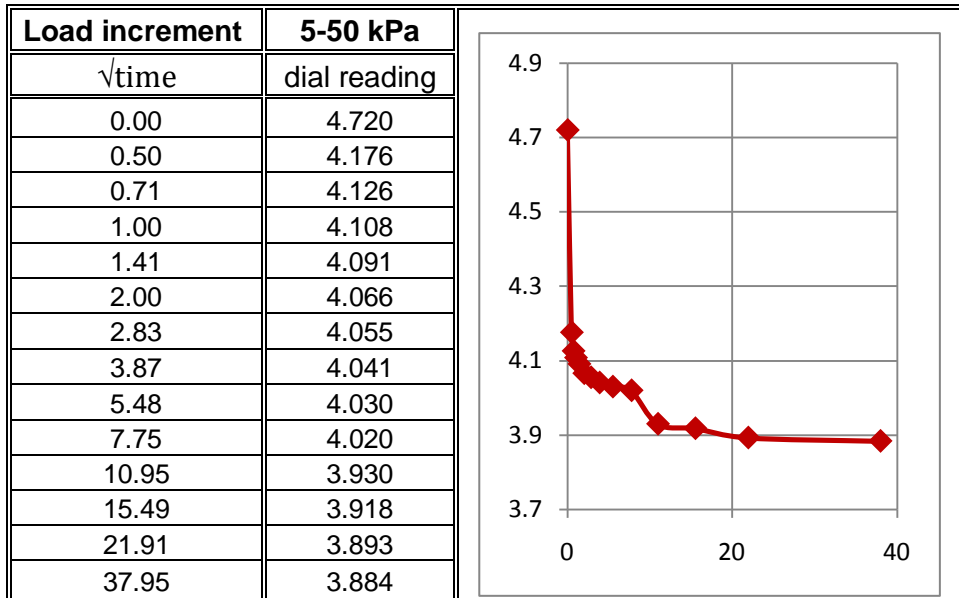
Load increment	400-800 kPa
$\sqrt{\text{time}}$	dial reading
0.00	2.391
0.50	2.092
0.71	1.992
1.00	1.984
1.41	1.958
2.00	1.936
2.83	1.908
3.87	1.860
5.48	1.856
7.75	1.828
10.95	1.803
15.49	1.770
21.91	1.710
37.95	1.670



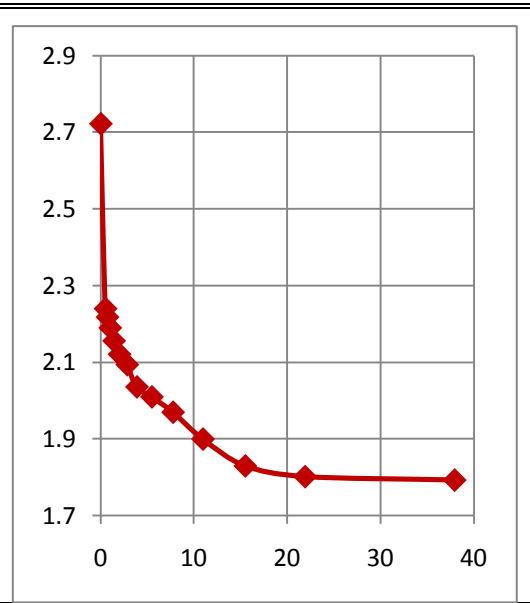
Load increment	800-1600 kPa
$\sqrt{\text{time}}$	dial reading
0.00	1.670
0.50	1.442
0.71	1.408
1.00	1.388
1.41	1.359
2.00	1.316
2.83	1.261
3.87	1.219
5.48	1.178
7.75	1.150
10.95	1.134
15.49	1.118
21.91	1.106
37.95	1.094



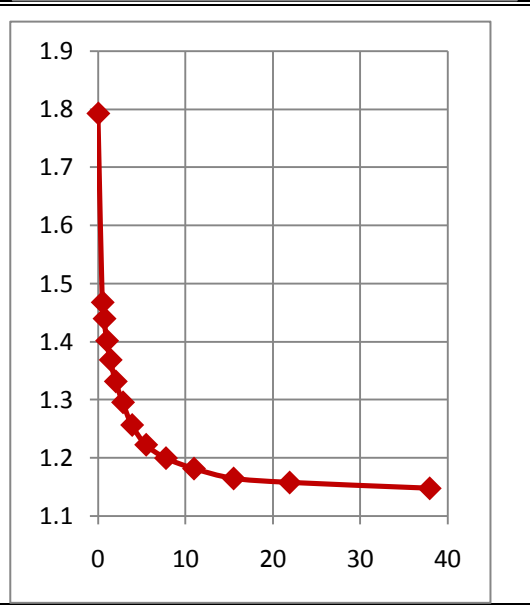
Sample No.:	TP4-2	Location:	Awelya
Sample Depth, m:	3.00		
[A] In the beginning of the test		[B] In the end of the test	
Sample type :	Disturbed	Final Moisture Content, %	48.62
Ring Area, cm ² :	19.625	Dry specimen wt (ms), gm:	67.32
Height of sample, mm:	20	Dry density, g/cm ³	1.07
Seating Load, Kpa	5	Height of Solids(Hs), mm	12.54
Initial Void Ratio, eo:	0.57	Final Void Ratio, ef:	0.23
Initial moisture content, %	24.50		
Specific Gravity:	2.74		
Wet density, g/cm ³	1.97		



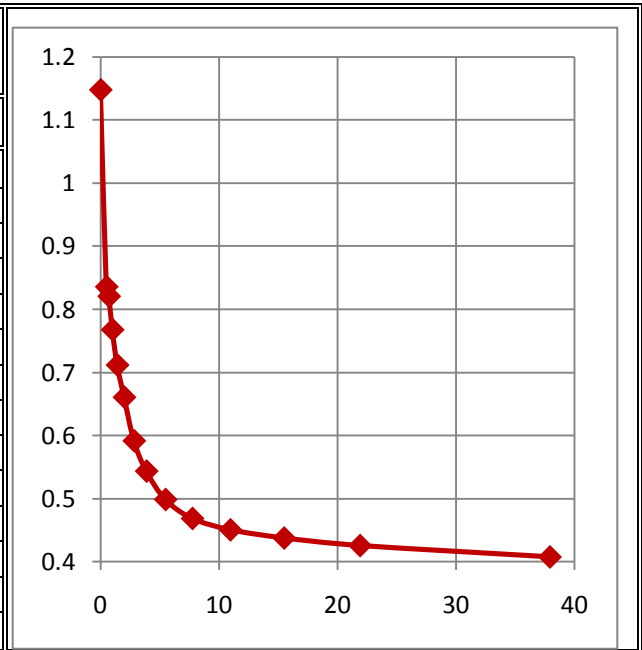
Load increment	200-400 kPa
$\sqrt{\text{time}}$	dial reading
0.00	2.722
0.50	2.240
0.71	2.218
1.00	2.190
1.41	2.156
2.00	2.121
2.83	2.094
3.87	2.036
5.48	2.010
7.75	1.970
10.95	1.900
15.49	1.830
21.91	1.802
37.95	1.793



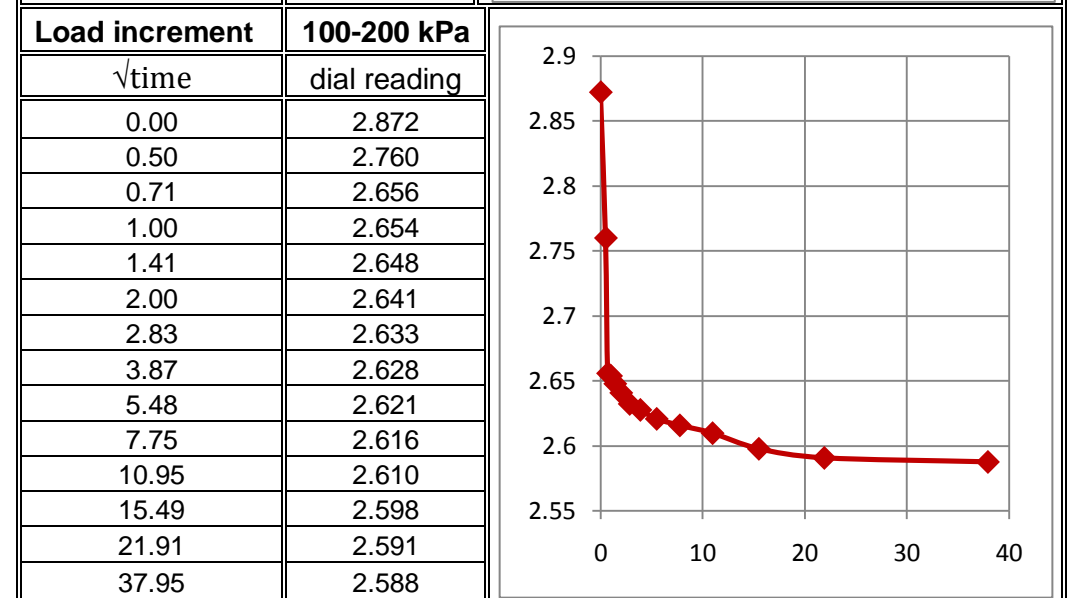
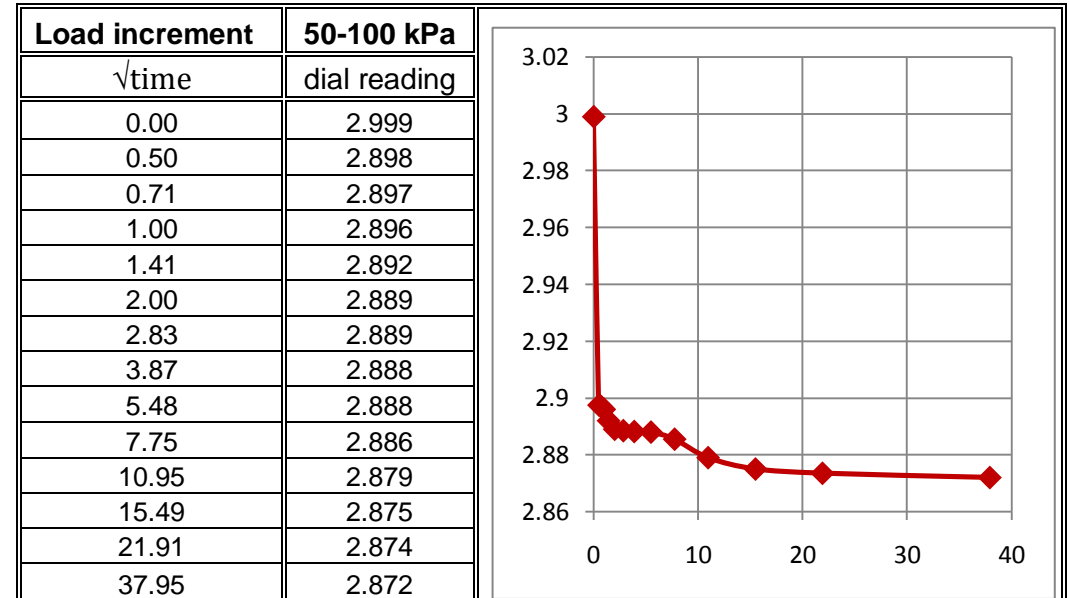
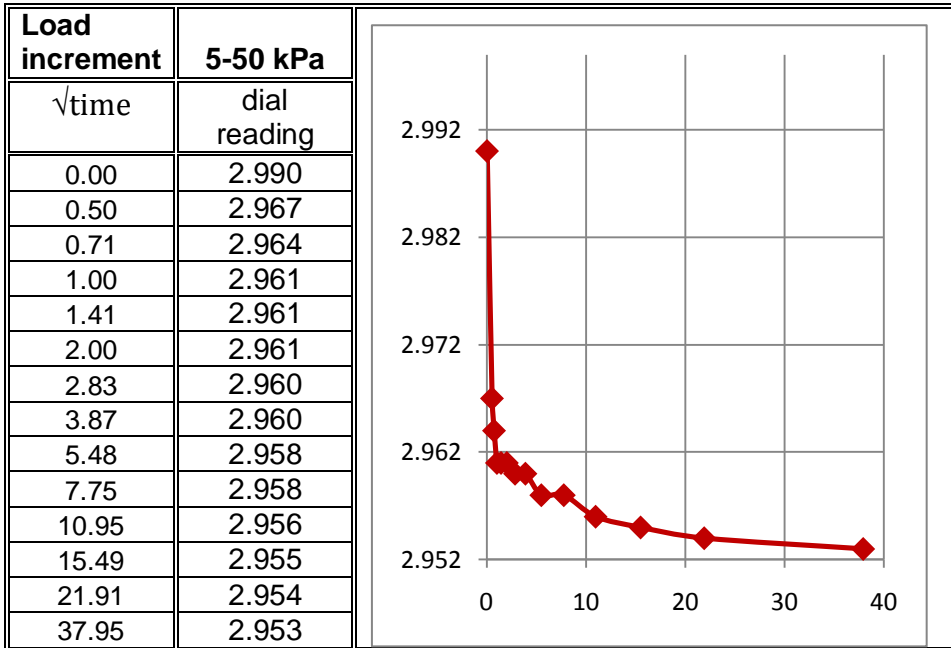
Load increment	400-800 kPa
$\sqrt{\text{time}}$	dial reading
0.00	1.793
0.50	1.468
0.71	1.440
1.00	1.402
1.41	1.369
2.00	1.332
2.83	1.296
3.87	1.257
5.48	1.223
7.75	1.200
10.95	1.182
15.49	1.165
21.91	1.158
37.95	1.148



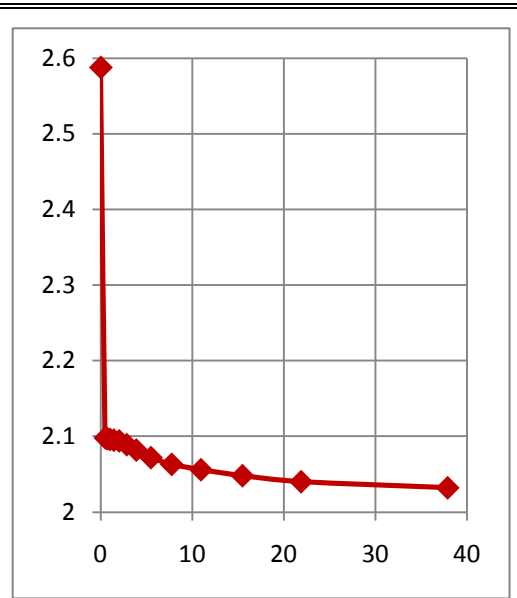
Load increment	800-1600 kPa
$\sqrt{\text{time}}$	dial reading
0.00	1.148
0.50	0.836
0.71	0.821
1.00	0.768
1.41	0.712
2.00	0.661
2.83	0.592
3.87	0.544
5.48	0.499
7.75	0.469
10.95	0.451
15.49	0.438
21.91	0.426
37.95	0.408



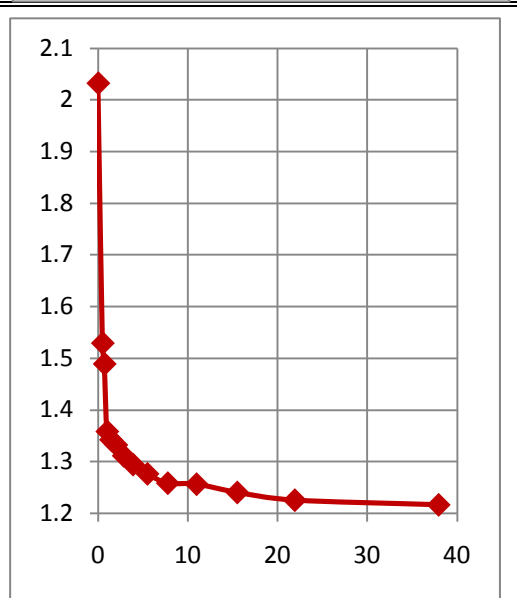
Sample No.	TP5-1	Location:	Kolfe
Sample Depth, m:	1.50		
[A] In the beginning of the test		[B] In the end of the test	
Sample type :	Disturbed	Final Moisture Content, %	28.09
Ring Area, cm ² :	19.625	Dry specimen wt (ms), gm:	56.05
Height of sample, mm:	20	Dry density, g/cm ³	1.02
Seating Load, Kpa	5	Height of Solids(Hs), mm	10.75
Initial Void Ratio, eo:	0.86	Final Void Ratio, ef:	0.63
Initial moisture content, %	24.30		
Specific Gravity:	2.66		
Wet density, g/cm ³	1.93		



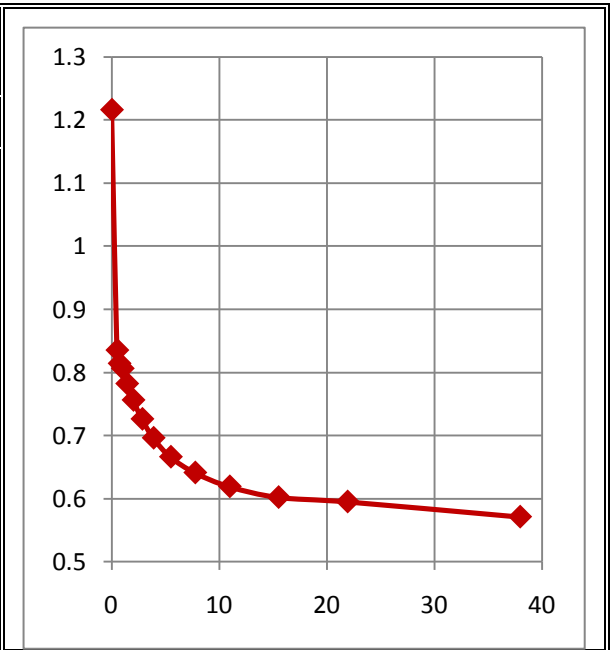
Load increment	200-400 kPa
$\sqrt{\text{time}}$	dial reading
0.00	2.588
0.50	2.098
0.71	2.097
1.00	2.096
1.41	2.095
2.00	2.094
2.83	2.089
3.87	2.082
5.48	2.072
7.75	2.063
10.95	2.056
15.49	2.048
21.91	2.040
37.95	2.032



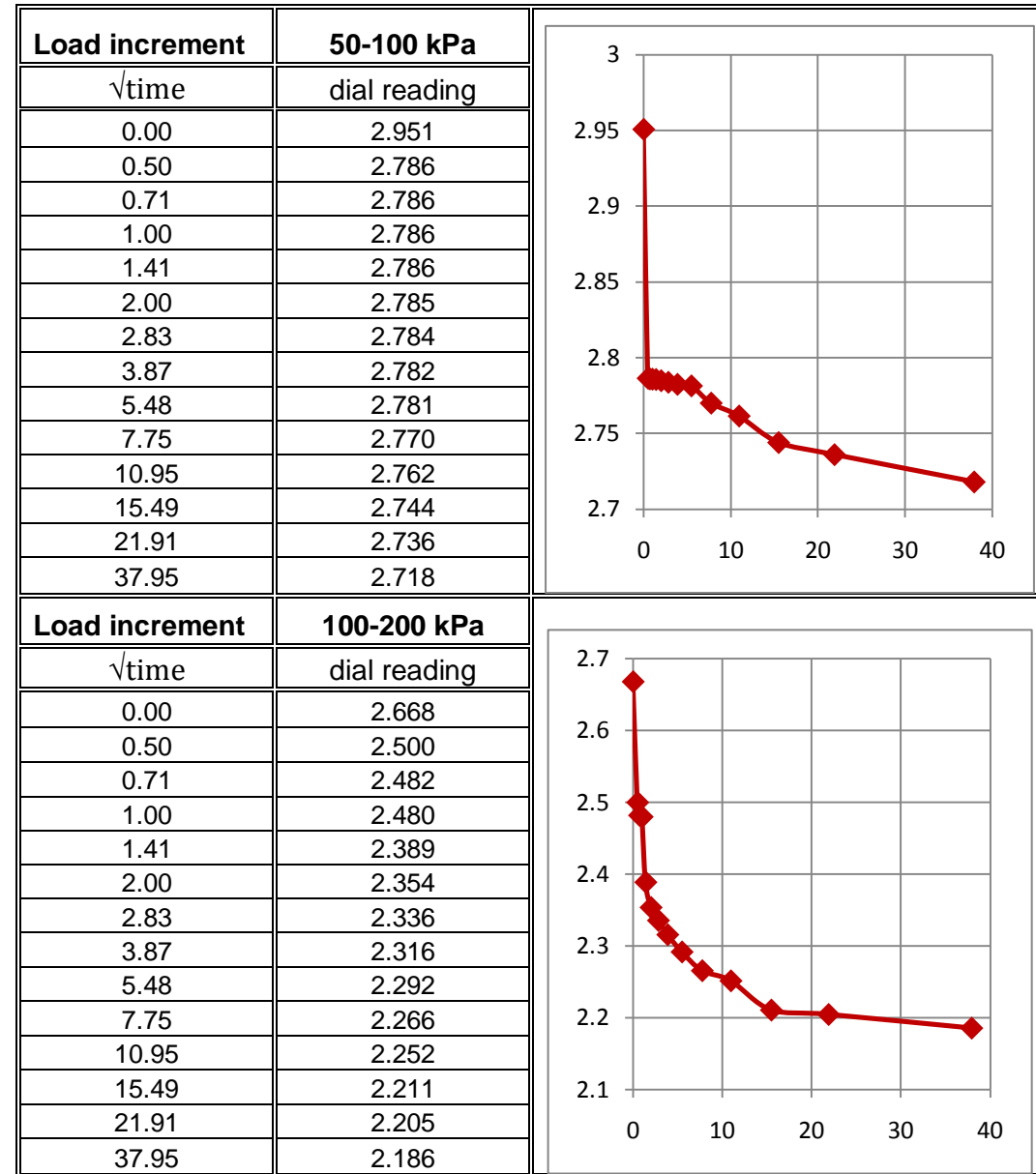
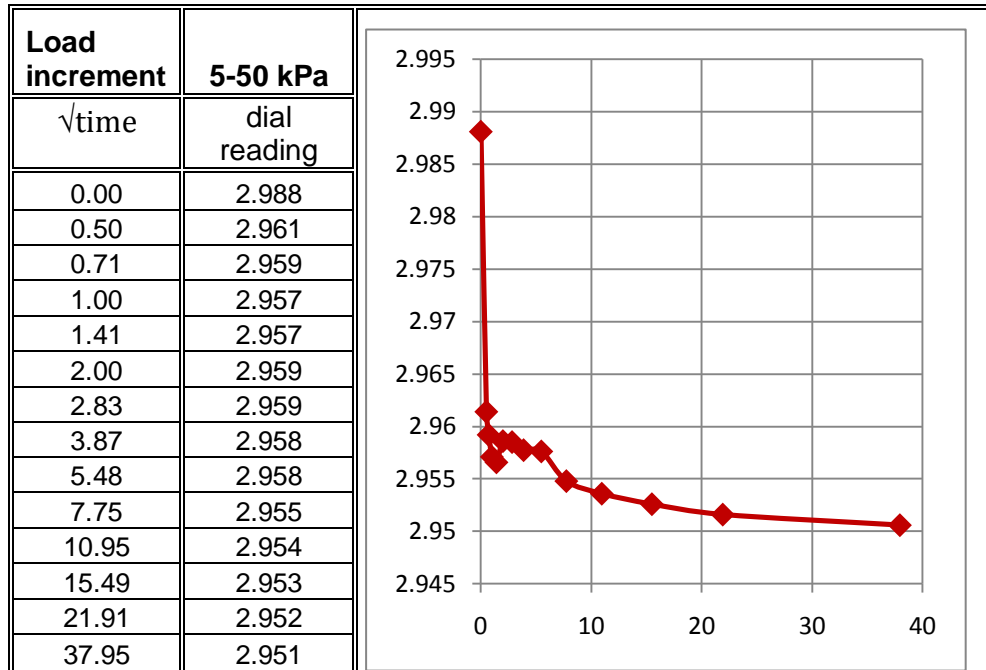
Load increment	400-800 kPa
$\sqrt{\text{time}}$	dial reading
0.00	2.032
0.50	1.529
0.71	1.489
1.00	1.358
1.41	1.342
2.00	1.332
2.83	1.311
3.87	1.294
5.48	1.276
7.75	1.258
10.95	1.256
15.49	1.240
21.91	1.225
37.95	1.216



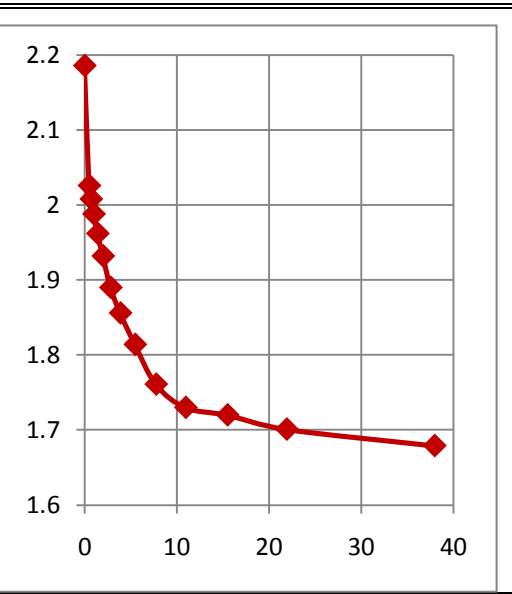
Load increment	800-1600 kPa
$\sqrt{\text{time}}$	dial reading
0.00	1.216
0.50	0.835
0.71	0.814
1.00	0.806
1.41	0.782
2.00	0.756
2.83	0.726
3.87	0.696
5.48	0.666
7.75	0.641
10.95	0.619
15.49	0.602
21.91	0.595
37.95	0.571



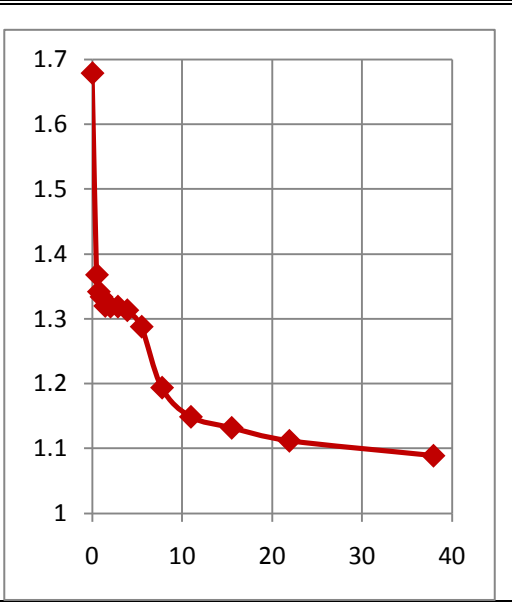
Sample No.:	TP5-2	Location:	Kolfe
Sample Depth, m:	3.00		
[A] In the beginning of the test		[B] In the end of the test	
Sample type :	Disturbed	Final Moisture Content, %	32.78
Ring Area, cm ² :	19.625	Dry specimen wt (ms), gm:	52.51
Height of sample, mm:	20	Dry density, g/cm ³	1.02
Seating Load, Kpa	5	Height of Solids(Hs), mm	9.78
Initial Void Ratio, eo:	1.04	Final Void Ratio, ef:	0.81
Initial moisture content, %	26.00		
Specific Gravity:	2.74		
Wet density, g/cm ³	1.92		



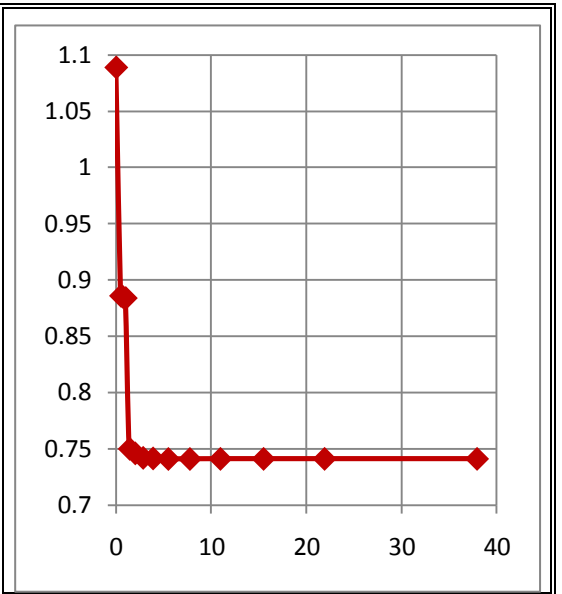
Load increment	200-400 kPa
$\sqrt{\text{time}}$	dial reading
0.00	2.186
0.50	2.026
0.71	2.008
1.00	1.988
1.41	1.962
2.00	1.932
2.83	1.890
3.87	1.856
5.48	1.814
7.75	1.761
10.95	1.730
15.49	1.720
21.91	1.701
37.95	1.679



Load increment	400-800 kPa
$\sqrt{\text{time}}$	dial reading
0.00	1.679
0.50	1.368
0.71	1.342
1.00	1.334
1.41	1.320
2.00	1.319
2.83	1.319
3.87	1.313
5.48	1.288
7.75	1.194
10.95	1.149
15.49	1.132
21.91	1.112
37.95	1.089

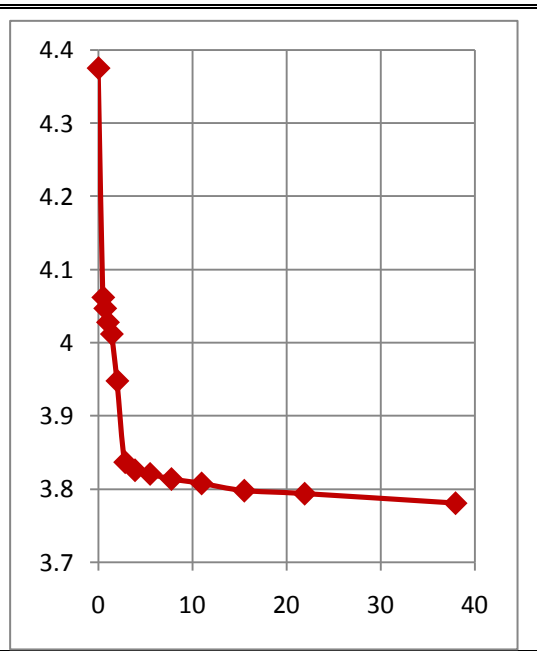


Load increment	800-1600 kPa
$\sqrt{\text{time}}$	dial reading
0.00	1.089
0.50	0.886
0.71	0.885
1.00	0.884
1.41	0.750
2.00	0.746
2.83	0.742
3.87	0.742
5.48	0.741
7.75	0.741
10.95	0.741
15.49	0.741
21.91	0.741
37.95	0.741

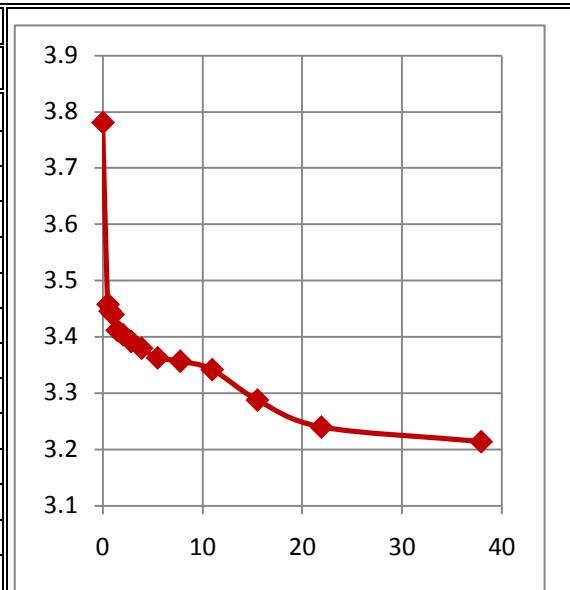


Sample No.	TP6-1	Location:	Shegole
Sample Depth, m:	1.50		
[A] In the beginning of the test		[B] In the end of the test	
Sample type :	Disturbed	Final Moisture Content,%	36.04
Ring Area,cm2:	19.625	Dry specimen wt (ms), gm:	52.85
Height of sample,mm:	20	Dry density,g/cm3	1.15
Seating Load,Kpa	5	Height of Solids(Hs), mm	9.85
Initial Void Ratio, eo:	1.07	Final Void Ratio, ef:	0.68
Initial moisture content,%	29.00		
Specific Gravity:	2.74		
Wet density,g/cm3	1.91		

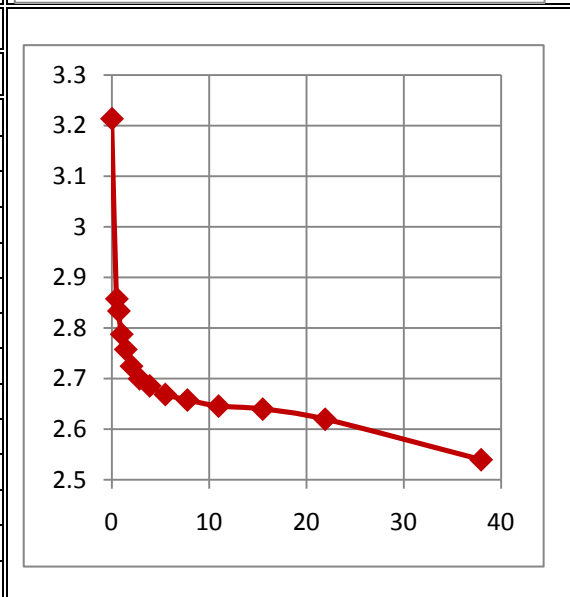
Load increment	5-50 kPa
$\sqrt{\text{time}}$	dial reading
0.00	4.375
0.50	4.062
0.71	4.047
1.00	4.028
1.41	4.012
2.00	3.948
2.83	3.837
3.87	3.826
5.48	3.821
7.75	3.814
10.95	3.808
15.49	3.798
21.91	3.794
37.95	3.781



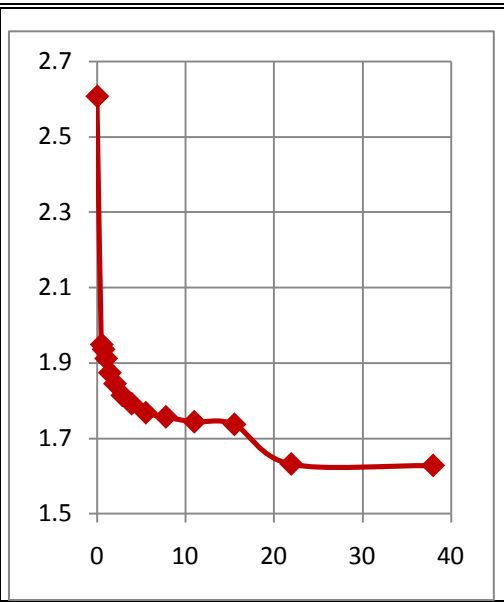
Load increment	50-100 kPa
$\sqrt{\text{time}}$	dial reading
0.00	3.781
0.50	3.458
0.71	3.446
1.00	3.440
1.41	3.412
2.00	3.404
2.83	3.392
3.87	3.380
5.48	3.363
7.75	3.357
10.95	3.342
15.49	3.288
21.91	3.240
37.95	3.214



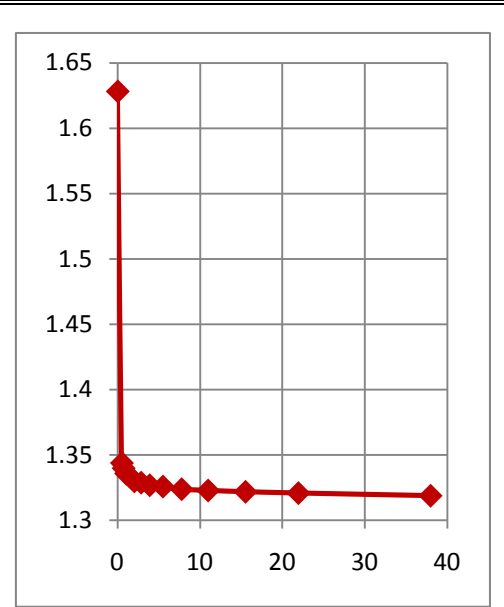
Load increment	100-200 kPa
$\sqrt{\text{time}}$	dial reading
0.00	3.214
0.50	2.858
0.71	2.834
1.00	2.788
1.41	2.758
2.00	2.725
2.83	2.700
3.87	2.686
5.48	2.669
7.75	2.658
10.95	2.646
15.49	2.640
21.91	2.620
37.95	2.540



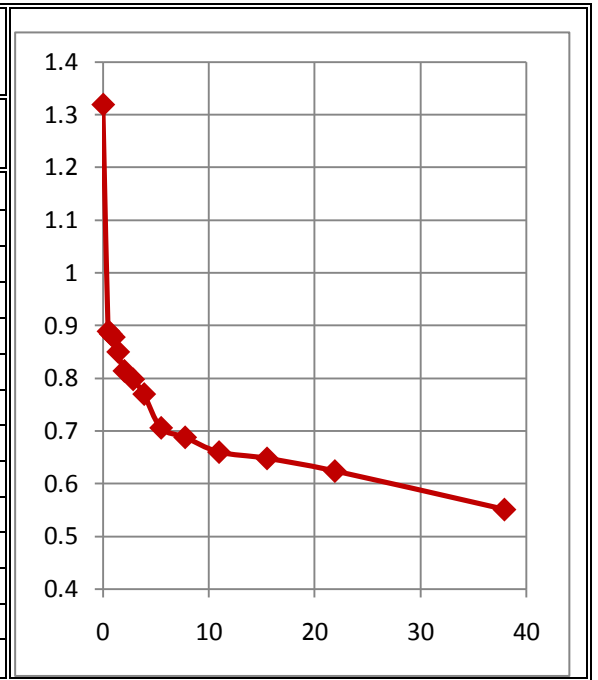
Load increment	200-400 kPa
$\sqrt{\text{time}}$	dial reading
0.00	2.608
0.50	1.949
0.71	1.936
1.00	1.912
1.41	1.874
2.00	1.845
2.83	1.814
3.87	1.792
5.48	1.768
7.75	1.757
10.95	1.744
15.49	1.737
21.91	1.632
37.95	1.628



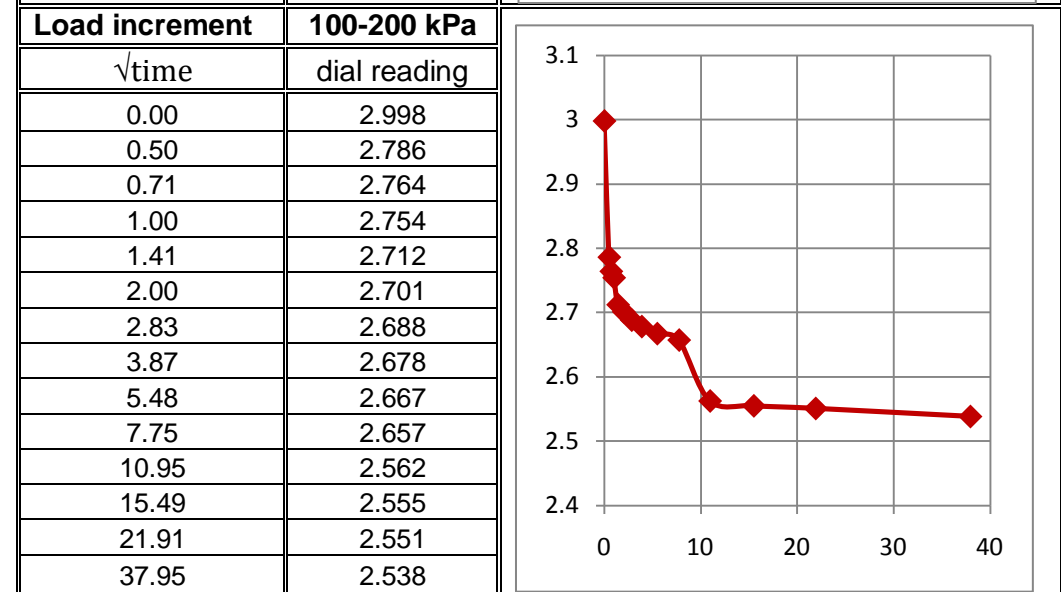
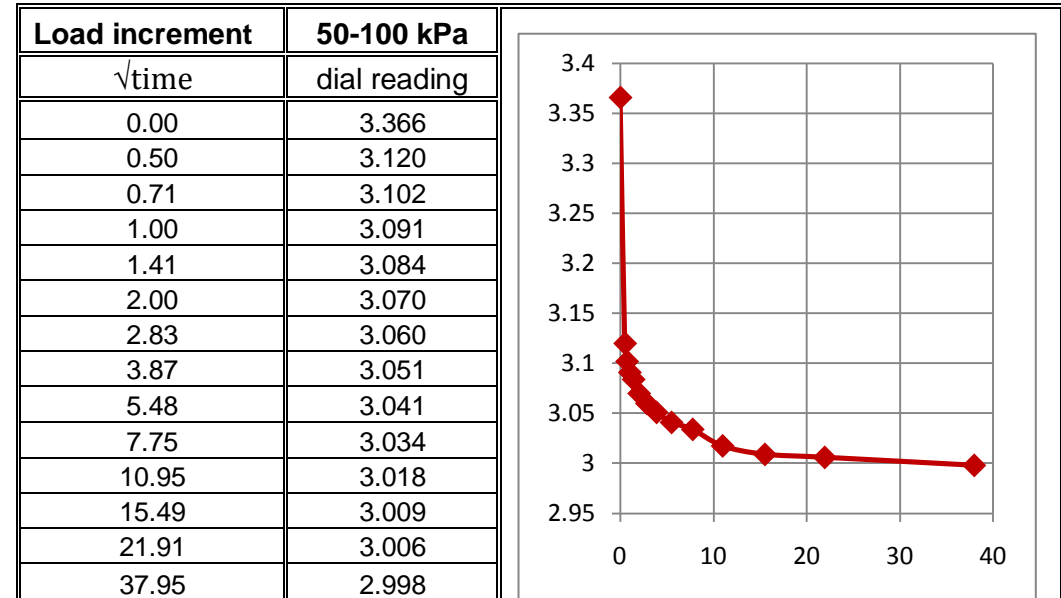
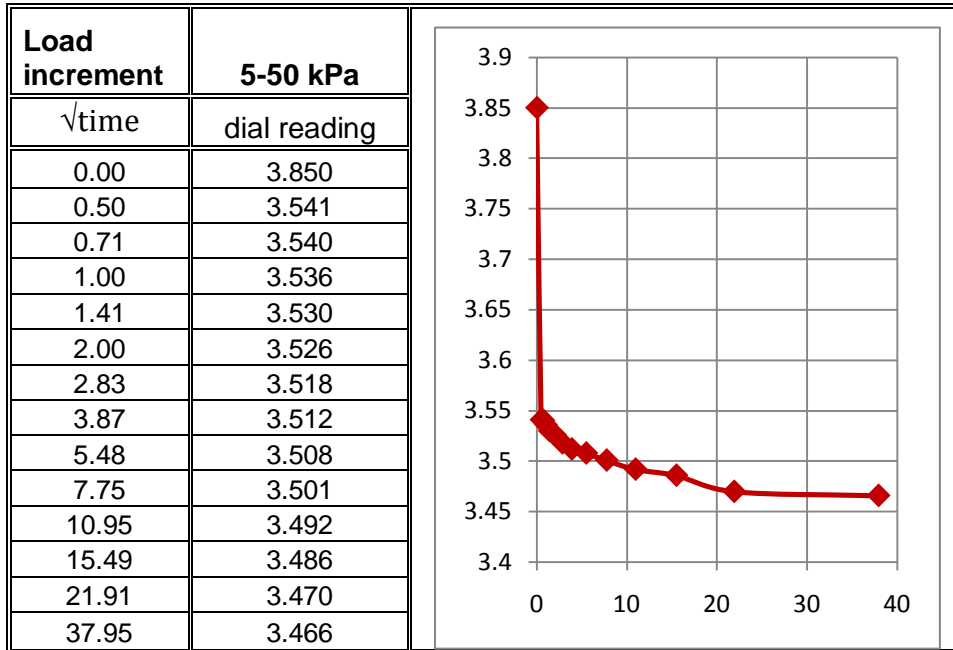
Load increment	400-800 kPa
$\sqrt{\text{time}}$	dial reading
0.00	1.628
0.50	1.344
0.71	1.340
1.00	1.336
1.41	1.334
2.00	1.330
2.83	1.329
3.87	1.327
5.48	1.326
7.75	1.324
10.95	1.323
15.49	1.322
21.91	1.321
37.95	1.319

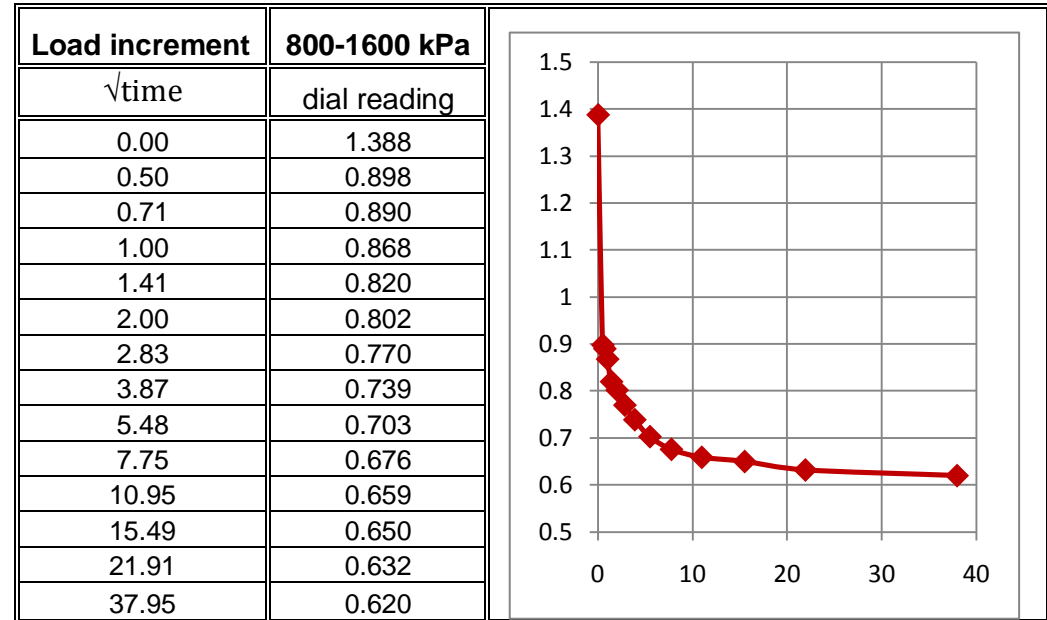
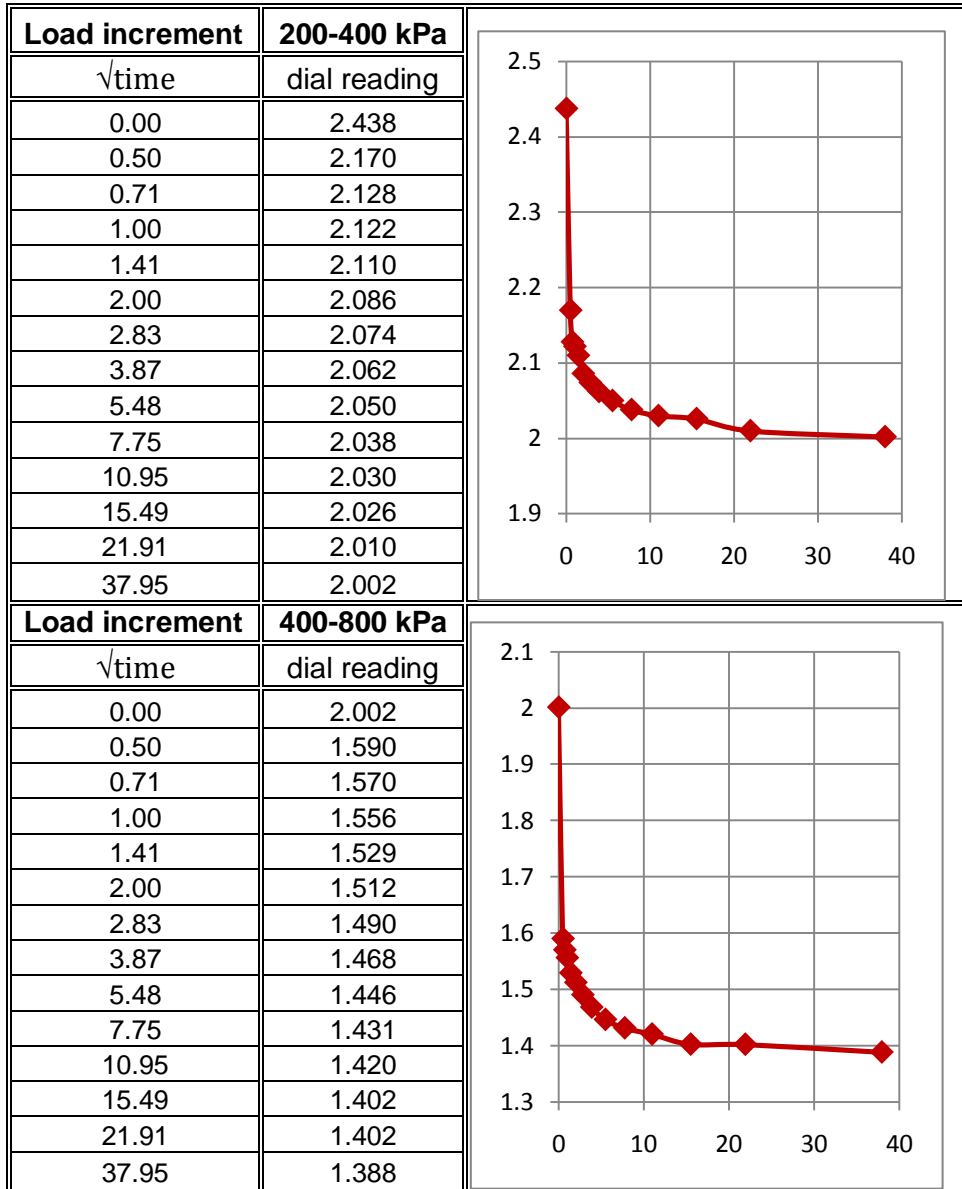


Load increment	800-1600 kPa
$\sqrt{\text{time}}$	dial reading
0.00	1.319
0.50	0.889
0.71	0.884
1.00	0.878
1.41	0.850
2.00	0.814
2.83	0.798
3.87	0.770
5.48	0.706
7.75	0.688
10.95	0.660
15.49	0.648
21.91	0.624
37.95	0.551



Sample No.	TP6-2	Location: Shegole	
Sample Depth, m:	3.00		
[A] In the beginning of the test		[B] In the end of the test	
Sample type :	Disturbed	Final Moisture Content, %	31.70
Ring Area, cm ² :	19.625	Dry specimen wt (ms), gm:	50.27
Height of sample, mm:	17.6	Dry density g/cm ³	1.18
Seating Load, Kpa	5	Height of Solids(Hs), mm	9.19
Initial Void Ratio, eo:	0.90	Final Void Ratio, ef:	0.55
Initial moisture content, %	27.10		
Specific Gravity:	2.79		
Wet density, g/cm ³	1.96		





II. Coefficient of compressibility (C_c) values and e versus $\log p$ Curves

Table AIV-1: Coefficient of compressibility (C_c) for Addisu Gebeya, sample TP1-1

Applied pressure ,P (kPa)	Final dial reading ,mm	Final Specimen Height ,mm	Void Ratio, e	
5	5.000	20.00	1.14	
5	4.980	19.98	1.14	
50	4.608	19.61	1.10	$C_c=0.199$
100	3.644	18.64	1.00	
200	2.728	17.73	0.90	
400	1.93	16.93	0.81	
800	0.964	15.96	0.71	
1600	0.406	15.41	0.65	

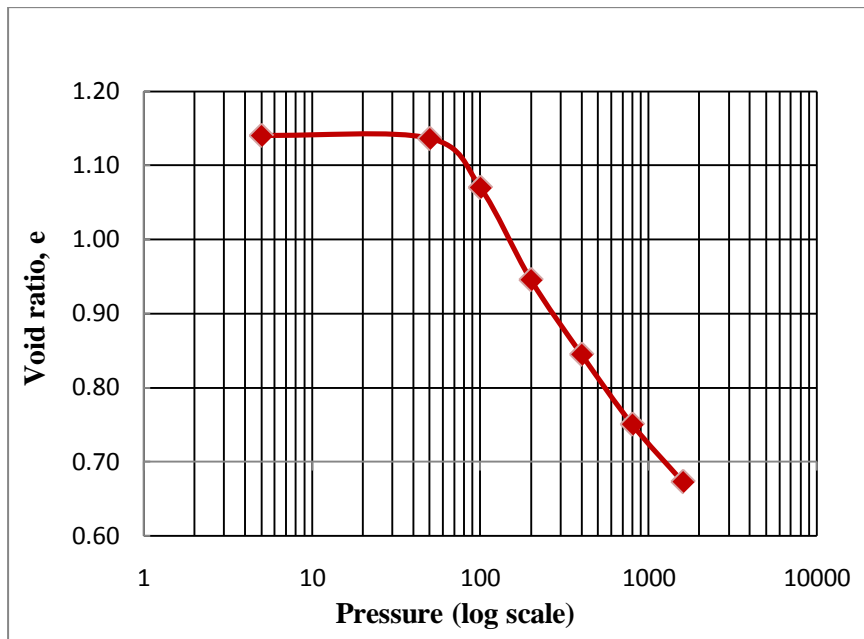


Figure AIV-1: e -Log p Curve for Addisu Gebeya, sample TP1-1.

Table AIV-2: Coefficient of compressibility (C_c) for Addisu Gebeya, sample TP1-2

Applied pressure ,P (kPa)	Final dial reading ,mm	Final Specimen Height ,mm	Void Ratio, e	
5	6.000	20.00	0.95	$C_c=0.191$
5	5.314	19.31	0.88	
50	4.924	18.92	0.84	
100	3.861	17.86	0.74	
200	2.907	16.91	0.65	
400	1.810	15.81	0.54	
800	1.336	15.34	0.49	
1600	0.632	14.63	0.43	

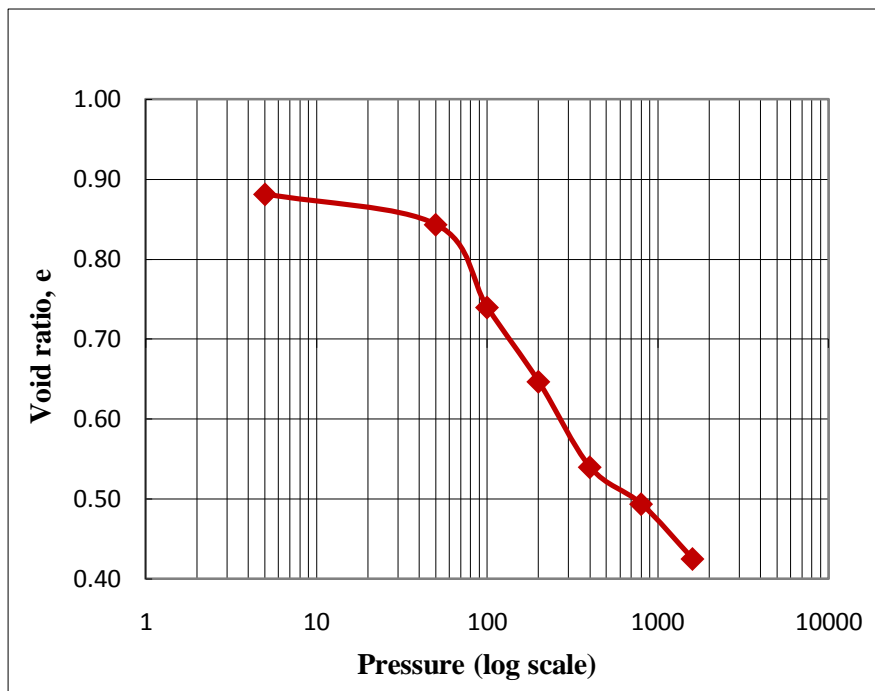


Figure AIV-2: e-Log p Curve for Addisu Gebeya, sample TP1-2.

Table AIV-3: Coefficient of compressibility (Cc) for Atena Tera, sample TP2-1

Applied pressure ,P (kPa)	Final dial reading ,mm	Final Specimen Height ,mm	Void Ratio, e	
5	5.000	20.00	0.96	
5	4.960	19.96	0.96	
50	4.533	19.53	0.92	Cc=0.203
100	3.967	18.97	0.86	
200	3.114	18.11	0.78	
400	2.254	17.25	0.69	
800	1.631	16.63	0.63	
1600	0.914	15.91	0.56	

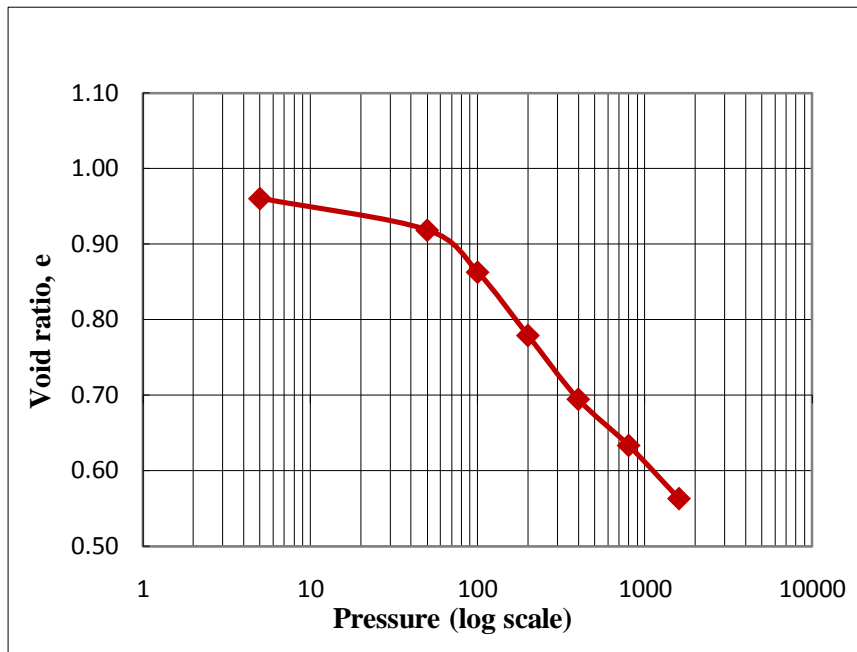


Figure AIV-3: e-Log p Curve for Atena Tera, sample TP2-1.

Table AIV-4: Coefficient of compressibility (Cc) for Atena Tera, sample TP2-2

Applied pressure ,P (kPa)	Final dial reading ,mm	Final Specimen Height ,mm	Void Ratio, e	
5	3.000	20.00	1.05	
5	2.962	19.96	1.05	
50	2.797	19.80	1.03	Cc=0.227
100	2.634	19.63	1.02	
200	2.322	19.32	0.98	
400	1.868	18.87	0.94	
800	1.537	18.54	0.90	
1600	0.871	17.87	0.83	

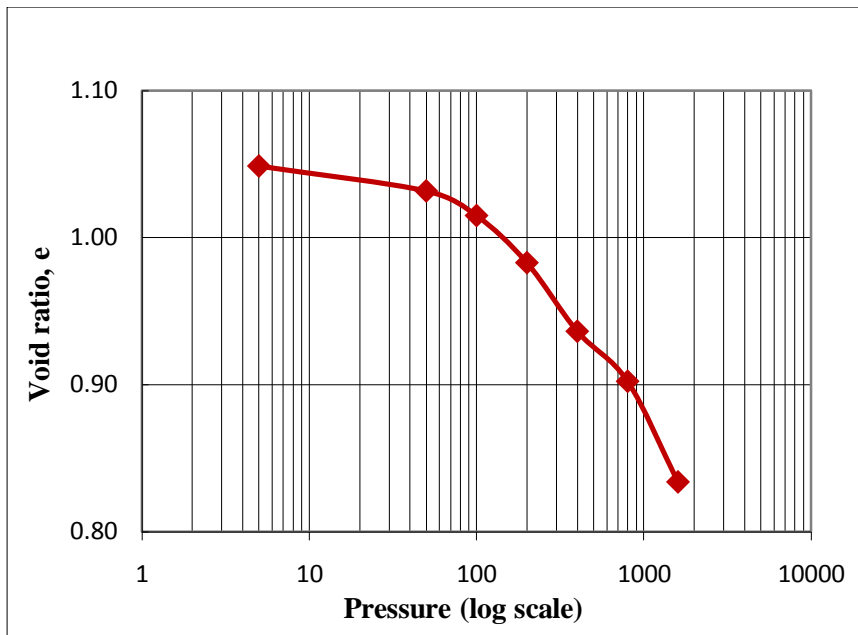


Figure AIV-4: e-Log p Curve for Atena Tera, sample TP2-2.

Table AIV-5: Coefficient of compressibility (Cc) for Athari, sample TP3-1

Applied pressure, P (kPa)	Final dial reading, mm	Final Specimen Height, mm	Void Ratio, e	
5	5.000	20.00	0.97	Cc=0.209
5	4.480	19.48	0.92	
50	4.300	19.30	0.90	
100	3.846	18.85	0.86	
200	3.234	18.23	0.80	
400	2.479	17.48	0.72	
800	1.785	16.79	0.65	
1600	0.988	15.99	0.57	

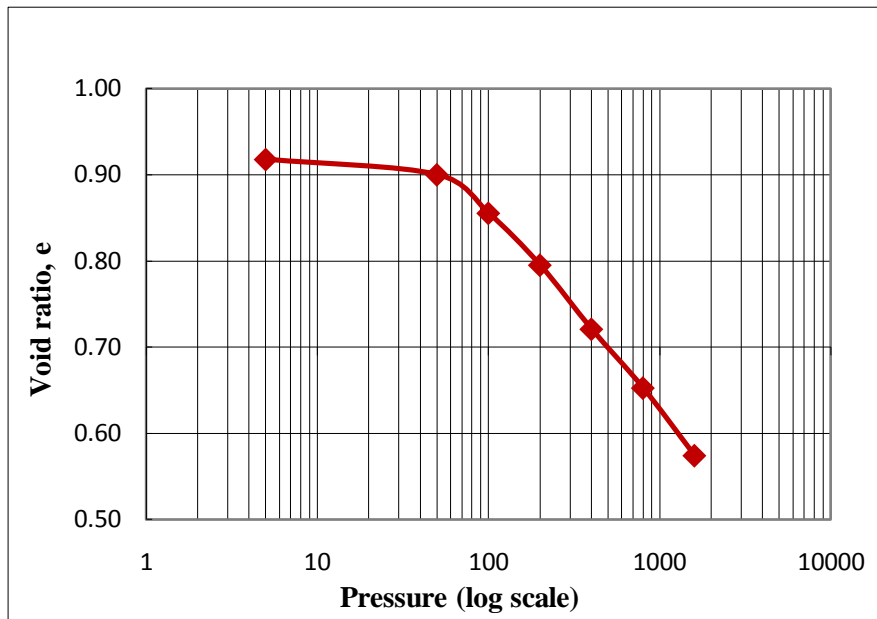


Figure AIV-5: e-Log p Curve for Athari, sample TP3-1.

Table AIV-6: Coefficient of compressibility (Cc) for Athari, sample TP3-2

Applied pressure ,P (kPa)	Final dial reading ,mm	Final Specimen Height ,mm	Void Ratio, e	
5	6.000	20.00	0.97	
5	5.150	19.15	0.89	
50	4.801	18.80	0.85	Cc=0.225
100	4.208	18.21	0.80	
200	3.148	17.15	0.69	
400	2.340	16.34	0.61	
800	1.662	15.66	0.54	
1600	0.965	14.97	0.48	

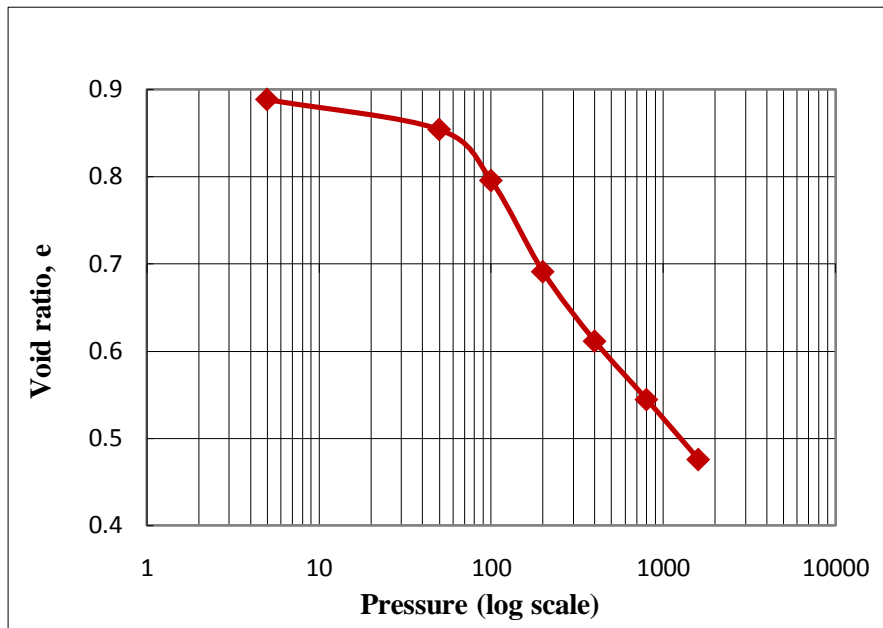


Figure AIV-6: e-Log p Curve for Athari, sample TP3-2.

Table AIV-7: Coefficient of compressibility (Cc) for Awelya, sample TP4-1

Applied pressure ,P (kPa)	Final dial reading ,mm	Final Specimen Height ,mm	Void Ratio, e	
5	5.000	20.00	0.84	Cc=0.176
5	4.980	19.98	0.84	
50	4.624	19.62	0.81	
100	3.636	18.64	0.72	
200	2.982	17.98	0.66	
400	2.391	17.39	0.60	
800	1.670	16.67	0.54	
1600	1.094	16.09	0.48	

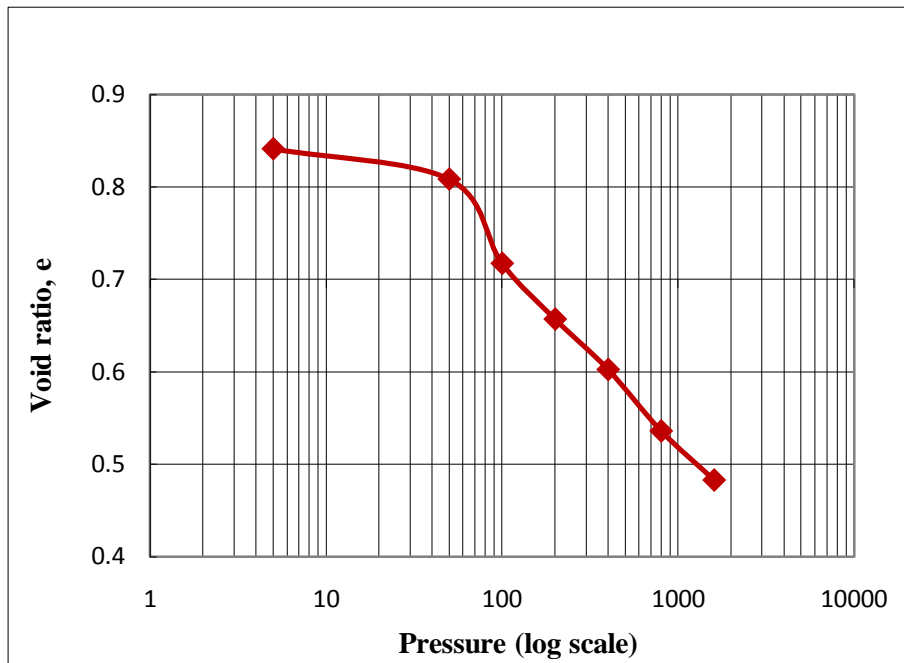


Figure AIV-7: e-Log p Curve for Awelya, sample TP4-1.

Table AIV-8: Coefficient of compressibility (Cc) for Awelya, sample TP4-2

Applied pressure ,P (kPa)	Final dial reading ,mm	Final Specimen Height ,mm	Void Ratio, e	
5	5.000	20.00	0.60	Cc=0.180
5	4.720	19.72	0.57	
50	3.884	18.88	0.51	
100	3.315	18.32	0.46	
200	2.697	17.70	0.41	
400	1.793	16.79	0.34	
800	1.148	16.15	0.29	
1600	0.408	15.41	0.23	

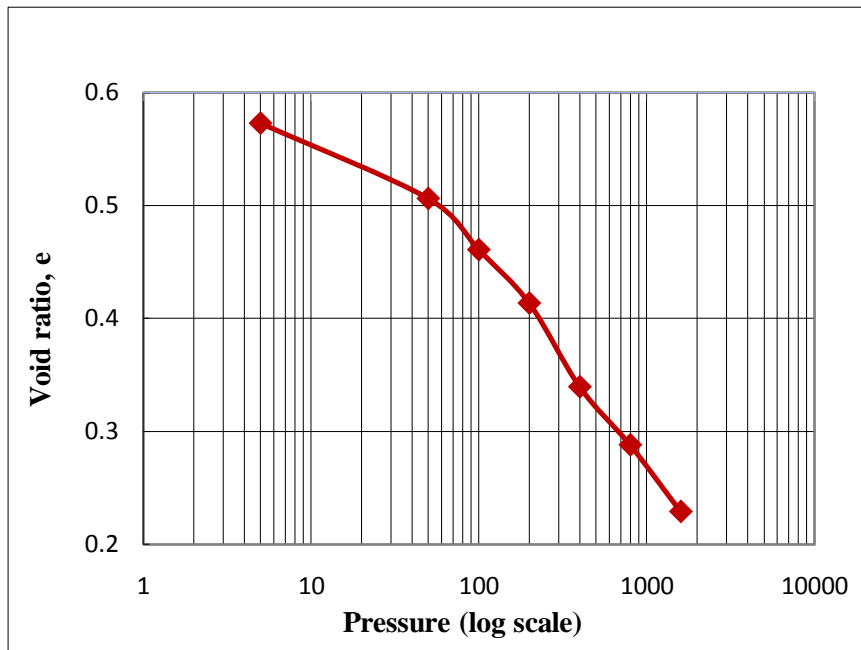


Figure AIV-8: e-Log p Curve for Awelya, sample TP4-2.

Table AIV-9: Coefficient of compressibility (Cc) for Kolfe, sample TP5-1

Applied pressure ,P (kPa)	Final dial reading ,mm	Final Specimen Height ,mm	Void Ratio, e	
5	3.000	20.00	0.86	
5	2.999	20.00	0.86	
50	2.999	20.00	0.86	Cc=0.199
100	2.872	19.87	0.85	
200	2.588	19.59	0.82	
400	2.032	19.03	0.77	
800	1.216	18.22	0.69	
1600	0.571	17.57	0.63	

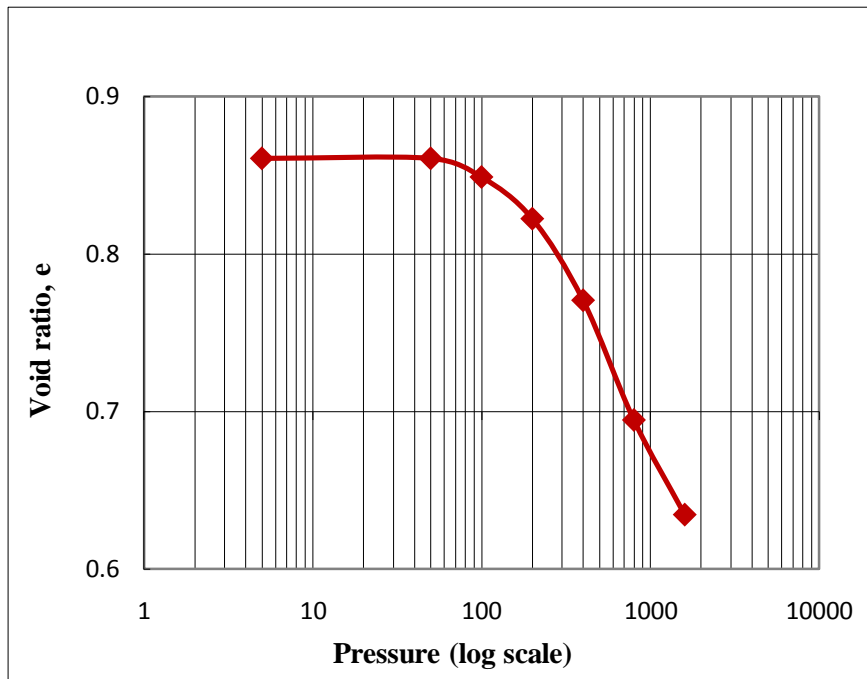


Figure AIV-9: e-Log p Curve for Kolfe, sample TP5-1.

Table AIV-10: Coefficient of compressibility (Cc) for Kolfe, sample TP5-2

Applied pressure, P (kPa)	Final dial reading, mm	Final Specimen Height, mm	Void Ratio, e	
5	3.000	20.00	1.05	
5	2.988	19.99	1.04	
50	2.951	19.95	1.04	Cc=0.186
100	2.668	19.67	1.01	
200	2.186	19.19	0.96	
400	1.679	18.68	0.91	
800	1.089	18.09	0.85	
1600	0.741	17.74	0.81	

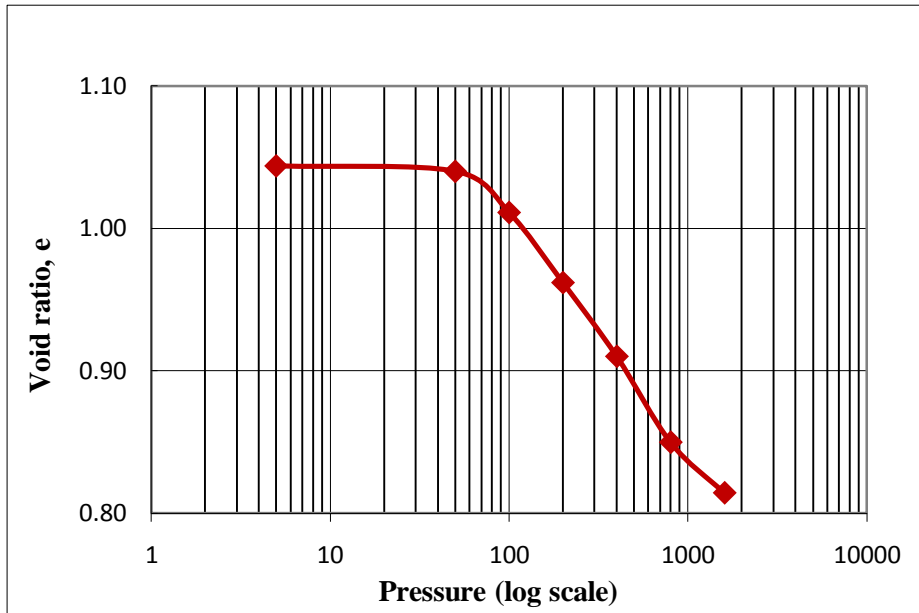


Figure AIV-10: e-Log p Curve for Kolfe, sample TP5-2.

Table AIV-11: Coefficient of compressibility (Cc) for Shegole, sample TP6-1

Applied pressure ,P (kPa)	Final dial reading ,mm	Final Specimen Height ,mm	Void Ratio, e	
5	4.000	20.00	1.03	
5	4.375	20.38	1.07	
50	3.781	19.78	1.01	Cc=0.209
100	3.214	19.21	0.95	
200	2.540	18.54	0.88	
400	1.628	17.63	0.79	
800	1.319	17.32	0.76	
1600	0.551	16.55	0.68	

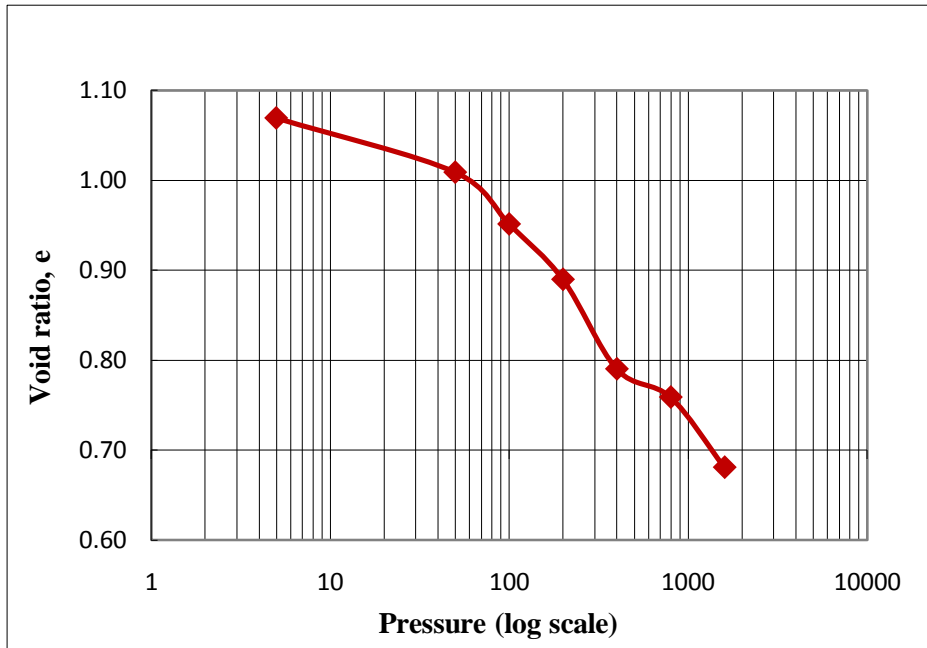


Figure AIV-11: e-Log p Curve for Shegole, sample TP6-1.

Table AIV-12: Coefficient of compressibility (Cc) for Shegole, sample TP6-2

Applied pressure ,P (kPa)	Final dial reading ,mm	Final Specimen Height ,mm	Void Ratio, e	
5	4.000	17.60	0.91	Cc=0.180
5	3.850	17.45	0.90	
50	3.366	16.97	0.85	
100	2.998	16.60	0.81	
200	2.438	16.04	0.74	
400	2.002	15.60	0.70	
800	1.388	14.99	0.63	
1600	0.620	14.22	0.55	

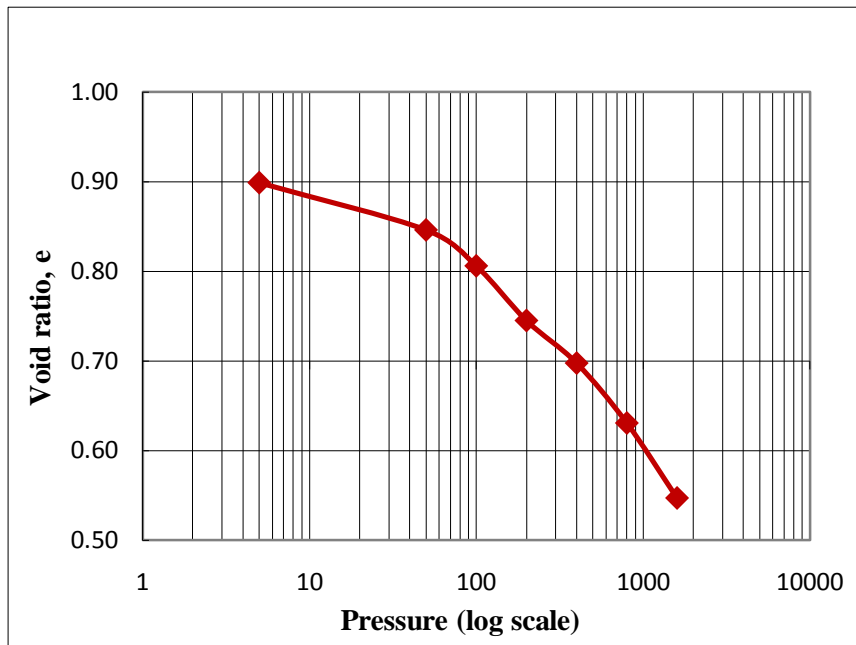


Figure AIV-12: e-Log p Curve for Shegole, sample TP6-2.

III.Pre consolidation pressure (P_c)

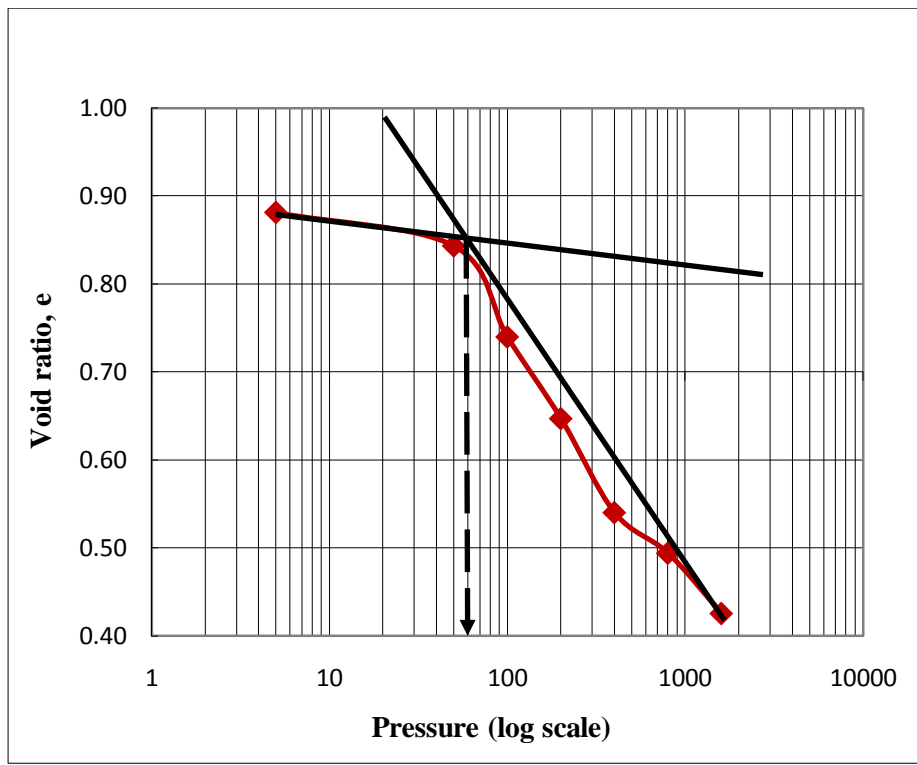


Figure AIV-13: e-Log p Curve for Addisu Gebeya, sample TP1-2.

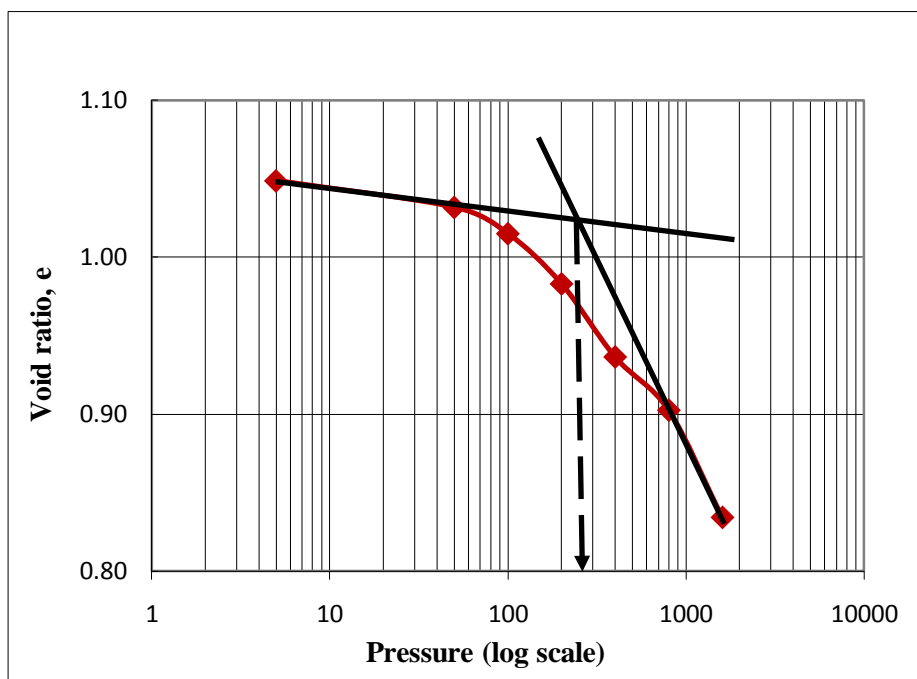


Figure AIV-14: e-Log p Curve for Atena Tera, sample TP2-2.

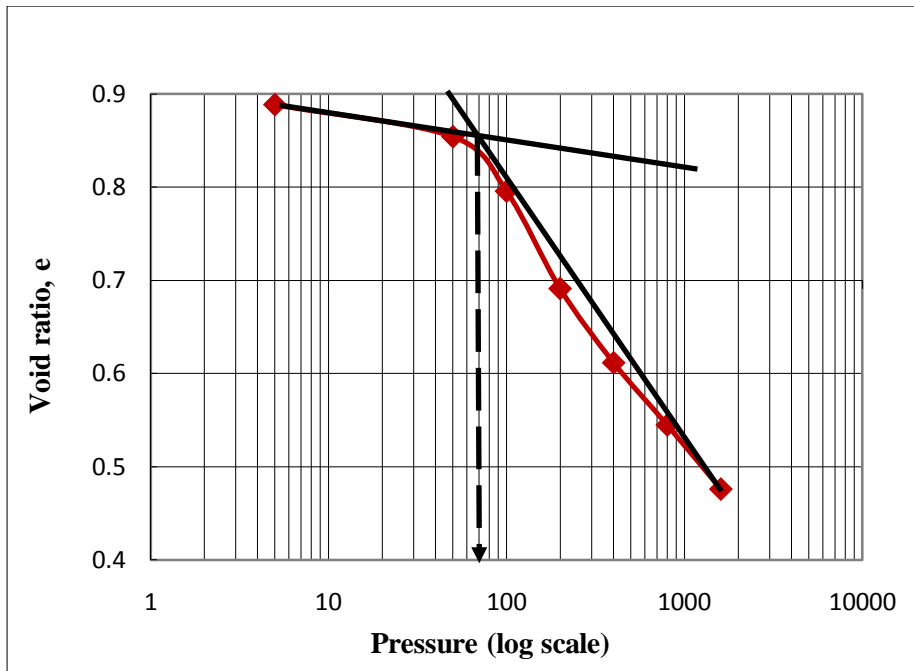


Figure AIV-15: e-Log p Curve for Athari, sample TP3-2.

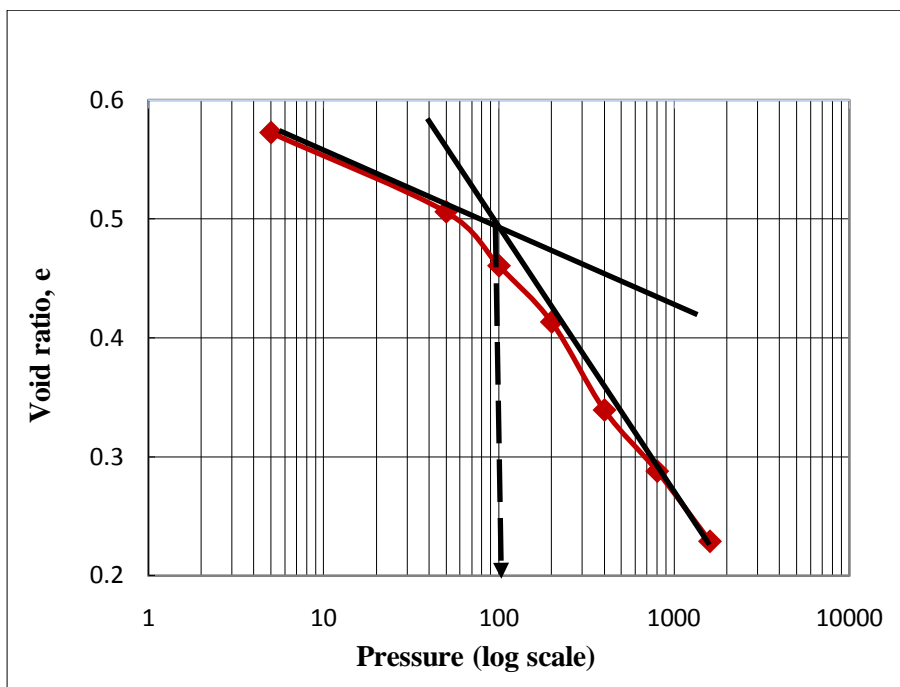


Figure AIV-16: e-Log p Curve for Awelya, sample TP4-2.

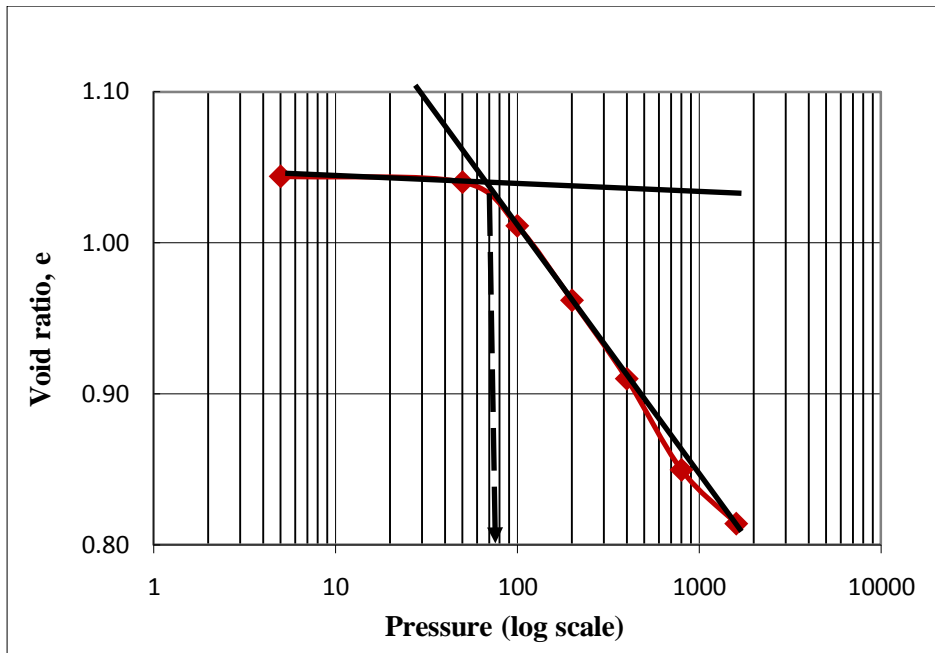


Figure AIV-17: e-Log p Curve for Kolfe, sample TP5-2.

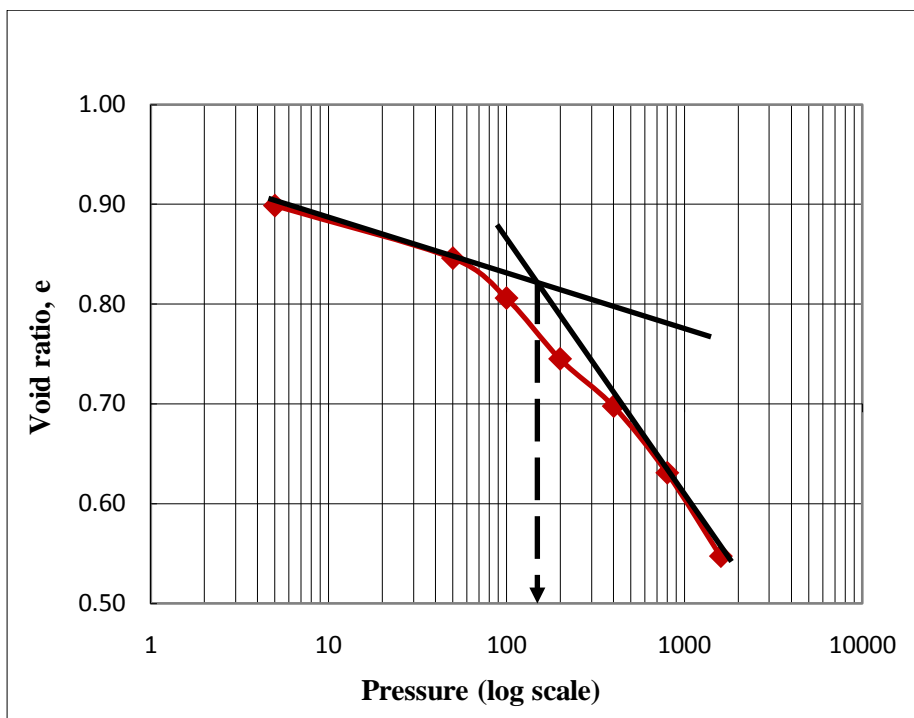


Figure AV-18: e-Log p Curve for Shegole, sample TP6-2.

V. Triaxial compression (isotropic consolidation) test results

1. Addisu gebeva site, sample TP-1-2-Calculation of λ and Γ

✓ Specific volume calculation

Specific volume is volume of sample at any stage to solid grains. The specific volume for each specimen calculated using the following relationship:

$$\nu = 1+e \quad \text{where, } e = \text{void ratio}$$

$$\nu = \text{specific volume}$$

Void ratio (e) is determined from the following relationship:

$$e_o = \frac{G_s \gamma_w (1+w)}{\gamma_{wet}} - 1$$

And $\gamma_{wet} = \gamma_{dry}(1+w)$

$$\gamma_{dry} = \rho g$$

Where $G_s = \text{specific gravity} = 2.72$

$\gamma_w = \text{unit weight of water} = 9.81 \text{ KN/m}^3$

$w = \text{water content} = \text{OMC} = 25\%$

$\gamma_{wet} = \text{wet unit weight of the soil, KN/m}^3$

$\gamma_{dry} = \text{dry unit weight of the soil, KN/m}^3$

$\rho = \text{dry density of the soil} = \text{MDD} = 1.58 \text{ gm/cm}^3$

$g = \text{gravity} = 9.81 \text{ m/s}^2$

There for:

$$\gamma_{dry} = 1.58 * 9.81 = 15.4998 \text{ KN/m}^3$$

$$\gamma_{wet} = 15.499(1+0.25) = 19.375 \text{ KN/m}^3$$

$$e_o = \frac{2.72 * 9.81(1+0.25)}{19.375} - 1 = 0.72$$

$$\nu_o = 1 + 0.72 = 1.72$$

Then, the specific volume at each increment of load (loading stage) determined as:

$$\nu = \frac{V_o}{V_o - \text{cumulative volume change at that stage}}$$

V_o

Where $V_o = \text{initial volume of the sample} = 461.814 \text{ cm}^3$

LOADING STAGE ,VOLUME CHANGE			
Load .kPa	Volume change at each loading, cc	Cumulative Volume change at each loading ,cc	Specific volume at each increment
490	0	0	1.72
490 to 540	1.68	1.68	1.714
540 to 590	3.07	4.75	1.702
590 to 640	2.06	6.81	1.695
640 to 690	0.44	7.25	1.693

From 490 kPa to 540kPa

$$\nu = 1.72 (461.814 - 1.68) = 1.714$$

461.814

From 540 kPa to 590kPa

$$\nu = 1.72 (461.814 - 1.68 - 3.07) = 1.702$$

461.814

From 590 kPa to 640kPa

$$\nu = 1.72 (461.814 - 1.68 - 3.07 - 2.06) = 1.695$$

461.814

From 640 kPa to 690kPa

$$\nu = 1.72 (461.814 - 1.68 - 3.07 - 2.06 - 0.44) = 1.693$$

461.814

- ✓ For isotropic compression, where $\sigma_1 = \sigma_2 = \sigma_3$, P (mean normal stress) is given by:

$$P = \frac{(\sigma_1 + \sigma_2 + \sigma_3)}{3} = \sigma_3$$

3

Cell pressure, σ_3 (kPa)	Mean normal stress, P (kPa)	ln P
490	490	6.19
540	540	6.29
590	590	6.38
640	640	6.46
690	690	6.54

The summary of the above calculations is presented below:

From graph below the capital gamma (Γ) determined as: the value of specific volume when the mean normal stress (lnp) is 1kPa.

$$\text{I.e. } y = -0.0856x + 2.2503$$

$$\Gamma = -0.0856 * \ln 1 + 2.2503 = 2.22503$$

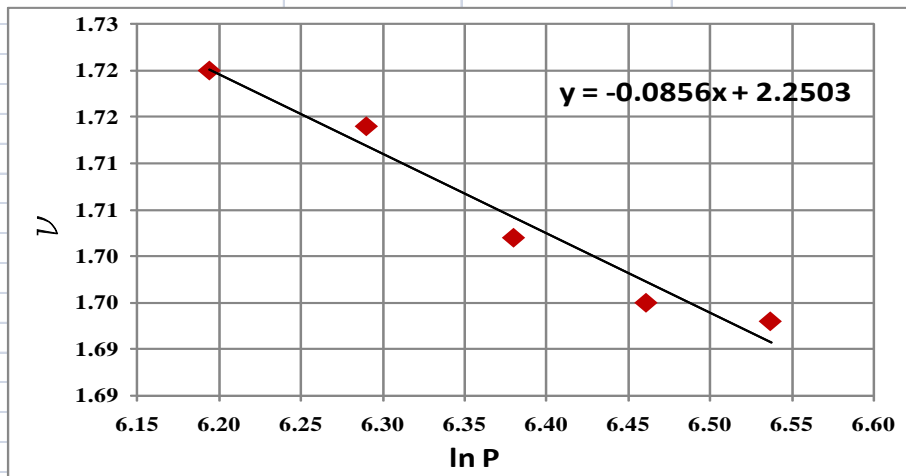
Also from the graph, one can determine the compression index λ (the slope of the line) = 0.0856.

Site	Adisu gebeya	Depth,m	3.0
OMC ,%	25	γ_{wet} (KN/m ³)	19.375
MDD,g/cm ³	1.58	e_o	0.72
Gs	2.72	$\nu_o=1+e_o$	1.72
Initial sample volume ,cm ³	461.814	γ_w (KN/m ³)	9.81

LOADING STAGE ,VOLUME CHANGE

Load.kPa	Volume change at each loading,cc	Cumulative Volume change at each loading,cc	Specific volume at each increment
490	0	0	1.72
490 to 540	1.68	1.68	1.714
540 to 590	3.07	4.75	1.702
590 to 640	2.06	6.81	1.695
640 to 690	0.44	7.25	1.693

Cell pressure, σ_3 (kPa)	Mean normal stress, P (kPa)	ln P	Specific volume, ν
490	490	6.19	1.72
540	540	6.29	1.714
590	590	6.38	1.702
640	640	6.46	1.695
690	690	6.54	1.693



In similar way for rest of the sites the value of the critical state parameters (Γ and λ) was determined and the summary of the result is presented below.

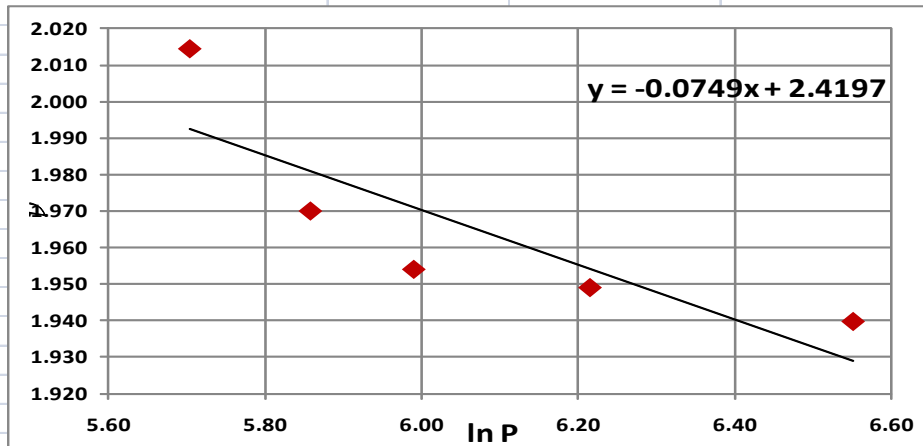
2. Atena tera site, sample TP-2-2

Site	Atena tera	Depth,m	3.0
OMC ,%	33.06	γ_{wet} (KN/m ³)	17.883
MDD,g/cm ³	1.37	e_o	1.0145
Gs	2.76	$\nu_{o=1+e_o}$	2.0145
Initial sample volume ,cm ³	86.193	γ_w (KN/m ³)	9.81

LOADING STAGE ,VOLUME CHANGE

Load.kPa	Volume change at each loading,cc	Cumulative Volume change at each loading,cc	Specific volume at each increment
300	0	0	2.0145
300 to 350	1.9	1.9	1.97
350 to 400	0.8	2.7	1.954
400 to 500	0.2	2.9	1.949
500 to 700	0.4	3.3	1.9397

Cell pressure, σ_3 (kPa)	Mean normal stress, P (kPa)	ln P	Specific volume, ν
300	300	5.70	2.015
350	350	5.86	1.970
400	400	5.99	1.954
500	500	6.22	1.949
700	700	6.55	1.940



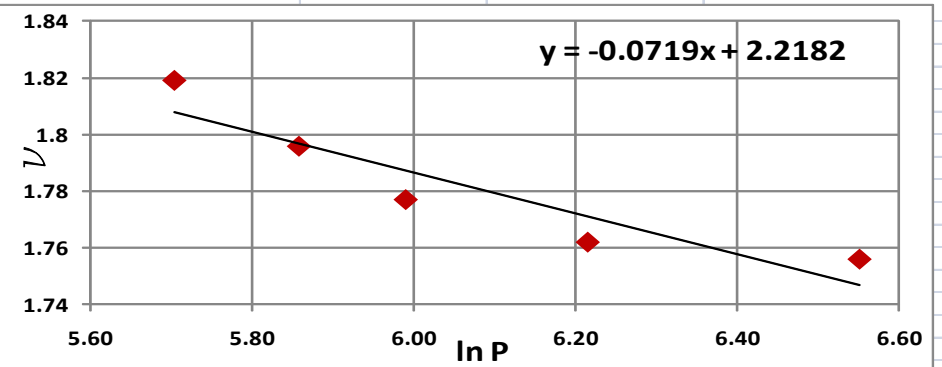
3. Athari site, sample TP-3-2

Site	Athari	Depth,m	3.0
OMC ,%	29	γ_{wet} (KN/m ³)	18.856
MDD,g/cm ³	1.49	e_o	0.819
Gs	2.71	$\nu_{o=1+e_o}$	1.819
Initial sample volume ,cm ³	86.193	γ_w (KN/m ³)	9.81

LOADING STAGE ,VOLUME CHANGE

Load.kPa	Volume change at each loading,cc	Cumulative Volume change at each loading,cc	Specific volume at each increment
300	0	0	1.819
300 to 350	1.1	1.1	1.796
350 to 400	0.85	1.95	1.777
400 to 500	0.72	2.67	1.762
500 to 700	0.3	2.97	1.756

Cell pressure, σ_3 (kPa)	Mean normal stress, P (kPa)	ln P	Specific volume, ν
300	300	5.70	1.819
350	350	5.86	1.796
400	400	5.99	1.777
500	500	6.22	1.762
700	700	6.55	1.756



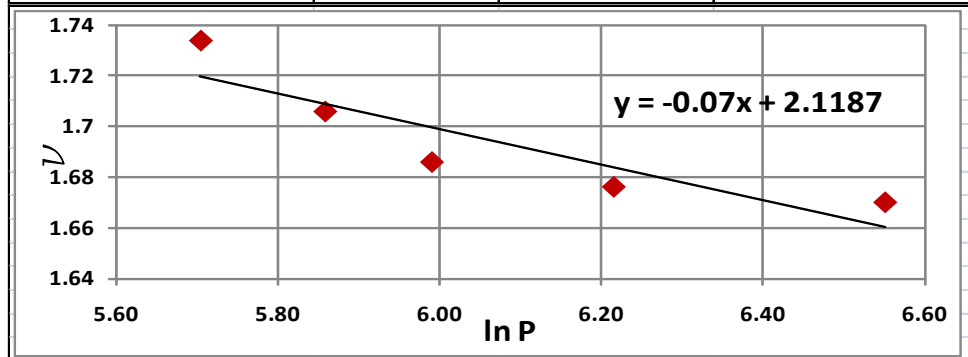
4. Awelya site, sample TP-4-2

Site	Awelya	Depth,m	3.0
OMC ,%	24.5	γ_{wet} (KN/m ³)	19.297
MDD,g/cm ³	1.58	e_o	0.734
Gs	2.74	$\nu_o=1+e_o$	1.734
Initial sample volume ,cm ³	86.193	γ_w (KN/m ³)	9.81

LOADING STAGE ,VOLUME CHANGE

Load.kPa	Volume change at each loading,cc	Cumulative Volume change at each loading,cc	Specific volume at each increment
300	0	0	1.734
300 to 350	1.4	1.4	1.706
350 to 400	0.9	2.3	1.686
400 to 500	0.5	2.8	1.676
500 to 700	0.3	3.1	1.670

Cell pressure, σ_3 (kPa)	Mean normal stress, P (kPa)	ln P	Specific volume, ν
300	300	5.70	1.734
350	350	5.86	1.706
400	400	5.99	1.686
500	500	6.22	1.676
700	700	6.55	1.670



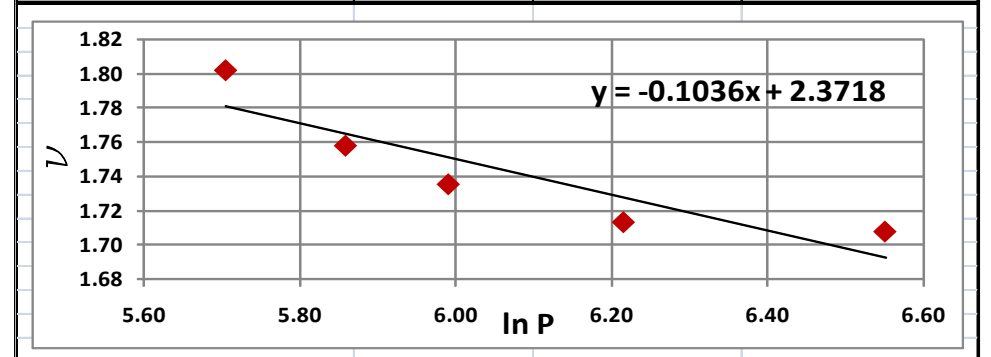
5. Kolfe site, sample TP-5-2

Site	Kolfea	Depth,m	3.0
OMC ,%	26	γ_{wet} (KN/m ³)	18.79
MDD,g/cm ³	1.52	e_o	0.802
Gs	2.74	$\nu_o=1+e_o$	1.802
Initial sample volume ,cm ³	65.21	γ_w (KN/m ³)	9.81

LOADING STAGE ,VOLUME CHANGE

Load.kPa	Volume change at each loading,cc	Cumulative Volume change at each loading,cc	Specific volume at each increment
300	0	0	1.802
300 to 350	1.6	1.6	1.758
350 to 400	0.7	2.3	1.736
400 to 500	0.8	3.1	1.713
500 to 700	0.2	3.3	1.708

Cell pressure, σ_3 (kPa)	Mean normal stress, P (kPa)	ln P	Specific volume, ν
300	300	5.70	1.802
350	350	5.86	1.758
400	400	5.99	1.736
500	500	6.22	1.713
700	700	6.55	1.708



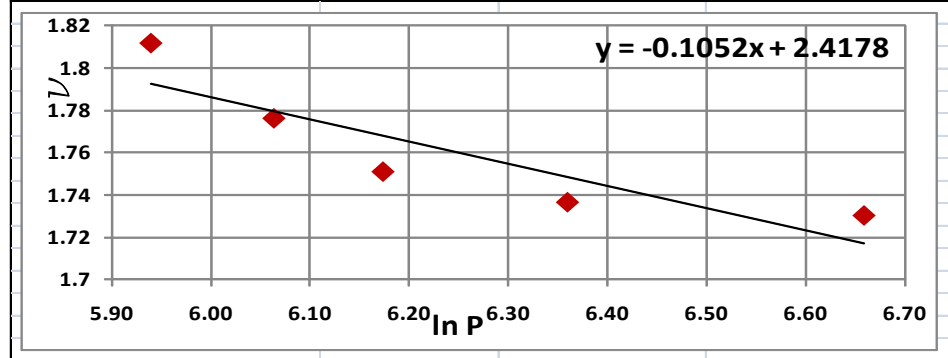
Shegole site, sample TP-6-2

Site	Shegole	Depth,m	3.0
OMC ,%	27.1	γ_{wet} (KN/m ³)	19.2
MDD,g/cm ³	1.54	e_o	0.812
Gs	2.79	$\nu_o=1+e_o$	1.812
Initial sample volume ,cm ³	86.193	γ_w (KN/m ³)	9.81

LOADING STAGE ,VOLUME CHANGE

Load.kPa	Volume change at each loading,cc	Cumulative Volume change at each loading,cc	Specific volume at each increment
380	0	0	1.812
380 to 430	1.7	1.7	1.776
430 to 480	1.1	2.8	1.751
480 to 580	0.7	3.5	1.737
580 to 780	0.3	3.8	1.730

Cell pressure, σ_3 (kPa)	Mean normal stress, P (kPa)	ln P	Specific volume, ν
380	380	5.94	1.812
430	430	6.06	1.776
480	480	6.17	1.751
580	580	6.36	1.737
780	780	6.66	1.730



Appendix –B:

(Photos of site and laboratory tests)



Figure B-1: Extracting disturbed soil sample.



Figure B-2: Loading one dimensional consolidation machine.



Figure B-3: mounted soil sample on triaxial machine.



Figure B-4: conducting isotropic consolidation triaxial compression test.

DECLARATION

I, the undersigned, declare that this thesis is my original work performed under the supervision of my research advisor Prof. Alemayehu Teferra and has not been presented as a thesis for a degree in any other university. All sources of materials used for this thesis have also been duly acknowledged.

Name: Yodit Muluneh

Signature: _____

Place : Addis Ababa institute of technology (AAiT)

Addis Ababa University

School of graduate studies

Addis Ababa.

Date : July, 2012